ANTHRAX EDEMA TOXIN IMPAIRS NEUTROPHIL ACTIN-BASED MOTILITY BY STIMULATING VASP PHOSPHORYLATION

By

SARAH E. SZAROWICZ

A DISSERTATION PRESENTED TO THE GRADUATE SCHOOL
OF THE UNIVERSITY OF FLORIDA IN PARTIAL FULFILLMENT
OF THE REQUIREMENTS FOR THE DEGREE OF
DOCTOR OF PHILOSOPHY

UNIVERSITY OF FLORIDA
2010

To all who have believed in me, cultured my intellectual curiosity, academic interest throughout my lifetime, making this milestone possible

ACKNOWLEDGMENTS

I thank my chair and members of my supervisory committee for their mentoring. I thank my loving husband for all of his support and love, which motivated me to complete my studies. I also thank my parents for their loving encouragement and support throughout my academic career.

TABLE OF CONTENTS

page

LIST OF TABLES

LIST OF FIGURES

Abstract of Dissertation Presented to the Graduate School
of the University of Florida in Partial Fulfillment of the
Requirements for the Degree of Doctor of Philosophy

ANTHRAX EDEMA TOXIN IMPAIRS NEUTROPHIL
ACTIN-BASED MOTILITY BY STIMULATING VASP PHOSPHORYLATION
By

Sarah E. Szarowicz

May 2010

Chair: Frederick Southwick
Major: Medical Sciences - Microbiology and Immunology

Inhalation anthrax can lead to sepsis and death within days. The fulminate nature of illness reveals minimal elevation of peripheral polymorphonuclear (PMNs) counts at time of hospital admissions indicating a profound impairment of the innate immune response. Edema toxin (ET) is one of the major *Bacillus anthracis* virulence factors and consists of edema factor (EF) and protective antigen (PA). Low concentrations of ET (100-500 ng/ml of PA and EF) significantly impair human PMN chemokinesis, chemotaxis, and their ability to polarize. These changes are accompanied by a significant reduction in chemoattractant-stimulated PMN actin assembly. ET also causes a significant decrease in *Listeria monocytogenes* intracellular actin-based motility within HeLa cells. These defects in actin assembly are accompanied by a >50-fold increase in intracellular cyclic AMP and a >4-fold increase in the activation of protein kinase A (PKA). Our studies have shown that anthrax lethal toxin (LT) also impairs neutrophil actin-based motility, and we now find that LT combined with ET causes an additive inhibition of PMN chemokinesis, polarization, chemotaxis, and FMLP (N-formyl-met-leu-phe)-induced actin assembly. Our studies have shown that anthrax LT blocks the Hsp27 phosphorylation cycle, impairing actin assembly and chemotaxis.

However, the complete molecular pathway leading to ET-induced impairment of actin-based motility has not yet been determined. *Listeria* infection of MVd7 cells (lack all members of the VASP protein family) transfected with different VASP constructs, as well as introduction of VASP-TAT recombinant proteins into human neutrophils point to the actin-regulatory protein VASP as the likely end target of edema toxin, and other cyclic AMP-inducing agents, that impairs actin-based motility. Phosphorylation of VASP serine-157 impairs actin-based motility, and introduction of a VASP pseudo-unphosphorylated construct completely neutralizes the ability of ET and forskolin plus IBMX (adenylate cyclase activating compound and cAMP phosphodiesterase inhibitor) to block actin-based motility. These findings reveal the primary pathway by which ET impairs neutrophil motility, and emphasizes the importance of the cAMP signaling pathway and VASP phosphorylation in the regulation of actin-based motility in neutrophils and *Listeria*.

CHAPTER 1
INTRODUCTION

Bioterrorism and Bacillus anthracis

In October 2001 *Bacillus anthracis* was used as a bioweapon, and this attack has rekindled scientific interest in anthrax pathogenesis (1). Once inhaled, *B. anthracis* can lead to sepsis, meningitis and death within days if not properly diagnosed and treated. Following the bioterrorist attacks, analysis of clinical findings revealed patients suffering with systemic anthrax had little to no increase in polymorphonuclear neutrophils (PMNs) in their blood (1). Also, pleural effusions from these patients demonstrated a paucity of white blood cells providing further evidence for poor chemotaxis to the area of infection (2). An understanding of how *B. anthracis* is able to escape the innate and adaptive immune responses may lead to new therapeutic strategies to improve the host immune response to anthrax.

History of *Bacillus anthracis* Microbiology

B. anthracis is a gram-positive spore forming rod that is the causative agent of anthrax (3). When grown in culture, *B. anthracis* forms a distinct boxcar chain. It is non-hemolytic and catalase positive. The thick capsule wall is visible after staining with McFaydean's methylene blue. When cultured on sheep blood agar, the bacteria form characteristic large white ovoid colonies with tacky consistency when touched with a loop. Also, *B. anthracis* is gamma phage-sensitive, distinguishing it from other species of bacilli.

Of historical interest, anthrax was the first disease for which a microbial origin was established (4). Robert Koch's paper in 1876 demonstrated rod-like bacteria in the blood/tissue of diseased animals, spore formation under starvation conditions, nutrient

induced transformation of the spores back to bacteria, and culturing of either form would lead to anthrax. Koch called the bacterium *B. anthracis* which was the name given by Cohn in 1875 (5). The work on anthrax led to the formulation of what is commonly referred to as Koch's postulates. Fundamental knowledge of the pathogenesis of anthrax progressed significantly due to the work of Koch and Pasteur.

Anthrax is primarily a zoonotic disease that affects herbivores and was believed to be first documented in the Bible as the fifth great plague of Egypt (6). Hippocrates named the disease "anthrax" (coal in Greek) due to the cutaneous black skin lesions that appear at the site of spore entry (7). Anthrax remained a major killer of livestock until the late 19th century. A striking feature of the disease is the suddenness of clinical pathology. Symptoms usually appear one to two days prior to death. Animals usually look depressed, display signs of cardiac and respiratory failure, mucosa become hemorrhagic, the throat and abdomen become swollen, and blood leaks from the vessels and fails to coagulate (6).

B. anthracis spores are highly resistant to killing and remain viable in soil for many years. The simplicity for its aerosilization and high mortality rate make it an ideal bioweapon. The CDC classifies it as a category A agent. There are many historical examples of *B. anthracis* being used in warfare. The Japanese contaminated food and water in the 1930's and 40's (8). The former Soviet Union weaponized *B. anthracis* during the 1970's in a factory in Sverdlovsk, where in 1979 there was an accidental release of anthrax leading to 68 deaths in surrounding towns (9). Most notable in the US was the attack in 2001 via the US mail that led to 22 cases and 5 deaths (10).

B. anthracis spores are dormant forms of the bacteria. Like seeds, they only germinate in a fertile environment. If inhaled, larger spores lodge in the upper respiratory tract, where they are less dangerous, but spores between 1 and 5 microns penetrate into the alveoli, tiny sacks in the lung. The LD50 is calculated to be 2,500-55,000 inhaled spores (10), however recent data suggests that as few as 1-3 spores may cause death (11). Once inside the host, the spores are able to germinate and initiate transcription of virulence factors to enhance immune evasion and survival within the host. *B. anthracis* spores are particularly resistant to extreme temperatures, low nutrients and harsh chemical environments. Spores can survive for decades in the environment (6). It is thought that people come into contact with anthrax primarily through infected herbivores.

The transformation of the spore into a vegetative cell is one of the key steps in the pathogenic cycle of anthrax, enabling bacteria to proliferate and synthesize virulence factors. Alveolar macrophages and dendritic cells are thought to be primary sites for germination (12-14). Guinea pigs were used as a model for spore uptake, and it was determined that spores are taken up by lung phagocytes within an hour, within four hours spores were detected in the lymph nodes, and within twenty-four hours the bacteria were proliferating in the blood (15). Non-human primates have also been used as a model system for spore uptake and it was determined that it takes six to eighteen hours for the spores to be taken up by lung phagocytes and transported to the lymph nodes (15, 16).

Germination is closely followed by the expression of toxin genes. Isolates are extremely uniform in chromosome composition. *B. anthracis* is phenotypically and

genotypically similar to *B. cereus* and *B. thuringenesis* except for two virulence plasmids *px01* and *px02*. *Px01* contains the genes that encode anthrax toxins: lef, pagA and cya (4). *Lef* encodes for lethal factor (LF), *pagA* encodes for the protective antigen (PA) and *cya* encodes for edema factor (EF). The *px01* plasmid also encodes the toxin gene transactivator *atxa* (17), and the plasmid-borne germination genes; *ger-xc*, *ger-a* and *ger-b* (18). Migot, et al. (19) found that *atxa* functions as a master regulator controlling *pxo1* and *px02* expression. *Atxa* is triggered at 37°C under high CO_2, which is a condition found in the host. *Px02* encodes for the poly D-glutamic acid protein capsule. The poly D-glutamic acid structure is unique, as glutamic acid used by other bacteria are typically a mixture of L and D isomers (20). The capsule has a negative charge, which inhibits macrophages from engulfing and destroying the vegetative cells, impeding the host's immune response. Thus, the capsule allows virulent anthrax bacilli to grow virtually unimpeded in the infected host (21). Little is currently known about the function of pXO2 open reading frames (ORFs) beyond the virulence genes associated with the capsule (*dep, capACB*, and *acpA)* (4).

Although pXO1 and pXO2 are considered major virulence factors, other virulence factors have been found including: anthrolysin O (22)and cholesterol dependent cytolysin, similar to cytolysins produced by pathogenic gram-positive bacteria such as *Listeria* and *Streptococcus* species (23, 24). Anthrolysin O is shown to lyse RBC, neutrophils, macrophages and lymphocytes *in vitro* in a dose dependent manner (25) and has been shown to induce pro-inflammatory responses as a Toll-like receptor (TLR) 4 agonist (26).

Anthrax Infections

Anthrax infection can be present in three very distinct forms depending on the site of entry. Symptoms and disease depend on the route of infection: cutaneous anthrax results when spores come into contact with an open wound, gastrointestinal anthrax results from the ingestion of contaminated meat or other contaminated products, and inhalation anthrax results from spores being inhaled into the lungs. Generally it is not spread person-person. Anthrax can also be contracted during a lab accident, mishandling of infected animals, and as a bioweapon.

Inhalational anthrax is almost 100% fatal if not diagnosed and treated promptly (1). Once spores are inhaled into the lungs, alveolar macrophages phagocytose the spores and carry them to the mediastinal lymph nodes where germination and subsequent rupture of macrophages occurs resulting in the release of vegetative bacteria into the blood stream (7). Initial clinical presentation includes flu-like symptoms for several days, followed by sudden respiratory collapse and sepsis, usually occurring within a 4-5 day period (27).

Gastrointestinal anthrax usually occurs when anthrax spores are consumed through ingestion of contaminated meat. Clinical signs are vomiting blood, severe diarrhea, acute inflammation of the intestinal tract, and loss of appetite. If the pathogen invades the bowels it can gain access to the bloodstream allowing for sepsis to occur. Gastrointestinal anthrax can be treated with antibiotics, but left untreated 25-60% of cases will result in death (28).

Cutaneous anthrax presents as black boil-like lesions on the skin. The lesions are often large, painless necrotic ulcers that usually form at the site of spore entry 2-5 days

post-exposure. Cutaneous anthrax is rarely fatal, but can progress to toxemia and death without proper treatment (28).

Anthrax Toxins

B. anthracis excretes three exotoxins; protective antigen (PA), edema toxin (ET) and lethal toxin (LT), which account for many of the clinical manifestations. PA is responsible for transporting EF and LF into the cytoplasm by a pH dependent endocytic event. As the pH becomes acidic the PA will form a pore allowing the release of toxins into the host cytosol (29, 30). Protective antigen is able to bind two separate receptors, TEM-8 (tumor necrosis factor-8) or CMG-2 (capillary morphogenesis protein-2) (31, 32). TEM-8 is expressed on tumor endothelial cells, and its only known function currently is to bind PA. CMG-2 functions in cellular interactions with laminin and the extracellular matrix through binding laminin and collagen IV (32). PA is an 83-kDa protein that is cleaved by furin (33), present on the cell surface, to a 63-kDa protein that is able to heptamerize and form a pore for the entry of EF and LF into the cell (34). Even though the heptameric PA-63 prepore has radial sevenfold symmetry, measurements by two independent methods have shown that the heptamer binds only three molecules of ligand under saturating conditions (35). The toxin-receptor complex is internalized primarily through clathrin-coated pits and is then trafficked to the early endosomes. The low pH conditions of the endosome facilitate the transition of PA-63 from a pre-pore to a pore and the unfolding of LF and EF. LT and ET are then released from PA-63 into the cytosol (Figure 1-1) (36).

LT is a zinc-metalloprotease that cleaves the N-terminal seven amino acids of mitogen-activated protein kinases 1-4, 6-7 (MAPKKs or MEKs) resulting in their inactivation (37, 38). MEK1/2 is in the ERK pathway that functions in cellular

proliferation, differentiation and survival. MEK3/6 is in the p38 pathway that functions in environmental stresses, cell growth, differentiation, cell-cycle arrest and apoptosis. The MEK4/7 is in the JNK pathway that functions in stress stimuli, T-cell differentiation and apoptosis. Inactivation of the MEK pathway allows for LT to affect many different cell types. LT is able to inhibit actin polymerization and thus chemotaxis in the neutrophil (39) and inhibits the proliferation and differentiation of monocytes (40). In neutrophils, LT not only impairs chemotaxis but also induces neutrophils to release factors that are hemolytic triggering the lysis of red blood cells (RBCs) (39, 41). LT is able to impair dendritic cells (DCs) by inhibiting the proinflammatory cytokines and co-stimulatory molecules necessary for stimulating antigen specific T cells (42). LT also induces apoptosis of macrophages (40), and inhibits phagocytic production of phospholipase A2 (43) and the glucocorticoid receptor responsible for inflammation (44).

ET functions as an adenylate cyclase that converts adenosine triphosphate (ATP) to cAMP (45). ET requires the uptake of extracellular calcium for generation of optimal cAMP response in neutrophils and macrophages (46). A rise in cAMP in neutrophils has been shown to inhibit phagocytosis of the avirulent Sterne strain of *B. anthracis* (47). cAMP is a second messenger, and its purposes include activation of protein kinases and regulating the effects of glucagon and adrenaline (48). By accumulating cAMP within the host cell, ET disrupts bacterialcidal functions of immune effector cells disabling the host defense mechanism. This may help facilitate the survival and replication of *B. anthracis* within the host. Unlike LT, ET has not been extensively studied, so not much is known about the effects on the host. ET not only has specific activity 1000 fold higher than mammalian adenylate cyclase (AC) but also

is also able to disrupt water homeostasis and other crucial pathways responsible for edema seen during infection (49). ET has been shown to block phagocytosis in neutrophils thereby increasing susceptibility to infection and impairing the innate immune response (49, 50). ET has also been shown to increase toxin receptor expression, resulting in increased rates of toxin internalization (51). ET and LT activities, cAMP and MEK cleavage, are likely to act synergistically to enhance pathogenesis.

cAMP Signaling

cAMP is an ancient and extremely important signaling molecule that is preserved from bacteria to humans (52). In eukaryotes, concentrations of cAMP are up regulated in response to activation of adenylate cyclase (AC) through G-protein coupled receptors (GPCRs) (53). cAMP or 3'-5'-cyclic adenosine monophosphate is a second messenger that is important for many different biological processes. Earl Sutherland discovered cAMP during studies of hormonal regulation of metabolism in mammalian heart and liver samples in 1958 (54). cAMP is derived from ATP and used for intracellular signal transduction, such as transferring the effects of hormones, which cannot pass through the cell membrane. cAMP is also used by cells to regulate metabolism, gene expression, cell cycle, cytoskeletal function, and proliferation (Figure 1-2) (53).

cAMP signaling involves the synthesis of cAMP by membrane-bound AC isoforms and subsequent diffusion through the cell to points of spatially restricted cAMP effector proteins like protein kinase A (PKA) (55). Hormones or neurotransmitters binding the GPCR-$\beta\gamma$, leads to the increase in AC, which then catalyzes ATP conversion into cAMP and inorganic pyrophosphate. cAMP is able to form discrete and often minute gradients within cells. Three different downstream effectors sample cAMP gradients: 1) cyclic

nucleotide gated ion channels, 2) EPAC and 3) PKA. Each of these effectors is solely activated by cAMP, and protein-protein interactions that maintain spatial resolution are essential for cellular signaling (56). There are several different classes of ACs. Heterogeneity exists between many organisms and cell types demonstrating there are a multitude of cellular processes that are regulated by cAMP. Mammals normally utilize class III AC, a family of transmembrane AC (tAC): tAC is directly regulated by heterotrimeric G-coupled proteins and generates cAMP in response to hormones and neurotransmitters, which signal through GPCR (57).

The AC has been divided into six different classes based on sequence homology within the catalytic portions. ACs from *E. coli* and other Gram-negative pathogens are classified as class I. Class II are the “toxins”. These AC are secreted and translocated into the host and disrupt the intracellular signaling by flooding the cell with supraphysiological levels of cAMP. This class contains ET from *B. anthracis*, ExoY of *Pseudomonas aeruginosa, Yersinia pestis*, and *Bordetella pertussis* (58). Eukaryotic AC belongs to class III, which are the broadest class. Class IV, V and VI are relatively newly identified classes and only contain a handful of prokaryotic members (57).

Phosphodiesterases (PDEs) are the only known route of cAMP degradation (59). PDEs control the magnitude and duration of cAMP regulated events (58). If AC is left unchecked it will rapidly increase in a uniform manner, which will have dire consequences for normal cellular function. To this end, cells express defined subsets of PDEs from eight different families of cAMP phosphodiesterases (60). The inability to generate and shape intracellular cAMP gradients depends on PDEs activity to degrade cAMP to 5’-AMP (55).

The concept of cAMP signaling compartmentalization was first introduced in 1981 by Brunton and is thought to allow for various effects on cellular targets (61). This idea came about with the discovery of A-Kinase anchoring proteins (AKAP). AKAP bind directly to the regulatory subunit of PKA to target the kinase to defined cellular locations (62). In creating a signaling network, enzymes are needed to activate and hydrolyze cAMP. AKAPs are uniquely equipped to modulate spatial and temporal PKA signaling (63).

PKA

An important role of PKA is in the cAMP-dependent regulation of the cytoskeleton and cell movement. PKA is promiscuous with targets found in the membrane, cytoplasm, nucleus and nearly all families of cytoskeletal networks (64). The requirement for tight control and regulation of PKA activity during cell migration is supported by reports of both stimulatory and inhibitory effects of PKA on cell migration (65-67).

PKA is heterotetrameric enzyme comprising two regulatory (R) subunits and two catalytic subunits (C). Four R subunits are encoded by four separate genes (R1α, RIβ, RIIα, and RIIβ), while three genes encode for the C unit (α, β, and γ) (68). There are two types of PKA holoenzymes, Type I and Type II, which are defined by their R subunits. The R subunit has four functions: 1) maintain holoenzyme in an inactive state, 2) releases an active C subunit upon the cooperative binding of two cAMP per R subunit, 3) the N-terminus mediates dimerization, and 4) interacts with AKAPs (63). The C subunit can be down-regulated by phosphorylation (69). Down-regulation of PKA

occurs by a feedback mechanism: one of the substrates activated by PKA is a PDE that converts cAMP to 5'-AMP (63).

Inactive PKA holoenzyme exists as a homodimer made up of two R and two C subunits. In the "inactive" state, C subunits are bound to R subunits. In the "active" state the R subunits are released and the C subunits are free to phosphorylate substrates they come into contact with (Figure 1-3). Protein phosphorylation allows eukaryotic cells to translate extracellular signals into a bio-response.

AKAPs have been linked not only to PKA compartmentalization but also to the cytoskeleton. AKAP-Lbc has been linked with the actin cytoskeleton through its interaction with the Rho GTPases and is able to promote GPCR-dependent stress fiber formation (70, 71). AKAP13 has been linked with the actin cytoskeleton by gravin (72) and a close relative SSeCKs (Src-suppressed C-kinase substrate) (73), as well as WASp and verprolin homology protein-1 (WAVE1) (74).

Members of the functionally related but structurally diverse AKAP family compartmentalize PKA. AKAP typically compartmentalizes RII to various subcellular regions of structures and has been used as an valuable tool for measuring the impact of cAMP/PKA signaling (70, 75). Also, AKAPs direct the assembly of multi-enzyme complexes that are capable of integrating multiple input signals to control phosphorylation of a target with great specificity (75). PKA has positive and negative effects on cytoskeletal organization. These effects are not due to a cAMP/PKA blanket effect but rather to a balance of cAMP/PKA in space and time that is crucial for its effects on the cytoskeleton and cell migration (66, 70).

Actin Structure and Function

The actin cytoskeleton is a dynamic structure that plays an important role in many ongoing processes like immune response, homeostasis and blood vessel preservation. Actin is a globular 42-kDa protein with an ATP binding site in the center of the molecule. Monomeric actin, termed "G-actin" will dimerize or form a trimer, which serves as a site for nucleation and further growth of the actin filament. ATP is hydrolyzed immediately after the molecule is incorporated into an actin filament. The ADP is trapped in the actin filament until it depolymerizes, then an exchange can occur. G-actin forms F-actin efficiently (the filament) in the presence of ATP, Mg+ and K+. Actin behaves like other polymers, above critical concentration of G-actin the molecules will polymerize into filaments. Below the critical concentration, actin filaments will depolymerize. Actin filaments are polar structures that have two distinct ends: the plus end (barbed end) and the minus end (pointed end) (76). Monomers can add or leave the barbed end at much faster rates then the pointed end of the filament (77).

Actin polymerization has three distinct stages: nucleation, elongation and steady state. The nucleation stage is the rate-limiting step in actin assembly and requires the binding of three actin monomers to initiate actin assembly. The elongation phase is the period of rapid addition of monomers to the filaments. The steady state phase occurs when the addition of actin monomers onto filaments is equal to the disassembly of monomers from the filament. The concentration of monomers left in solution at steady state is called the critical concentration (Figure 1-4) (76).

Actin Binding Proteins

There are several classes of actin-binding proteins that are required to control actin assembly. Thymosinβ4 is a small protein which binds actin monomers and inhibits

the association of actin with either the plus or minus end of the actin filament and prevents exchange of the bound nucleotides (78). Recruitment of actin monomers depends on another monomer-binding protein called profilin. Profilin binds to the face of the actin monomer opposite the ATP-binding cleft, blocking the side of the monomer that associates with the minus end of the filament. The profilin-actin complex can readily access the free plus end, which causes a change in conformation that reduces actin's affinity for profilin, subsequently profilin falls off leaving the actin filament one subunit longer. Profilin's ability to move sequestered actin subunits onto the growing end of the filament is critical for filament assembly at the plasma membrane. Besides binding to actin and phospholipids, profilin binds to various other intracellular proteins that help to localize profilin to sites of rapid actin assembly (79, 80).

Capping proteins, such as CapZ and CapG, bind filament ends and prevent further polymerization (81). Once the actin filament is capped it cannot continue to grow nor can it be disassembled. CapG is sensitive to both calcium levels in the cell and PI(4,5)P2 (81).

Actin severing and cross-linking proteins, such as gelsolin and ADF-cofilin, bind sides of filaments and then sever the filaments (82, 83). These actin regulatory proteins enhance the depolymerization of filaments. Gelsolin binds pre-existing actin filaments and then severs the filaments. This severing is important for remodeling of the actin cytoskeleton by creating new barbed ends for filament growth (84).

Nucleation is the rate-limiting step in actin assembly and is template-driven by the Arp2/3 complex (85). Arp2/3 binds the pointed ends of actin monomers and nucleates actin assembly. Arp2/3 complex can also bind the sides of actin filaments to create a

'Y' shape that branches at a 67° angle (85). The Arp2/3 complex is activated by small GTPases, Rac, Rho and Cdc42 (86). Rho activation is responsible for formation of stress fibers and focal contacts. Rac activation leads to the formation of lamellipodia while Cdc42 forms filopodia. (Filopodia are long finger-like projections of tightly bundled actin filaments.) Small GTPases bind and activate N-WASP, WASp (87) and ActA components of *Listeria monocytogenes* (88), which then binds to Arp2/3 allowing for the nucleation of actin filaments.

Neutrophil Function

Neutrophils are the most abundant type of white blood cell (WBC) in mammals and form an essential part of the innate immune response. The main physiological activities of neutrophils are adherence and migration, degranulation and release of inflammatory mediators, phagocytosis and apoptosis (89). Neutrophils arise in the bone marrow from myeloid progenitor cells, which differentiate in response to specific growth factors (90). Neutrophils enter into circulation in an immature band state. Unlike mature neutrophils, band cells possess few cytoplasmic granules and lack the segmented nucleus characteristic of a mature neutrophil. Mature neutrophils synthesize minimal amounts of protein. Instead, much of what the neutrophil requires for its response is found pre-packaged in the cells' cytoplasmic granules and thus is immediately available for cellular functions (90, 91).

After release into the blood, the life span of the neutrophil is limited to five-six hours (92). During a disease process, functionally mature neutrophils are released from the bone marrow, due to mature neutrophils exploiting functional attributes. The level of circulating neutrophils remains fairly constant in healthy adults, although the levels will

quickly rise during infection. Neutrophils are extremely active and maintain blood levels of 10,000 cells/ml in a healthy adult (91).

Neutrophils respond to factors secreted by bacteria during the host response, as well as to factors generated during activation of the coagulation cascade, including bioactive lipids released by platelets during clotting. The cell also responds vigorously to host-derived substances, which accumulate at sites of previously damaged tissues (93). Microbial factors that initiate the neutrophil to respond are secreted by the invading pathogen or activate chemokines and cytokines of the host's innate immune response, which activates the host's complement system resulting in the generation of potent neutrophil agonists like C5a. Neutrophils are also able to respond to the synthetic tripeptide, formylated methionyl-leucyl-phenylanine (FMLP), which is derived from bacteria, in much the same way it responds to microbial pathogens. In addition, cytokines such as tumor necrosis factor (TNF) and IL-8 (94), as well as many growth factors, including granulocyte macrophage colony-stimulating factor (GM-CSF) (91, 95, 96) help to fine-tune the neutrophil signaling pathway resulting in enhanced neutrophil response.

The mammalian TLR family is known to consist of thirteen members and play a crucial role in innate immunity. As microbe-recognition receptors, TLRs mediate cellular responses to a large array of microbial ligands, including LPS, proteins and nucleic acids. Activation of different TLRs leads to various downstream responses that help tailor the immune response to be effective against specific pathogens (97). Human neutrophils express all currently known TLRs. TLR stimulation on neutrophils can result

in the shedding of L-selectin, reduction in chemotaxis, increased phagocytosis, priming of superoxide, and the production of a number of chemokines and cytokines (91).

Chemokines are leukocyte attractants divided into two major groups based upon the positions of the first two cysteine residues in their primary sequence the “C-X-C” and the “C-C” (93). RANTES (acronym for regulated upon activation of normal T cell expressed and secreted), macrophage inflammatory protein-1α (MIP-1α), MIP-1β and MIP-1γ are members of the CC chemokine subfamily produced by neutrophils. By contrast, the CXC subfamily exerts effects towards neutrophils (91). Cytokines and chemokines can be produce by neutrophils in three ways. Cytokines are stored in granules until stimulated by inflammatory mediators like IL-8 causing the neutrophil to degranulate and release cytokines (98). Neutrophils also have the ability to cleave surface-bound inactive cytokines from their plasma membrane (99). Human neutrophils have the capacity to produce a number of CXC chemokines, including IL-8, growth-regulated oncogene alpha (GROα), IFN-γ, and cytokine induced neutrophil chemoattractant (CINC) (91). However, when compared to macrophages, neutrophils are responsible for less than 2% of the total cytokine array (100).

The containment and killing of bacteria are the major functions of neutrophils in host defense. After penetrating the body, factors released by the pathogen activate complement or other inflammatory cells, which attract neutrophils to the site of invasion. After the pathogen attaches to the neutrophil surface receptor, they are rapidly sequestered into phagolysosomes and then killed through the release of granules and from the production of oxygen radicals. Neutrophils undergo degranulation to release proteases and reactive oxygen species into the surrounding tissue to kill invading

pathogens. Neutrophil possess at least three types of granules: primary granules containing the enzyme myeloperoxidase, secondary granules containing hydrolytic enzymes and other antibacterial components, and less dense tertiary granules which fuse with the plasma membrane and alter the cytoskeletal architecture and location of the oxidative generating NADPH oxidase by translocating components to the plasma membrane (101). It is important that once the infection is cleared that neutrophils are removed, and there is a fine line that separates beneficial from detrimental tissue damage or inflammation. The primary role of the neutrophil is to phagocytose and kill the pathogen that has invaded the host, limiting the infection. To accomplish this task the neutrophil has the ability to undergo dynamic actin remodeling to allow for chemotaxis to the site of infection (102).

Neutrophils are among the first cells to arrive at the site of infection and are important contributors to the acute inflammatory response (103, 104). The neutrophil can sense as small as a 5-10% difference in the concentration of a chemoattractant. As the neutrophil rolls along the blood-vessel wall, the L-selectin on its surface binds to carbohydrate structures, such as sialyl-Lewisχ, found on the adhesion molecules of the vascular endothelium, and rolling is eventually halted. As the neutrophil becomes activated, it replaces L-selectin with other cell-surface adhesion molecules, such as integrins; these molecules bind E-selectin, expressed on the surface of the vascular endothelium in response to inflammatory mediators such as bacterial lipopolysaccharides (LPS) and the cytokines IL-1 and TNFα. The activated neutrophil then enters the tissues through diapedisis, where it is attracted to the infection site by a

number of chemoattractants. The neutrophil can then phagocytose and kill the pathogen (Figure 1-5) (105).

Our lab has previously shown that both LT and ET impair the ability of neutrophils to assemble and disassemble actin filaments (39, 106). Unstimulated neutrophils contain 60-70% of total actin in monomeric form (~200 μM) (107). It is therefore important for the cell to synthesize proteins that directly regulate actin monomer function. Neutrophils are the first line of defense during bacterial infections and are able to quickly crawl, or chemotax, to the site of infection, and defects in the ability of PMNs to chemotax severely compromises the innate immune response (108, 109). Neutrophils migrate by membrane protrusions at the leading edge of the cell, which are formed by the assembly of branched actin filaments and the continued polymerization of actin allows for the physical movement of the cell (110). The mechanism(s) coordinating these events are poorly understood, however, it is well known that cAMP, via activation of PKA, can inhibit neutrophil migration (111-113).

Neutrophil Chemotaxis

Cell motility is a fundamental cellular process that is essential to many biological processes such as embryonic development, immune system function and wound healing (63). For cells to move they must be able to sustain shape and interact with the surrounding environment. As a cell moves on a substrate (the extracellular matrix if the cell moves inside an organism or a cover slide if it moves outside an organism), it experiences external forces, which include the viscous force or resistance from the surrounding medium and cell-substrate interaction forces, and internal forces that are generated by the cytoskeleton. In most animal cells, the cytoskeleton is the essential

component in creating these motility-driving forces. All spatial and mechanical functions are performed by a system of filaments called the cytoskeleton, particularly the protein actin. The cytoskeleton provides support to the cell but must also undergo dynamic remodeling to facilitate cell movement (114).

The neutrophil actin cytoskeleton is a highly dynamic structure that rapidly adapts to the cell's demands in order to successfully utilize two of its most important features: motility and phagocytosis. Directional F-actin polymerization in the lamellipodia of a migrating human neutrophil is signaled by GPCRs. It is known that the ligation of chemoattractant receptors triggers the release of G-$\beta\gamma$ (115). Downstream from the GPCRs, is phosphatidylinositol 3-kinase-γ (PI3K), which regulates F-actin polymerization (116). Activation the Rho family GTPases has also been shown to be instrumental in orchestrating membrane protrusion and retraction in neutrophils (115). The Rho family GTPases have been shown to activate the nucleation promoting factor WAVE/Scar, one activator of the actin-related protein 2/3 (Arp2/3), and to promote the formation of free barbed ends (117) that in turn initiates cytoskeletal actin polymerization in the lamellipodia (118). The most prominent Rho GTPases in neutrophils are of the Rac subfamily, Cdc42 and Rac (119), which are capable of promoting actin polymerization. After chemoattractant GPCR stimulation, G-α activation leads to the accumulation of lipid products of PI3K, such as phosphatidlyinositol-3,4,5-triphosphate (PIP3), at the leading edge and the activation of Cdc42 and Rac, which promotes actin polymerization (120, 121). The small GTPases are thought to activate N-WASP (Wiscott-Aldrich syndrome protein), which results in Arp2/3 activation (122, 123). Arp2/3 nucleates new actin assembly (Figure 1-6). Unfortunately, most reviews

on neutrophil actin-based motility focus on G-proteins and phosphoinositides as key signaling molecules in actin assembly and do not review other potentially important molecules.

Listeria monocytogenes

L. monocytogenes is used extensively as a model system to identify key proteins involved in cell motility. *L. monocytogenes* is a Gram-positive intracellular bacterium that invades mammalian epithelial cells and propagates in the intestinal, feto-placental and blood brain barriers (124). *Listeria* is an intracellular pathogen, thus it avoids host defenses, immune response, and complex signaling (125). During intracellular growth, *Listeria* polymerizes the host actin at one pole of the bacteria, allowing the bacteria to move through the cytoplasm via actin-based motility (126). When *Listeria* encounters the plasma membrane it forms a membrane protrusion (filopodia) from the infected cell into an adjacent cell leading to the formation of a double membrane vacuole in the uninfected cell (127). Bacteria escape the double membrane vacuole and resume intracytosolic growth within the newly infected cell (128).

Listeria actin-based motility relies on ActA (126), a bacterial factor that mimics the nucleation promoting activity of WASp/WAVE family members (129), and by recruiting the Arp2/3 complex to the surface of the bacteria (130). WASp is activated by small GTPases Rac and Cdc42 (131).

Listeria uses internalin A (InlA), a cell wall covalently anchored protein, to bind to the cellular adhesion molecule E-cadherin and induce bacterial entry into polarized epithelial cells (132). *Listeria* also utilizes internalin B (InlB), which interacts with gC1qR and hepatocyte growth factor receptor Met to allow for entry into the polarized epithelial cell (133). *Listeria* hijacks the molecular machinery associated with the tail portion of E-

cadherin (132). α- and β-catenins are required to link the adherence junction (E-cadherin) to the underlying actin cytoskeleton (134). *Listeria* recruits these catenins to the entry site for actin remodeling to allow the bacterium to enter into the cell. After internalization, *Listeria* lyse the membrane compartment through bacteria phospholipases A and B as well as listerolysin O (LLO) (135). In the host cytoplasm, bacteria begin to multiply and use the cellular actin machinery of the host. Bacteria are initially coated with an actin cloud, consisting of new actin filaments that will rearrange themselves to form a comet shaped tail at the bacterial pole (136). Nucleation and elongation of actin filaments will provide the necessary propulsion to force the bacteria through the cell cytoplasm (137).

The characteristic actin rocket tail at one pole of the bacteria is formed by actin polymerization, which is initiated by a protein complex containing asymmetrical distributed bacterial surface protein ActA and several host proteins like VASP and Arp2/3 complex. ActA is necessary for *Listeria* motility(130).

The central region of ActA has four proline rich repeats of FPPPP or FPPPIP motifs (138, 139). These proline rich areas mimic the host cytoskeleton proteins vinculin and zyxin, which are associated with focal adhesions and stress fibers (138). The proline rich sequence in these proteins and ActA bind Ena/VASP family of proteins (139). Ena/VASP proteins localize to actin stress fibers, filopodia tips, the leading edge of cells, and are implicated in the actin-based processes of cell migration and axonal guidance (140). Ena/VASP is recruited to *Listeria* actin comet tails and increases bacterial speed and directional persistence (141, 142).

In extracts, *Listeria* actin-based motility requires very few host proteins to generate movement. Arp2/3 is required to nucleate actin assembly, while actin-depolymerizing factor (ADF) helps recycle monomers from filaments, and CapZ blocks the barbed ends of filaments (125). *Listeria* motility is enhanced by actin regulatory proteins, such as profilin, VASP and the actin bundling protein α-actinin (141).

VASP

Ena/VASP proteins are a structurally conserved family found in vertebrates, invertebrates and *Dictyostelium discoideum* cells (143). VASP was originally discovered and initially characterized as a substrate for cAMP and cGMP dependent protein kinases in human platelets (144-146). VASP is found not only in platelets, but also in many other cell types, including: leukocytes, T cells, smooth muscle, fibroblasts and cardiomyocytes (144, 147-149). Evidence for the role of Ena/VASP proteins in motility comes from the analysis of VASP deletion/overexpression on the motile behavior of living cells (140, 143, 150) and on actin-based motility of *Listeria* (151-153).

VASP is a 46-kDa membrane associated protein that is a member of the Enabled (Ena) family of proteins (111, 154). Two other mammalian family members, Mena (mammalian enabled) and EVL (Ena-VASP like), were identified by sequence similarity (155). VASP has a tripartite domain containing an N-terminal Ena/VASP homology 1 (EVH1) domain, a central proline-rich domain (PRR), and an EVH2 domain at the C-terminus (Figure 1-8) (156, 157). The EVH1 domain aids in the binding of Ena/VASP to proline rich ligands like vinculin and zyxin (158). The PRR domain contains binding sites for the actin-monomer binding protein profilin (159), Src homology 3 (SH3) and WW domain containing proteins (160), suggesting that VASP is a key element in

cytoskeletal reorganization. The EVH2 domain contains F- and G-actin binding sites and a coiled-coiled motif important for tetramerization (161).

VASP promotes actin filament elongation by delivering profilin G-actin complexes to the barbed end of a growing filament. VASP harbors three serine/threonine phosphorylation sites. Serine 157 (S157) is located N-terminally of the central PRR. Serine 239 (S239) and threonine 278 (T278) are within the EVH2 domain, adjacent to the G- and F-actin binding sites (156). The equivalents of VASP S157 and S239, but not T278, are found in Mena, whereas S157 is the only site found in EVL (Figure 1-8) (155). *In vivo*, S157 is preferentially phosphorylated by PKA whereas S239 and T278 are targeted by cGMP-dependent protein kinase (PKG) or AMP-activated protein kinase (AMPK) (162). Phosphorylation of VASP at S157 is thought to regulate its affinity for F-actin (163, 164) and play an important role in F-actin assembly at the lamellipodia, filopodia and focal adhesions (165). Phosphorylation affects the interaction of VASP with actin; however, the crucial phosphorylation site(s) involved remain unclear.

Several key factors support Ena/VASP proteins as important regulators in the actin cytoskeleton. They associate with the surface of motile *Listeria* in an asymmetric manner (155) and are necessary for efficient *Listeria* motility (139, 141, 151, 152). Ena/VASP proteins localize to areas of actin remodeling such as the front of spreading lamellipodia in motile cells (166), tips of growth cone filopodia, focal adhesions and cell junctions (155, 166-168). Despite the relevance of Ena/VASP proteins to dynamic actin-based processes their exact molecular functions remain elusive.

Filopodia

Two alternative forms of actin machinery coexist at the leading edge of most motile cells: lamellipodia which seem to be designed for persistent protrusion over a

surface, and filopodia which appear to perform sensory and exploratory functions to steer cells depending on cues from the environment (169). Lamellipodia have been investigated since the 1970's, however, filopodia have only recently emerged as important structures in wound healing, immune cell function and cell invasion (170).

Actin based filopodia protrusions, first described by Porter, Claude and Fullam as early as 1945 (171), are composed of tightly bundled parallel filaments 5-50 μm long and 0.1-0.5 μm thick (172). Despite the importance of filopodia in wound healing, metastasis, neuronal growth cone formation and embryonic development, the exact mechanism governing their initiation and formation has yet to be fully elucidated (173-176). Generally, filopodia are described as "antennae' or 'tentacles' that cells use to probe their microenvironment, serving as pioneers during protrusion. However, the roles of filopodia seem diverse and, in many cases, remain vague.

Small GTPases of the Rho superfamily are linked to the regulation of cell morphology and the actin cytoskeleton. The best-studied mammalian Rho GTPases are Rac1, Cdc42 and RhoA. RhoA is implicated in the formation of stress fibers and focal adhesions, while Rac1 promotes lamellipodium formation, and Cdc42 functions in the formation of filopodia (177). A large number of proteins that regulate the actin cytoskeleton have been shown to localize to filopodia and/or to regulate filopodia formation. Although many of these proteins are specific to only certain cell types, key sets of proteins seem to contribute to the generation of filopodia in diverse cell types and organisms (Table 1-1).

There are several model systems for filopodia formation; however, each model has a tip complex of proteins thought to mediate: lateral interactions between barbed

ends, bundling, and filopod extensions (178). It is important to note that some controversy still exists concerning the activities of individual proteins, and is likely that the relative importance of each in filopodia varies depending on the organism and cell type. A subset of uncapped actin filaments of the Arp2/3 network are targeted for continued elongation by formins and/or by ENA/VASP proteins (179). The barbed ends of these elongating actin filaments converge together through the motor activity of myosin-X, leading to the initiation of filopodia (180). The forces resulting from polymerization of tightly packed filaments are thought to result in the extension of the plasma membrane, and insulin-receptors substrate p53 (IRSp53) or inverse (I)-BAR-domain containing proteins might further facilitate plasma membrane protrusion by directly deforming the membrane. Alternatively, IRSp53 might sense the negative membrane curvature that is induced by pushing forces of elongation filaments and recruit other components to the site of filopodia initiation (181). Ena/VASP proteins can also function as initial F-actin cross-linking proteins in the tip of the elongating filopodia. The incorporation of the actin cross-linking protein fascin in the shaft of the filopodia generates a stiff actin filament bundle (182). However, the exact role of Ena/VASP during filopodia initiation and elongation still needs to be characterized along with understanding the function of myosin-X and its cargo-binding domain in the tips of filopodia (180). A full understanding will only come with a complete inventory of all the proteins and their specific functions within the dynamics of filopodia initiation and elongation (178).

ET Inhibits Neutrophil Motility by VASP Phosphorylation of S157

The downstream effects of ET activity have not been extensively studied, and it is only recently that we have begun to understand how ET impairs the host's innate

immune response. Other agents that elevate cAMP within the neutrophil result in the inhibition of a number of functions such as: phagocytosis, migration, spreading, oxidative burst and bacterial killing (183).

VASP localizes to regions of dynamic actin remodeling and promotes filament formation (155, 166, 184). Phosphorylation affects the interaction of VASP with actin; however, the crucial role of phosphorylation in the regulation of actin filaments remains to be clarified (163, 164, 185). *Listeria* infection of MVd7 cells (lack all members of the VASP protein family) transfected with different VASP constructs, as well as introduction of VASP-TAT recombinant proteins into human neutrophils, point to the actin-regulatory protein VASP as the likely end target of edema toxin and other cyclic AMP-inducing agents that impair actin-based motility. Phosphorylation of VASP serine-157 impairs actin-based motility, and introduction of a VASP pseudo-unphosphorylated construct completely neutralizes the ability of ET and forskolin plus IBMX (adenylate cyclase activating compound and cAMP phosphodiesterase inhibitor) to block actin-based motility. These findings reveal the primary pathway by which ET impairs neutrophil motility, and emphasizes the importance of the cAMP signaling pathway and VASP phosphorylation in the regulation of actin-based motility.

Table 1-1. Key proteins involved in filopodia formation

Protein	**Proposed activities and functions**
Cdc42	Small GTPase that induces filopodia formation
RIF	Small GTPase that promotes the formation of long filopodia through the forming protein Dia2
Arp2/3 Complex	Actin filament nucleator that generates the formation of a branched lamellipodial F-actin network
WASP/WAVE	Proteins that activate the F-actin nucleation activity of the Arp2/3 downstream of Rho family GTPases
Dia2	Protein that induces the formation of unbranched actin filaments in filopodia
Ena/VASP	Factors that promote actin filament elongation, anti-branching and/or bundling to induce filopodia formation
Myosin-X	Motor protein that promotes filopodia formation by converging filament barbed ends together and by transporting proteins to filopodial tips
Fascin	Major F-actin cross-linking protein of filopodia
IRSp53	Scaffolding protein that also deforms membranes to promote the formation of plasma-membrane protrusions
LPR1	Lipid phosphatase-related protein that induces filopodia formation through a currently unidentified mechanism

This table has been modified from Faix et al. (182).

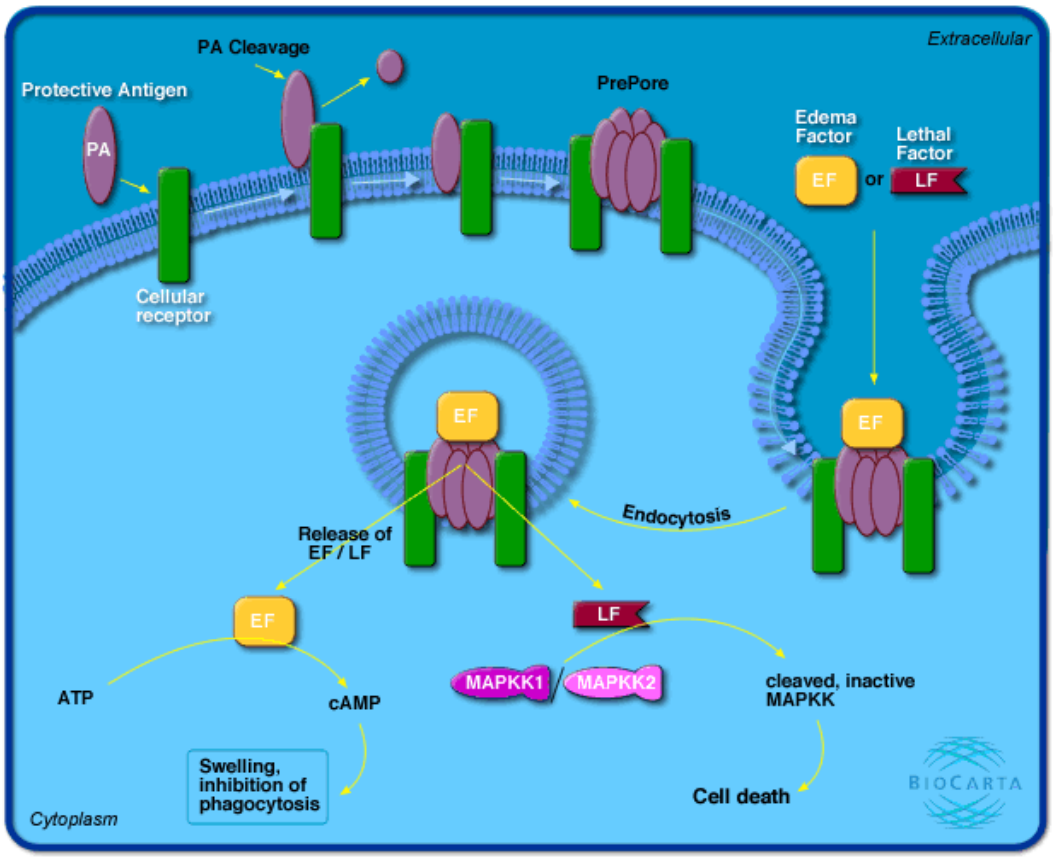

Figure 1-1. Anthrax toxins. The toxins produced by *Bacillus anthracis* are derived from three proteins: edema factor (EF), lethal factor (LF), and protective antigen (PA). The entry of toxin into cells begins with the recognition of cellular receptors in the plasma membrane by PA. Proteolytic cleavage of cell-bound PA creates a smaller fragment that then multimerizes into a pore-like structure in the plasma membrane. The LF and EF proteins bind to the PA pre-pore, followed by internalization of the entire structure through receptor-mediated endocytosis. In the endosomal compartment, the acidic pH causes a conformational change that inserts PA fragments and releases LF and EF into the cytoplasm. In the cytoplasm, LF acts as a protease that cleaves MAP kinase, inhibiting pathways that rely on this kinase family and causing cell death. EF is an adenylate cyclase that inhibits the immune response and increases swelling and edema due to increased cAMP levels (186). Reproduced with permission of BioCarta and author Glenn Croston.

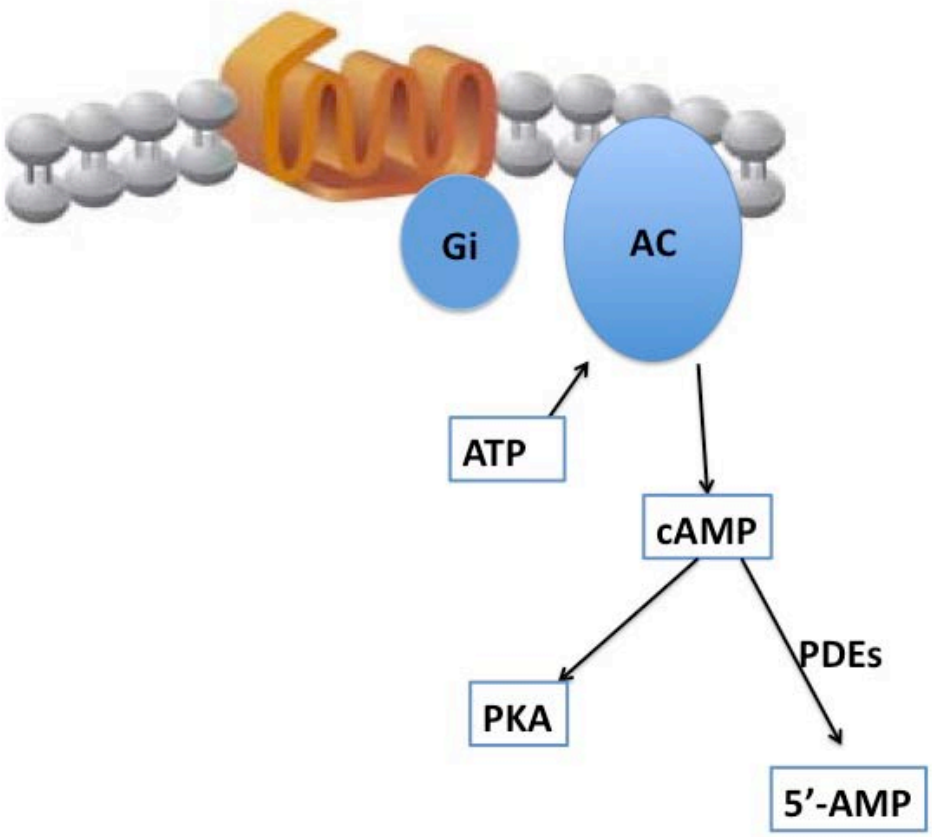

Figure 1-2. cAMP signaling pathway. An amine receptor is activated by binding to a specific ligand. The ligand-bound receptor then activates a stimulatory G protein (Gs), which leads to an increase in the enzymatic activity of adenylate cyclase (AC). Adenylate cyclase catalyzes the conversion of ATP to cAMP. As the intracellular concentration of cAMP increases, cAMP-dependent PKA is activated and phosphorylates different target proteins on serine and threonine residues. Phosphodiesterases (PDEs) break down cAMP into 5'-AMP (63).

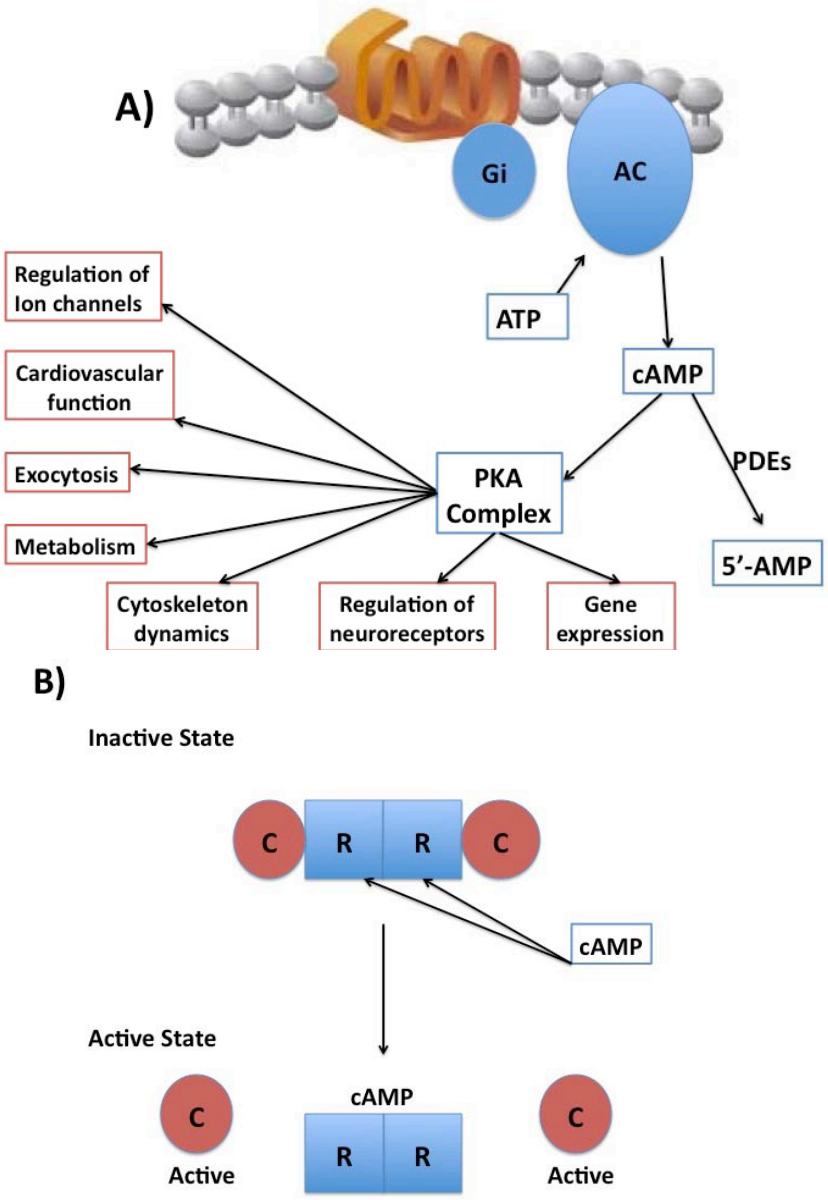

Figure 1-3. PKA signaling pathway. A) PKA signaling is a widely used intracellular pathway and is the major route for channeling the second messenger cAMP signal. cAMP binding to the PKA complex leads to dissociation of the catalytic subunits from the holoenzyme. PKA cross-talks or integrates with other signaling pathways. The PKA signaling pathway has been implicated in many cellular and physiological processes, from metabolism and reproduction, to cardiac function, memory and learning. B) Each regulatory subunit has two distinct sites for binding cAMP (called A and B), located in different domains. cAMP binding to B induces conformational change, unmasking A allowing for cAMP to bind to A releasing the catalytic subunit (63).

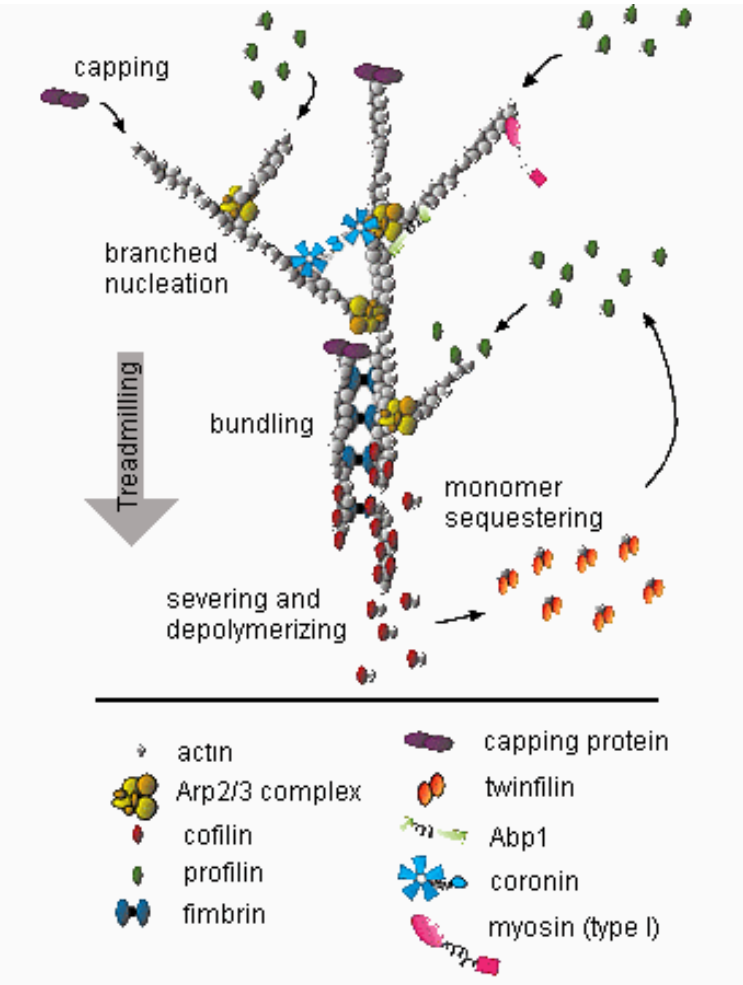

Figure 1-4. Actin structure. All of the diverse actin structures found in cells are assembled from the same basic building blocks (globular actin monomers) into filaments, which are then organized by actin-associated proteins into specialized arrays with distinct architectures and dynamic properties. Reproduced with permission of Dr. Bruce Goode from his website: bio.brandeis.edu.

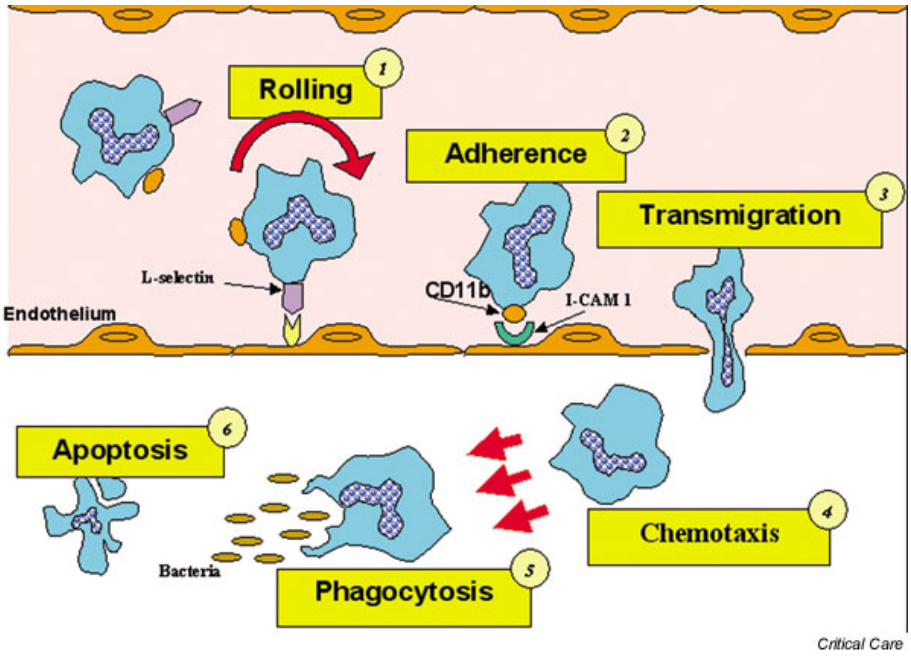

Figure 1-5. Neutrophil function. Neutrophil delivery in the postcapillary venule. ICAM, intercellular adhesion molecule. 1) Neutrophils are found rolling through the vascular endothelium; 2) neutrophils begin to slow down by the use of L-selectin; 3) neutrophils adhere to the endothelium; 4) neutrophils diapedisis through the vascular endothelium; 5) neutrophils chemotax to the site of infection; and 6) neutrophils undergo phagocytosis of the bacteria/pathogen. Reproduced with permission from Critical Care press and authors.

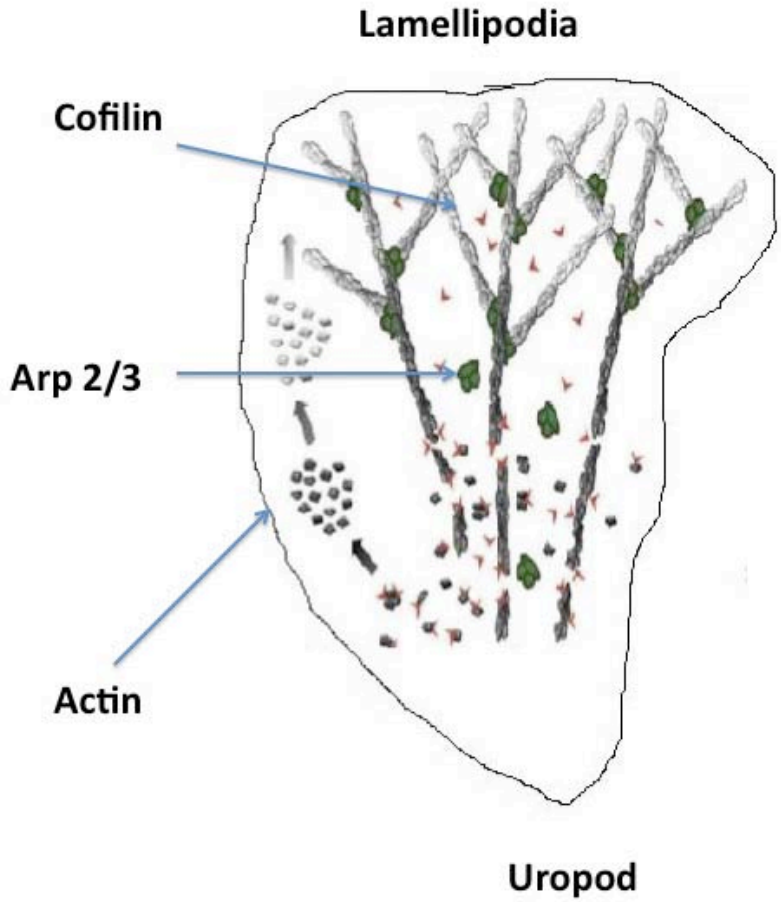

Figure 1-6. Neutrophil actin-based motility. A polarized, migrating neutrophil requires rapid assembly and disassembly of actin filaments, which is controlled by the heterotrimeric GPCR pathway. The G-$\beta\gamma$ subunit activates small GTPases such as Rac, Rho, and Cdc42. The small GTPases are thought to activate N-WASP, which results in Arp2/3 activation. Arp2/3 can nucleate new actin assembly (122, 187).

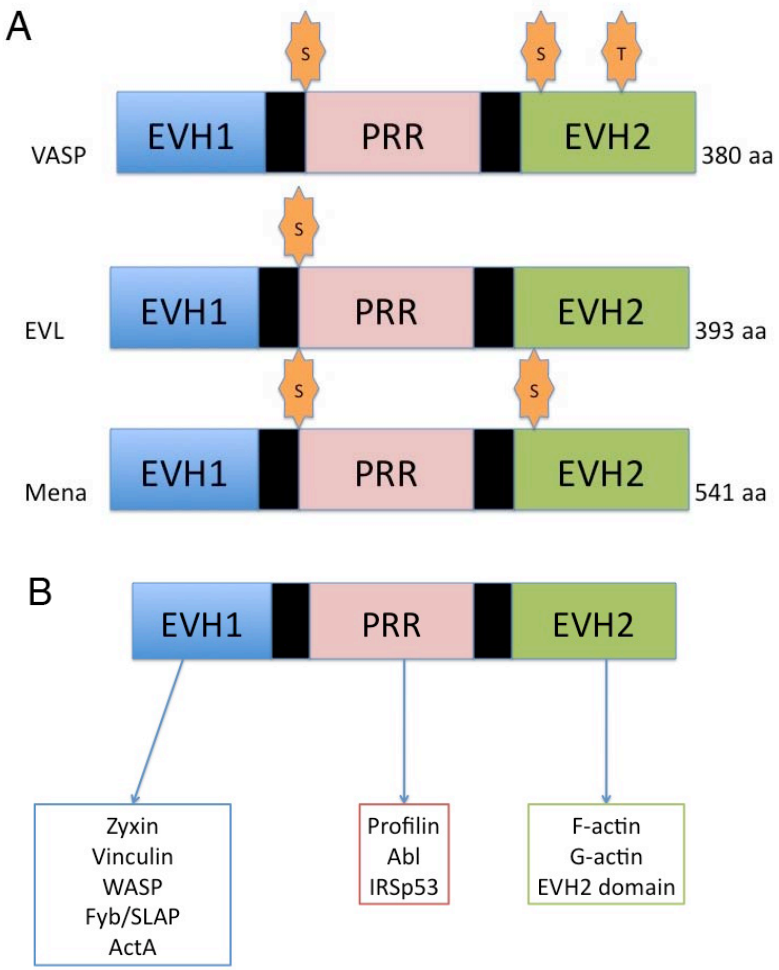

Figure 1-8. VASP structure. (A) Domain organization of Ena/VASP proteins. EVH1: Ena/VASP Homology 1, PRR: proline-rich region, LERER: region harboring LERER repeats, Q-rich: glutamine-rich region, EVH2: Ena/VASP Homology 2. Serine and Threonine phosphorylation sites are indicated as orange stars. (B) Major binding partners for the EVH1, EVH2 and PRR regions of Ena/VASP proteins (157).

CHAPTER 2
LITERATURE REVIEW ON NEUTROPHILS AND ANTHRAX

Anthrax Clinical Data

Inhalation anthrax can lead to sepsis and death within days if not diagnosed early and treated effectively (27). Epidemiological analyses of the anthrax bioterrorist attacks in 2001 indicated a mean duration of 4.5 days between exposure and symptom onset in the 6-inhalation anthrax cases for whom the exposure dates could be determined. Analyses of the clinical findings from 10 of the 11-inhalation anthrax cases revealed normal or minimally elevated peripheral PMN counts at the time of hospital admission, despite high level *B. anthracis* bacteremia (1). Furthermore, heavily infected pleural fluid demonstrated a paucity of white blood cells. In the fatal cases, mediastinal infection was associated with marked edema and hemorrhage, but minimal infiltration by acute inflammatory cells (2). Similarly, experimentally induced inhalation anthrax in monkeys was associated with edema and hemorrhage of the mediastinum and pulmonary interstitium with absent or modest infiltration by neutrophils (188). These findings suggest an impaired delivery of neutrophils to the sites of infection during the early stages of systemic *B. anthracis* infection.

Neutrophils constitute the first line of defense against bacterial infections. These phagocytic cells are able to quickly chemotax to the site of infection, and defects in neutrophil chemotaxis compromise the innate immune response. Chemotaxis is accompanied by shape changes that are mediated by rapid assembly and disassembly of actin filaments (189). Actin polymerization is dependent on elongation of existing filaments catalyzed through uncapping and/or severing of existing filaments and catalysis of their elongation through members of the Ena/VASP and formin family of proteins.

This process of elongation is followed by the appearance of new branches through activation of the Arp2/3 complex. Stimulation of Arp2/3 may be controlled through Rac-dependent activation of the Scar/WAVE and WASp complexes (190). *B. anthracis* acts to limit chemotaxis by targeting any of the aforementioned mechanisms by which the neutrophil creates new actin. There is substantial evidence to support the possibility of a defect in neutrophil chemotaxis as evidenced by the autopsy results and hospital admissions finding from the inhalation anthrax cases during the bioterrorist anthrax scare of 2001 (1).

Previous Studies with ET and Neutrophils

The effects of ET on neutrophil chemotaxis has not been visited in nearly twenty years (191). Little is known about the effects of ET on cell motility. Only recently have investigators been able to express ET in *E. coli* and have shown that this purified recombinant protein has binding affinity and biological activity comparable to those of the purified toxins from *B. anthracis* (192, 193). Twenty years ago the target of ET, an adenylate cyclase, was determined to be increased intracellular cAMP levels (194). A few years later it was determined that both ET and LT increased PMN chemotaxis. However, this previous study was performed without being able to determine the activity of the toxins, and the researchers did not detect a significant increase in intracellular cAMP levels (191). During *et al.* (39) revisited effects of LT on neutrophil chemotaxis and found that purified toxin inhibited neutrophil chemotaxis and this effect required two hours to achieve maximal inhibition. When taken together, the clinical and research data call for a re-evaluation of effects of ET on neutrophils.

Only recently have researchers found that both LT and ET exhibit distinct inhibitory effects on FMLP and C5a receptor-mediated superoxide production (49). Anthrax

toxins are able to effectively suppress human neutrophil-mediated innate immunity by inhibiting their ability to generate superoxides for bacterial killing (49). During cases of anthrax-related meningitis it has been found that ET suppresses the blood brain barrier's recruitment of neutrophils due to a down-regulation in neutrophil chemoattractants IL-8, CXCL-1 and CXCL-2 (195). I have chosen to study the effects of anthrax ET and ET+LT on neutrophils actin-based motility, as well as determine the exact mechanism of ET's action on actin assembly.

CHAPTER 3
MATERIALS AND METHODS

Toxin Purification

Edema factor (EF) was expressed and purified from *E. coli* as previously described (generous gift from Dr. Wei-Jen Tang, University of Chicago) (193). Briefly, for high-level gene expression, pPN-EF was transformed in *E. coli* SG13009 (pREP4) competent cells. Cultures were induced for four hours with IPTG and subsequent analysis confirmed EF was mainly localized to the cytosol. EF was purified from the cytosol with a 50% Ni-nitrilotriacetic acid resin. Affinity chromatography resulted in 456-fold purification of EF. EF was further purified by Sepharose cation-exchange column, concentrated down and stored at -80°C in aliquots (192). Protective antigen (PA) and lethal factor (LF) were purified from *B. anthracis* as previously described (generous gift from Dr. Conrad Quinn, CDC) (196). Briefly, culture media were filtered through a 0.22 μM filter, followed by diethylaminoethyl cellulose (DEAE) anion exchange chromatography. The resulting toxin components were then subjected to gel filtration and hydrophobic interaction fast protein liquid chromatography (FPLC) as previously described. Cultures of 15 liters were found to generally yield 8 mg of PA, 13 mg of LF, and 8 mg of EF with purity assessed by coomassie blue staining to be 90% (196).

Chemicals Used

Positive controls for cAMP are Forskolin (Fsk, Sigma-Aldrich), 3-isobutyl-1-methylaxthine (IBMX, Sigma-Aldrich) and 6-db-cAMP (Biolog, Life Sciences). Three different MEK inhibitors were used: p38 inhibitor is SB203580 (Calbiochem), Erk1/2 inhibitor is PD98059 (Calbiochem), and the JNK inhibitor is SP600125 (Sigma). Antibodies used: anti-MEK antibody (Cell Signaling), P S157 VASP (Cell Signaling) and

anti-VASP (BD Bioscience).

Neutrophil Isolation and Toxin Treatment

Human neutrophils were purified using a Ficoll-Hypaque gradient media (ICN Biomedical, Irvine, CA). The study followed US Department of Health and Human Services guidelines and was approved by the Institutional Review Board at the University of Florida. Healthy volunteer donors (total of 7 subjects) ranged in age from 24-58 years, and included both males and females of Caucasian and Asian descent. Purified neutrophils were resuspended in RPMI with L-glutamine (Mediatech), and adjusted to 1 X 10^6 cells/ml. Neutrophils were treated with varying concentrations of EF + PA, LF + PA or PA + LF + EF for two hours at 37°C while gently rotating the cells to prevent clumping or cell activation. For experiments with ET and LT, a 1:1 mass ratio of PA to EF or LF was used. We found that a weight ratio PA to EF to 2:1 had identical effects to a 1:1 ratio. For experiments combining all three toxins, the PA concentration was increased to 1 µg/ml to assure sufficient binding sites for both EF and LF. For the majority of experiments control cells were incubated with buffer alone. To assure the specificity of our findings for each experimental condition cells were incubated with EF, LF and PA alone. Neutrophils were studied immediately after the two hours of incubation, and experiments were completed within four to five hours of blood drawing.

Cell Culture

HeLa cells were grown in Dulbecco's modified eagles media (DMEM) with 4.5 g/L glucose supplemented with 10% fetal bovine serum (FBS) and 5% penicillin and streptomycin (Cellgro.) Cells were grown to 70-80% confluence. Cells were used at passage 5-20. MVd7 (rat fibroblast cell-line devoid of Ena/Mena/VASP), MVd7 egfp-VASP, and MVd7 egfp VASP S157A stablely transfected cell lines were grown in

Immorto media (DME with 15% FBS, 5% penicillin and streptomycin, 5% L-Glutamine and 50 U/ml of mouse interferon gamma {Gibco}). MVd7 cells were transiently transfected with Lipofectamine 2000 (Invitrogen) and analyzed 24-36 hours later.

Annexin V Staining, Analysis for Necrosis and Nitroblue Tetrazolium Assay

Annexin V staining was performed on neutrophils using the annexin V-Fluos Staining Kit (Roche) combined with propidium iodide to assess necrosis, and 10,000 cells were analyzed by FACS as previously described (39). To further assess necrosis in separate experiments, cells were mixed in a one to one ratio with 0.4% Trypan Blue (Sigma). Samples were then loaded onto a hemacytometer, allowed to sit for two minutes, and the intracellular content of trypan blue was determined by light microscopy. Two hundred cells were analyzed for each condition. The NBT test was performed before and after stimulation with a final concentration of 200 ng/mL of phorbol myristate acetate (Sigma), in accordance with the manufacturer's protocol. One hundred cells were analyzed for each condition.

Neutrophil Chemokinesis, Chemotaxis and Polarity

Neutrophil chemokinesis, chemotaxis and polarization were performed as previously described (39). Briefly, untreated ET, LT and ET+LT treated PMNs ($1X10^5$ cells in 2ml of RPMI) were added to a 35mm glass bottom microwell dish (Matek) coated in 0.1% fibronectin (Sigma). For chemokinesis experiments, 1 µM FMLP (N-formyl-met-leu-phe) was added to each plate five minutes prior to time-lapse phase contrast video imaging. Images were captured at 10s intervals using an inverted Zeiss microscope and a cooled charge-coupled–device camera (model C5985; Hamamatsu). The velocity of PMNs was determined using the Metamorph software track image program (Universal Imaging). The percent of polarized PMNs (a distinct lamellipod and

uropod) was assessed 15 minutes after the addition of FMLP. Chemotaxis toward a gradient was assessed using a FemtoJet needle (0.5um tip, Eppendorf) containing a concentration of 10 μM FMLP. The tip of the needle was placed just inside the visual field, and chemoattractant was infused into buffer solution at a pressure of 15 psi using an Eppendorf micromanipulator. The velocity of movement toward the needle was measured by time-lapse video microscopy at 10s intervals. In addition to anthrax toxins, in selected experiments cells were treated with 10 μM of Forskolin (Sigma-Aldrich) and 100 μM 3-isobutyl-1-methylaxthine (IBMX, Sigma-Aldrich) for 15 minutes at 37°C.

Whole Cell cAMP Levels

cAMP levels in human neutrophils and HeLa cells were determined using an enzyme-linked immunoassay (Amersham Biosciences) as previously described (49). Briefly cAMP levels in human neutrophils were determined using the cAMP Biotrak Enzymeimmunoassay System (Amersham Biosciences). Human neutrophils were suspended at 1 x 10^6 cells/ml in DMEM and were either left untreated or were treated with the indicated amounts of toxins for various time points at 37°C. Positive controls were treated with forskolin (10 μM, final) plus 3-isobutyl-1-methylxanthine (IBMX) (100 μM, final) for 15 min at 37°C. Neutrophils (1 x 10^6) from each group were assayed in duplicate on 96-well tissue culture plates and lysed using the supplied lysis buffer. Supernatants were then collected and cAMP concentrations were determined according to the manufacturer's instructions.

PMN Phalloidin and CD11/CD18 Staining and Fluorescence-Activated Cell Sorting (FACS) Analysis

Phalloidin staining was performed as previously described (39). Briefly, after

incubation for two hours at 37°C with PA + EF (ET), PA + LF (LT) or both toxins (PA + LF + EF) neutrophils were exposed to 1 µM FMLP (Sigma-Aldrich) for 0, 5, 10, 15, 30, 60, and 120 seconds. Cells were fixed at these time points with a final concentration of 3.7% formaldehyde followed by permeabilization with 0.2% Triton and staining with Alexa 488 phalloidin stain for 30 minutes (Invitrogen-Molecular Probes). In separate experiments, live PMN were stained using CD11/CD18 primary antibody (Abcam) at 2.5 µg/ml followed by secondary antibody mouse IgG H&L conjugated with HRP at a 1:100 dilution in PBS (Invitrogen). Immediately following staining, cells were subjected to FACS analysis.

Measurement of Phosphorylated PKA

PKA phosphorylation was determined using the PKA Assay Kit (Upstate Cell Signaling Solutions) with [γ-32,P] ATP (PerkinElmer.) Neutrophils were treated with 500 ng/ml of ET and incubated at 37°C for 2h or treated with the positive control, 6-db-cAMP, at 100 µM for 1h (Biolog, Life Science Institute.) Cells were lysed using non-denaturing lysis buffer (1% Triton X-100, 50 mM TrisCl, 150 mM KCl, 50 mM EDTA, 0.2% NaA2, 200 mM imidazole, 100 mM NaFl, 100 mM Na3VO4) containing a complete mini protease inhibitor cocktail tablet (Roche). As previously described (197), phosphorylation of PKA was determined using 25 µg of radiolabeled protein lysate by measuring the transfer of radioactive phosphate from ATP into Kemptide.

***Listeria monocytogenes* and *Shigella flexerni* Infection and Phalloidin Staining**

Listeria monocytogenes infection and phalloidin staining were performed as previously described (88). *Listeria* motility and tail lengths were determined four to six hours after the initiation of *Listeria* infection, as previously described (198). *Listeria*

infections were allowed to proceed for 2 hours before the addition of various concentrations of ET or LT from 50ng/ml to 500ng/ml or Fsk/IBMX (10 μM/100 μM). *Listeria* 10403S (1 X 10^6 cells/ml) were used to infect 1 X 10^5 HeLa cells, followed by the addition of 50 μg/ml gentamicin sulfate 60 min after infection to prevent extracellular growth. *Listeria* motility was observed three to four hours after infection by using phase microscopy as described above. Velocity measurements were determined using the Axiovert imaging software. *Shigella flexerni* infection was performed as previously described (199), and velocities were determined two and a half hours after infection. Briefly, Shigella (1 X 10^6) were used to infect 1 X 10^5 HeLa cells, followed by the addition of 50 μg/ml gentamicin sulfate 60 min after infection to prevent extracellular growth. *Shigella* motility was observed 1.5 to two hours after infection using phase microscopy as described above. Velocity measurements were determined using the Axiovert imaging software.

Neutrophils were fixed in 3.7% formaldehyde, permeabilized with 0.4% Triton, and incubated with Rhodamine-Phalloidin (Molecular Probes-Invitrogen). After treatment with anti-fading agent Fluoromont-G (Southern Biotech), the signal was visualized by Zeiss Confocal imaging system with a 63X oil-immersion lens (Zeiss).

Plasmid and Protein Purification

VASP point mutations were generated by site-directed mutagenesis using the QuikChange Multi Kit (Stratagene). Human VASP in the pEGFP-C1 vector (Clonetech) and primers (see Table 1) were used to exchange S157 and S239 with alanines (S157A, S239A) or acidic amino acids (S157D, S239D). Human VASP in the pQE-30 plasmid (kind gift of Dr. Dorothy Schafer, Associate Professor of Biology at the

University of Virginia) and primers (see Table 1) was used to exchange S157 and S239 for alanines and acidic amino acids. All constructs were verified by sequence analysis. VASP protein was purified as previously described (200).

VASP isoforms were transformed in BL21DE3 (Stratagene) cells. Cultures were grown at 37°C until OD600 was between 0.5-0.8, then induced with 0.1 nM of isopropryl-β-d-thiogalactopyranoside (IPTG) for five hours, followed by centrifugation at 5,000 G x 15 min at 4°C. Bacterial pellets were resuspended in cold PBS with protease inhibitors (Roche), 2 µl DNase and 2 mM β-ME and sonicated. Cell lysates were centrifuged at 17000 rpm for one hour at 4°C and the His-tagged constructs purified using a cobalt column using standard methods. Purity was assessed by commassie blue stained SDS-PAGE gels. Protein concentrations were determined using the Bradford Assay (Thermo-Scientific).

Cloning and Expression of TAT-VASP Isoforms

High-fidelity DNA Polymerase-Based PCR of the pEGFP-C1 VASP, pEGFP-C1 VASP S157A and pEGFP-C1 VASP S157D was used to amplify the various VASP isoforms using the primers listed in Table 1. The pTAT vector (generous gift of Dr. Steven Dowdy, Washington University, St. Louis, MO) has an N-terminal His6 leader followed by the 11 amino acid TAT protein transduction domain and a polylinker. The different products were cloned into the KpnI/SphI sites on the pTAT vector. The resulting constructs were confirmed by sequence analysis.

The pTAT-VASP isoforms were transformed in BL21DE3 (Stratagene), followed by induction with 500µM IPTG. After five hours of induction at 37°C, cells were harvested by centrifugation (5,000 X G for 15 min at 4°C). The pellet was resuspended

in ice-cold Buffer A (20 mM Tris, pH 7.5, 600 mM NaCl, 20 mM imidazole, 100 µg/ml of lysozyme and protease inhibitors {Roche}) followed by sonication and centrifugation (40,000 X g for 30 min at 4°C). Cell lysate was applied to a pre-equilibrated cobalt column followed by washes with Buffer A and elution in 40 ml of Buffer B (20 mM Tris, pH 7.5, 1 M NaCl and 250 mM Imidazole) and collected in 3-5 ml fractions. A 4-20% Tris SDS-PAGE gel was run on the fractions and samples were concentrated. S200 size exchange column was run using Buffer F (10 mM Na, K-PO4, pH 6.8 {Fisher-Scientific}, 600 mM NaCl, 5% glycerol, 1 mM β-mercaptoethanol) and collected in 3 ml fractions. A 4-20% Tris SDS-PAGE gel was run and fractions were concentrated down. The Bradford assay (Thermo-Scientific) was used to determine the protein concentration and 1 mg/mL of bovine serum albumin was added prior to storage of samples at -80°C.

PMN Isolation and Treatment with pTAT:

Human neutrophils were purified using a Ficoll-Hypaque Gradient as previously described (39). The study followed US Department of Health and Human Services guidelines and was approved by the Institutional Review Board at the University of Florida. Purified neutrophils were resuspended in RPMI with L-glutamine (Mediatech), and adjusted for 1 X 10^6 cells/ml. TAT fusion proteins were added to the final concentration of 5.2 ng/ml and placed at 37°C for 30 min while gently rotating the cells. Neutrophils were centrifuged at 1500 rpm for 5 min and extensively washed. Neutrophils were subsequently treated with 500 ng/ml of ET for two hours at 37°C while gently rotating the cells to prevent clumping or cell activation. Control cells were incubated with buffer alone. Neutrophils were studied immediately after the two hours

of incubation and experiments were completed within four to five hours of blood drawing. To determine the efficiency of protein delivery, neutrophils with TAT fusion protein were analyzed by immunoblotting.

To assess actin filament localization, neutrophils were fixed in 3.7% formaldehyde and permeabilized with 0.4% Triton and incubated with Rhodamine-Phalloidin (Molecular Probes-Invitrogen). After treatment with anti-fading agent Fluoromont-G (Southern Biotech), the signal was visualized by Zeiss Confocal imaging system with a 63X oil-immersion lens (Zeiss). Cell images were processed with Adobe Photoshop Software.

Quantitative Western Blots

Cells were lysed in non-denaturing lysis buffer (1% Triton X-100, 50 mM Tris Cl ph 7.4, 150 mM KCl, 50 mM EDTA and 0.02% NaA_2) with PhosSTOP phosphatase Inhibitors (Roche) and EDTA free protease tablets were added (Roche). BCA assay (Pierce) was performed to determine protein concentration. Neutrophils were lysed in 2X SDS sample buffer. Samples were sonicated, iced and centrifuged to remove cellular debris. Fifty micrograms of lysate was separated by 12.5% SDS-PAGE, transferred to Polyvinylidene fluoride (PVDF) membrane, incubated with anti-VASP (BD Bioscience) at 1:1000 overnight at 4°C, washed in TBS-T and incubated with 1:10,000 goat anti-mouse for one hour at room temperature. The wash was repeated and VASP and phosphorylated VASP at S157 was detected by using the SuperSignal Chemiluminescence detection system (Pierce) and quantitated using a FluorImager and ImageQuant Software (Molecular Dynamics). Phosphorylation of VASP on S157 or pseudophosphorylated mutant S to D 157results in a slowing of electrophoretic mobility

migrating as 50-kD polypeptide; while unphosphorylated and pseudounphosphorylated VASP migrate as 46-kD polypeptide (111, 144, 145).

Low Speed Actin Bundling Assay

G-actin was first polymerized at room temperature in 1X Bundling Buffer (2.5 mM HEPES pH 7.4, 10 mM KCl, 0.2 mM MgCl2, 0.2 mM EGTA) for 30 min. F-actin was incubated with 1 µM of bundling protein in 1X Bundling Buffer for one hour. The samples were centrifuged at low speed (10,000 X g for 15 min), the supernatant and pellet fractions were separated on 8-16% SDS-PAGE gel, fixed and stained in coomassie blue.

Pull-Down Assay

For his-tag pull-down assays, MVd7 -/- cells were grown to confluence and lysed in 40mM Hepes-NaOH, pH 7.4, 150 mM NaCl, 1% NP-40, PhosSTOP phosphatase Inhibitors (Roche) and EDTA free protease tablets were added (Roche), and incubated with 42.5 ng TAT-VASP constructs. Sample analysis was performed at the University of Florida Interdisciplinary Center for Biotechnology Research. Briefly, samples were run on 10% Tris-Glycine SDS gel. Gel plugs were washed, equilibrated, and treated with trypsin, as previously described (201). Generated peptides were analyzed using LC-MS/MS. Three database search engine and quantitative proteomic software; Mascot 2.1, Scaffold 1.6, and ProQuant 1.1.

Statistical Analysis

The Kruskal-Wallis test for multiple comparisons and the Fischer's exact test were used to determine statistical significance. In all experiments except for FACS

analysis, n refers to the number of cells analyzed. Results are the average from three separate experiments unless otherwise noted.

Table 3-1. Primers for the generation of VASP mutations by site-directed mutagenesis

Point Mutation	Primer Sequence
S157A	5'-C ATA GAG CGC CGG GTC **GCC** AAT GCA GGA GGC-3'
S157D	5'-C ATA GAG CGC CGG GTC **GAC** AAT GCA GGA GGC-3'
S239A	5'-AA CTC AGG AAA GTC **GCC** AAG CAG GAG GAG GCC T-3'
S239D	5'-AA CTC AGG AAA GTC **GAC** AAG CAG GAG GAG GCC T-3'

CHAPTER 4
RESULTS

Bacillus anthracis Edema Toxin Impairs Neutrophil Actin-Based Motility

Anthrax ET is Active in Human Neutrophils

To determine if ET entered both human neutrophils and HeLa cells, we performed an ELISA based assay to measure intracellular cAMP levels. Neutrophils and HeLa cells exposed to increasing concentrations of ET (50-1000 ng/ml of a 1:1 weight ratio of EF and PA, see Fig. 4-1A figure legend) for two hours demonstrated a progressive rise in intracellular cAMP, reaching a maximum of > 50 fold above untreated cells, $p<0.0001$ for 300 ng/ml to 1000 ng/ml plus Fsk/IBMX compared with control (Fig. 4-1 A-D). In neutrophils, this marked increase in cAMP was similar in magnitude to that induced by the cAMP agonists Fsk combined with IBMX (Fig. 4-1A). (Fsk resensitizes cell receptors by activating the enzyme adenylyl cyclase and increasing the intracellular levels of cAMP. IBMX is a competitive nonselective phosphodiesterase inhibitor, which raises intracellular cAMP. This makes the combination of Fsk and IBMX an ideal positive control.) In HeLa cells ET caused a greater rise in cAMP levels than these agonists (Fig. 4-1C). These effects were shown to be time dependent in neutrophils and HeLa cells since prolonged exposure was associated with a progressive accumulation of cAMP. (Fig. 4-1B, 4-1D). cAMP levels in neutrophils treated with 500 ng/ml of ET for a minimum of one hour and Fsk/IBMX were considered statistically significant at $p<0.0001$ as compared to control. Similarly the levels of cAMP in HeLa cells treated with 500 ng/ml of ET for a minimum of one hour and Fsk/IBMX were considered statistically significant at $p<0.0001$ compared to control. Exposure of human neutrophils and HeLa cells to PA, EF, or LF alone had no effect on

cAMP levels (data not shown).

Cellular cAMP's main downstream effector protein is PKA (202). For assessment of PKA phosphorylation, cell extracts from untreated neutrophils were compared to extracts from cells treated with 6-db-cAMP (positive control) or treated with 500 ng/ml of ET. ET treatment of neutrophils resulted in a four-fold increase P^{32} incorporation into PKA ($p<0.001$)(Fig. 4-1E). This is the first time that ET-induced P^{32} incorporation in PKA has been demonstrated in neutrophils.

Effects of ET on Apoptosis, Necrosis, and Nitroblue Tetrazolium Reduction

To ensure that the effects of ET on motility were not the result of apoptosis, we compared Annexin V staining in ET-treated cells to those exposed to buffer. Propidium iodide exclusion was also measured to assess necrosis. As observed previously with LT (39), exposure of concentrations up to 500 ng/ml of ET did not significantly increase neutrophil apoptosis and resulted in only low levels of necrosis, as compared to buffer alone (Table 4-1). Similarly, these concentrations of ET minimally affected HeLa cell apoptosis and necrosis (Table 4-1). To further assess cell viability, the ability of control, ET, and ET + LT treated cells to exclude trypan-blue was assessed. Under control conditions 99% of PMNs excluded trypan-blue. After ET treatment (100-500 ng/ml, 1:1 weight ratio), 96-97% of cells excluded trypan-blue, and following ET + LT treatment (50 ng-500 ng/ml of ET and LF combined with 1 µg of PA), 93-94% of cells excluded the dye. To further assure that PMN functions unrelated to actin-based motility remained intact, we compared the ability of control and ET-treated, as well as ET + LT treated PMNs to reduce NBT. The reduction of this dye to a blue precipitate reflects the generation of superoxide. We found a comparable percentage of NBT positive cells in phorbol myristate acetate–stimulated PMN: control, 91%; ET treated 89% (PA 500

ng/ml + EF 500 ng/ml) and ET + LT treated, 91% (PA 1 μg/ml + EF 500 ng/ml + LF 500 ng/ml) (p=1.0, Fisher's exact test.)

PMN Chemokinesis and Chemotaxis

We have previously shown that exposure to LT significantly impairs neutrophil chemotaxis and chemokinesis (39); however, during systemic anthrax infection, neutrophils are exposed to both LT and ET. Therefore, we examined the effects of ET alone, as well as the combination of ET and LT, on human neutrophil motility. The velocity of chemokinesis was significantly reduced by treatment with ET, a reduction in velocity being observed at concentrations of 50 ng/ml at a $p<0.0001$ with maximal reduction in velocity of 40% being observed at 300-500 ng/ml (Fig. 4-2A). Dual treatment with ET and LT had additive inhibitory effects on the velocity of chemokinesis, causing a maximal inhibition of 80% at a concentration of 250 ng/ml for both toxins (Fig. 4-2B). When the concentration of ET combined with LT was raised to 300 ng/ml, neutrophils no longer adhered to the surface; therefore, our chemokinesis and chemotaxis experiments combining both toxins, and the individual concentrations of EF and LF did not exceed 250 ng/ml. ET and LT alone at concentrations up to 1000 ng/ml had no measurable effect on adherence, indicating that these effects required the activities of both toxins (data not shown).

In control neutrophils, exposure to FMLP resulted in a distinct polarized morphology, a high percentage of cells forming broad lamellipodia at the leading edge and small uropodia at the rear (Fig. 4-2C, E). Exposure to ET alone markedly impaired the ability of neutrophils to polarize, maximum inhibition being seen at the same concentrations that maximally slowed chemokinesis, 300-500 ng/ml ($p<0.001$) (Fig. 4-2 E). This difference is highly significant ($p<0.001$) except at 50 ng/ml ($p>0.5$). Exposure

of neutrophils to dual toxin treatment resulted in greater inhibition than either toxin alone, while maximum reductions in the percentage of polarized cells was observed at 250 ng/ml ($p<0.0001$, Fisher's exact test) (Fig. 4-2D and F). ET treatment also reduced the speed of neutrophil directed migration or chemotaxis. Treatment with 300 ng/ml or higher concentration of ET reduced mean chemotactic velocity by 50% ($p<0.0001$) (Fig. 4-2G). Under these same conditions, LT also caused a concentration-dependent reduction in chemotaxis velocity, and a maximum inhibition of nearly 50% was observed at concentrations between 250-500 ng/ml ($p<0.0001$) (Fig. 4-2H). Dual toxin treatment also inhibited chemotaxis, maximal inhibition of 80% being observed at 250 ng/ml of the combination ($p<0.0001$) (Fig. 4-2I). Thus, as observed for chemokinesis and polarity, the combination of LT and ET had additive inhibitory effects on chemotaxis. PA, EF, or LF alone at concentrations of 500 ng/ml had no significant effect on chemokinesis or chemotaxis; velocities were identical to control cells (data not shown).

We sought to determine the time of maximum effects on neutrophils exposed to ET. Neutrophils were treated with buffer only (Ctl), 10 mM Fsk or 500 ng/ml of ET for 1 hour to two hours followed by time-lapse video imaging. The significant increase in cAMP levels is first noted one hr after ET treatment ($p<0.0001$). Even a slight increase in cAMP leads to inhibition of phagocytosis (203), superoxide killing (204), and bacterial killing of cells (49). The mean velocity of ET treated neutrophils was significantly decreased at one and two hours compared with buffer only (Fig. 4-3A). Neutrophils were treated with 500 ng/ml of ET for one or two hours and were not significantly different ($p=0.96$), leading us to conclude the increase in cAMP at one hour is sufficient to cause maximal effects.

In control neutrophils, exposure to FMLP resulted in a distinctly polarized morphology, a high percentage of cells forming broad lamellipodia at the leading edge and small uropodia at the rear (Fig. 4-3B). Exposure to 500 ng/ml of ET markedly impaired the ability of neutrophils to polarize ($p<0.0001$) with no statistical difference between one and two hours of exposure ($p=1.0$).

CD11/CD18 Expression in Neutrophils

Signaling via the adhesion molecules of the β_2 integrin family, CD11b/CD18 plays an essential role in PMN recruitment and activation during inflammation (205). ET induced reductions in chemotaxis and chemokinesis could in part be mediated by a change in the surface expression of these adherence molecules. Therefore, we examined the effects of treatment with 500 ng/ml ET and Fsk/IBMX on the PMN surface marker expression of CD11b/CD18. No significant differences in surface expression were observed as compared to control neutrophils ($p=0.143$) (Fig. 4-4A). Similarly, LT at concentrations up to 500 ng/ml had no effect on the surface expression of CD11b/CD18 (Fig. 4-4A). However, when EF, LF and PA were combined a concentration dependent decrease in receptor surface expression was observed (Fig. 4-4B). Minimal effects were seen at 100 ng/ml ($p=0.9857$, not statistically significant); however, a 50% reduction in expression was observed at 300 ng/ml ($p<0.001$). PA, LF, and EF alone (500 ng/ml) had no effects on surface expression (data not shown).

Effects of ET Alone and ET Combined with LT on Neutrophil Actin Assembly

Neutrophil chemotaxis requires rapid assembly of actin filaments at the leading edge, and ET-induced impairment of chemotaxis could be mediated by inhibition of neutrophil actin assembly. As assessed by Alexa-phalloidin staining of filamentous actin and FACS analysis, ET treatment resulted in a delay in FMLP-stimulated actin

assembly, a reduction in the maximum actin filament content ($p<0.001$) (Fig 4-5A open circles), and the extent of inhibition was comparable to treatment with 500ng/ml of LT ($p<0.001$) (Fig. 4-5A, open squares) (39). The combination of PA + EF + LF (ET + LT) resulted in an additive reduction in F-actin content ($p<0.001$), suggesting that EF and LF impair neutrophil actin assembly by different signaling pathways (Fig. 4-5A, closed squares). PA, EF, or LF alone at 500 ng/ml had no significant effect on FMLP-stimulated actin assembly, where F-actin content was nearly identical to neutrophils incubated in buffer (data not shown).

To further explore the effects of anthrax toxins on neutrophil actin assembly we, compared fluorescence micrographs of Alexa-phalloidin stained adherent neutrophils following exposure to 1 µM FMLP. Control neutrophils were polarized and demonstrated a high content of F-actin at the leading edge in lamellipodia (Fig. 4-5B). LT-treated adherent neutrophils appeared rounded with considerably reduced F-actin content (Fig. 4-5C). ET and ET + LT-treated neutrophils demonstrated a distinctly different distribution of filamentous actin as compared to control cells or cells treated with LT alone (Fig. 4-5D and 4-5E). Small discrete regions of increased F-actin content were noted throughout the horizontal plane of the cells. By shifting the Z-plane of focus in 0.5 µm steps beginning at the top of the cell, these F-actin structures were found to be in the lowest focal plane, adjacent to the slide surface (Fig. 4-5 F).

Effects of ET Alone and Combined with LT on *Listeria monocytogenes* and *Shigella flexeneri* Actin-Based Motility

Listeria monocytogenes (88, 128) and *Shigella flexneri* (206) both highjack the actin-regulatory system of host cells to induce the assembly of actin filaments. Both organisms bypass many of the signal transduction mechanisms required for receptor

mediated actin assembly, and we have used these model systems to further assess the effects of ET and the combination of PA + EF + LF on *in vivo* actin assembly. The velocity of bacterial movement directly correlates with the rate of actin assembly, and assuming that the rate of actin disassembly is constant, the length of each actin filament tail also directly correlates with the assembly rate of actin filaments within the tail (137, 207). Therefore, we examined the effects of these toxins on bacterial intracellular velocities and on actin tail lengths. Exposure of HeLa cells to 500 ng/ml ET resulted nearly 50% reduction in *Listeria* velocity ($p<0.001$), and treatment with Fsk/IBMX also reduced *Listeria* velocity ($p<0.001$)(Fig. 4-6A). *Listeria* actin tail lengths were comparably reduced ($p<0.001$) (Fig 4-6 B-D). The combination of PA + EF + LF (ET + LT) also impaired *Listeria* actin-based motility, with maximum inhibition occurring at a concentration of 50-100 ng/ml (Fig. 4-6 E, F). The maximal inhibition of the combined toxins was similar to that of ET or LT alone. PA, EF, or LF alone at 500 ng/ml had no significant effect on *Listeria* intracellular actin-based motility, velocity or tail length, being identical to cells treated with buffer alone (data not shown).

Treatment of *S. flexerni* infected HeLa cells with 500 ng/ml of ET minimally slowed the velocity of intracellular movement (mean control velocity: 0.125 ± 0.007 µm/s SEM, n= 270 vs. 0.109 ± 0.007 µm/s SEM, n = 315 for ET treated cells, $p = 0.07$). This finding is consistent with previous observations that Shigella and *Listeria* actin-based motility utilize different actin-regulatory proteins and signal transduction pathway (208). Shigella requires bacterial surface protein IcsA. IcsA directly attracts and activates the host cell protein N-WASP, and this protein in turn activates the Arp2/3 complex. Also, Shigella, unlike *Listeria*, does not require VASP for intracellular actin-based motility

(125).

VASP Phosphorylation Impairs Neutrophil and *Listeria* Actin-Based Motility

Effects of ET on VASP

Neutrophils were treated with 500ng/ml of ET for two hours and extracts were subject to quantitative western blot analysis. Equal amounts of neutrophils were analyzed for total VASP. Phosphorylation of VASP at S157 resulted in a change in electrophoretic mobility allowing relative quantification of both unphosphorylated and S157 phosphorylated VASP. Based on scanning densitometry, ET treatment for two hours resulted in a five-fold increase in phosphorylation on S157 as compared to cells incubated in buffer ($p<0.001$)(Fig. 4-7C, 4-7D). Forskolin, a cAMP signaling activator, mimiced the effects of ET treatment, resulting in a one-fold increase in VASP phosphorylation at S157 ($p=0.1036$, not significant).

Phospho-S157 anti-VASP antibody was used to detect localization phosphorylated VASP in human neutrophils, and in *Listeria* infected HeLa cells. Phospho-S157 localized to the lamellipodia and focal adhesions of neutrophils with greater intensity of staining in ET treated, as compared to neutrophils incubated with buffer alone. Some diffuse staining throughout the neutrophil was also apparent (Fig. 4-8A). Phospho-S157 was shown to localize around intracellular bacteria with much greater intensity than cells incubated in buffer alone (Fig. 4-8B).

Effects of Changes in VASP S157 Phosphorylation on Human Neutrophils

VASP phosphorylation at S157 may be regulating actin turnover during ET infection, thereby inhibiting the ability of the neutrophil to chemotax to the site of infection; however, neutrophils are refractory to transfection, limiting the number of approaches that can be used to gain insight into how this protein functions. A method

that has been successfully used to introduce proteins into primary human neutrophils while maintaining normal functional responses, involves the addition of a sequence derived from the HIV TAT protein linked to the protein of interest, which can then be introduced into intact neutrophils (209). The various VASP isoforms were cloned into the pTAT-HA vector at the KpnI/SphI restriction sites (Fig. 4-9A). The plasmids were transformed in BLD21 cells, subsequently cultured in Luria-Broth (LB) and induced for five hours with IPTG. S157A and S157D both were induced at three hours, whereas wild-type VASP was continuously produced without the need for induction (Fig. 4-9B). VASP is 46-kDa and with TAT we saw a band at ~54-kDa. Western blot analysis probing for anti-VASP confirmed VASP production (data not shown).

The samples were applied to a Cobalt column (Qiagen), and column fractions were analyzed by Coomassie blue staining of an SDS-polyacrylamide gel (Fig. 4-9C, representative of all three isoforms). The appropriate fractions were pooled together, run through a S200 (Qiagen) size exchange column to remove smaller protein contaminates, and again analyzed by Coomassie blue staining of an SDS-polyacrylamide gel (Fig. 4-9D).

We first estimated the concentration of VASP present in human neutrophils (Fig. 4-10A). Densitometric scans of the recombinant protein were plotted, and the amount of VASP protein in the lysate was interpolated from the linear portion of the curve. Based on this approach, we were able to estimate that neutrophils contain 0.1 ng of VASP per cell, or approximately 1.5% of the total protein found in human neutrophils.

The TAT VASP fusion proteins were added to a final concentration of 5.2 μg (Fig. 4-9E). To determine the efficiency of protein delivery, neutrophils with and without TAT-

VASP protein treatment were subject to extensive washes and analyzed by Western blot with anti-VASP antibody. After 30 min of TAT-VASP incubation approximately 85-90% of the TAT entered into the neutrophil and no longer appeared to be bound to the surface of the neutrophil after western blot analysis of cytoplasmic exacts devoid of cell membrane (data not shown).

After TAT-VASP protein treatment, neutrophils were incubated in buffer only or in 500ng/ml of ET for two hours at 37°C. The effects of TAT-VASP wild-type, TAT-VASP S157A, TAT-VASP S157D and control neutrophils treated incubated in buffer alone or ET were examined for effects on motility (Fig. 4-10B). As we have previously shown (106), ET significantly impaired neutrophil chemokinesis by 25-30% in control cells and TAT-VASP wild-type treated cells ($p<0.001$). ET treatment had no effect on chemokinesis of TAT-VASP S157A treated cells ($p>0.05$); however, TAT-VASP S157D treated cells incubated with buffer or ET demonstrated a significant reduction in neutrophil chemokinesis (25-30% decrease) ($p<0.01$ as compared to untreated neutrophils and neutrophils treated with wild-type TAT-VASP). These findings strongly suggest that ET-induced phosphorylation of VASP at S157 is responsible for ET mediated impairment of neutrophil motility.

In addition to chemokinesis, the effects of FMLP on neutrophil polarity was also examined. Untreated neutrophils, those treated with TAT-VASP wild-type protein and ET-treated TAT-VASP S157A neutrophils, demonstrated a distinctly polarized morphology, with a high percentage of cells forming broad lamellipodia at the leading edge and small uropodia at the rear (Fig. 4-10C). Exposure of cells with wild-type VASP to ET or cells containing TAT-VASP S157D incubated with buffer or ET

demonstrated marked impairment in the ability to polarize in response to the chemoattractant FMLP ($p<0.01$). These findings suggest that ET impairs neutrophil actin-based assembly by phosphorylating VASP S157.

Recent studies have implicated VASP in promotion of filopodial formation from the lamellipodium mesh network (210). Filopodia have been implicated in a number of diverse cellular processes including growth-cone formation, wound healing and metastasis (178, 211); therefore, we also explored the effects of various isoforms of VASP proteins on neutrophil filopodia formation (Fig. 4-10D, 4-10E). In response to phosphorylation of VASP as a consequence of ET exposure or by treatment with TAT-VASP S157D, the number of filopodia per cell was significantly increased as compared to control neutrophils ($p<0.001$), TAT-VASP wild-type and TAT-VASP S157A-treated neutrophils ($p>0.5$) (Fig.4-10D, 4-10E).

Effects of ET Induced VASP Phosphorylation on *L. monocytogenes* Actin-Based Motility

To unambiguously study the role of VASP protein in *Listeria* actin-based motility it was necessary to utilize a cell line that fails to express any of Ena/VASP proteins. This condition eliminates interference from the endogenous proteins (184, 212). MVd7 cells fulfill this condition, lacking all Ena/VASP proteins. As previously shown in the absence of transfection with VASP or VASP mutants, MVd7 cells supported only very slow intracellular *Listeria* velocities (Fig. 4-11A, CT). (MVd7 cells still have a small level of Mena remaining allowing for some *Listeria* motility.) This decrease in velocity was comparable to the slow velocities seen in cells transfected with S157D ($p>0.5$). MVd7 cells transfected with wild-type VASP were able to significantly increase *Listeria* velocities as compared to untransfected cells ($p<0.001$); however, ET treated MVd7

cells rescued with wild-type VASP reversed this effect, velocities being comparable to untransfected cells and cells rescued with S157D VASP. Rescue with S157A VASP resulted in a marked increase in the mean intracellular *Listeria* velocity and was significantly faster than MVd7 cells rescued with wild-type ($p<0.001$). Furthermore cells rescued with this mutant construct were resistant to the effects of ET treatment.

Because a significant increase in filopodia formation was observed in neutrophils containing S157 phosphorylated VASP, we sought to determine how the various isoforms of VASP proteins contribute to *Listeria*-induced membrane projections using MVd7 cells (Fig. 4-11B). Bacterial projection formation was significantly increased in MVd7 cells containing phosphorylated S157 VASP ($p<0.046$). The number of bacteria containing projections per cell was increased in MVd7 cells or cells rescued with wild-type VASP, treated with ET ($p=0.093$, not quite significant) and transfected with VASP S157D buffer ($p<0.046$), as compared to untransfected MVd7 cells or cells rescued with wild-type and S157A VASP. These findings suggest that VASP phosphorylation at S157 facilitates the ability of *Listeria* to form membrane projections important for cell-to-cell spread of the bacteria.

These findings were contrasted in MVd7 cells infected with *S. flexerni*. No significant difference in bacteria containing membrane projections was noted when comparing null cells to cells rescued with the three VASP constructs, MVd7 null cells forming 0.32 ± 0.032 (projections per cell $\pm$ standard error of the mean [SEM], MVd7 WT VASP: 0.25 ± 0.026, MVd7 S157A: 0.245 ± 0.027 and MVd7 S157D: 0.35 ± 0.05). Our findings are consistent with previous observations that *Shigella and Listeria* actin-

based motilities utilize different actin-regulating proteins and signal transduction pathways (208).

Effects of VASP S239 Phosphorylation on Human Neutrophils

Harbeck, et al. (185) previously showed in mouse VASP extracts that phosphorylation of S239 significantly impairs actin polymerization. S239 is preferentially phosphorylated by PKG, but it can also be phosphorylated by PKA; however, the preferred site for PKA is S157. Neutrophils were treated for two hours with buffer only, 10mM Fsk or 500ng/ml of ET. Immunoblotting using anti-Phospho S239 VASP antibody (Cell Signaling) confirmed slight phosphorylation in Fsk and ET treated cells (data not shown). To determine if the decrease in neutrophil actin assembly was the result not only of S157 phosphorylation, but also S239 phosphorylation, we transfected MVd7 cells with various VASP isoforms, followed by infection with *Listeria,* and incubation in buffer only or 500 ng/ml of ET (Fig. 4-12). Intracellular motility of *Listeria* was determined in MVd7 VASP wild-type (WT), S157A, S157D, S239A, S239D and MVd7 null cells treated with buffer only (CT) or ET. As we have previously shown (106), ET significantly impaired *Listeria* motility in wild-type cells. Control and ET treated S157A cells significantly increased *Listeria* motility over wild-type control ($p<0.001$); however, S157D and MVd7 null cells treated with buffer only or ET all showed a significant impairment in overall *Listeria* motility ($p<0.001$). Transfection of MVd7 null cells with S239A and S239D constructs were only able to rescue the wild-type *Listeria* phenotype to approximately 85%. ($p<0.0091$ and $p<0.0011$ respectively.) This set of experiments rescued with the S157 VASP construct reproduced our previous findings, while S239A and S239D had no effect on *Listeria*

velocity. These findings suggest that S239 does not play a significant role in ET mediated impairment of *Listeria* motility.

Effects of VASP Isoforms on Actin Bundling

In addition to examining the VASP function in cells and extracts, we examined the effects of recombinant VASP proteins on actin based bundling. Filopodia are highly dynamic finger-like cell protrusions filled with parallel bundles of actin filaments. A key player in the formation of filopodia across many species is VASP (143, 168). It has been proposed that the essential role of VASP for formation of filopodia is its ability to bundle actin filaments. Therefore to better understand the function of VASP in filopodium formation we examined the ability of purified native VASP, VASP S157A, VASP S157D, as well as alpha-actinin (positive control) to bundle purified skeletal muscle actin filaments.

As shown in Fig. 4-13, alpha-actinin enhanced the concentration of F-actin that sedimented after slow speed centrifugation ($p=0.002$). All three isoforms of VASP also enhanced F-actin sedimentation under the same conditions (Fig. 4-13A). No significant differences in supernatant and pellet were observed between the three proteins (P values between 0.13-0.59) (Fig. 4-13B). These findings suggest that all three isoforms are equally capable to efficiently bundle actin filaments and suggest that the differences in their ability to induce filopodia formation is likely to be the consequence of additional protein-protein interactions.

Pull-Down Assay

To explore the possibility of an additional protein binding partner being recruited by VASP S157 phosphorylation, MVd7 cells were treated with 6XHis tagged fusion

proteins followed by lysis and incubated with His-binding beads. Using this methodology we were unable to identify any proteins of interest (See Table 4-2).

Dual Toxin Affects on Human Neutrophils

ET and LT are Able to Enter Human Neutrophils

ET enters human neutrophils and HeLa cells as evidenced by a concentration dependent rise in cAMP levels (Fig. 4-1A-D). cAMP levels increase in a time and dose dependent manner.

Previous work from our lab (39) assessed LT activity in neutrophils. Neutrophil lysate extracts were subjected to western blot analysis using an antibody to detect the amino-terminus of MEK. The antibody identifies epitopes on the first seven amino acids of MEK, the region cleaved by LF, and loss of antibody cross-reactivity indicates proteolysis by LF. MEK cleavage in neutrophils and HeLa cells required two hours of treatment at 37°C with 50 ng/ml of LT (39).

Effects of ET+LT Interactions on cAMP Levels

To better understand the potential synergism of ET and LT, we exposed neutrophils and HeLa cells to increasing concentrations of ET and LT (50-500 ng/ml of a 1:1:1 weight ratio of PA, EF and LF). Two hours of dual toxin exposure significantly lowered the cAMP levels in neutrophils (Fig. 4-14A) and HeLa cells (Fig. 4-14C) than treatment with ET alone.

ET or LT binds with high affinity to the exposed domain sites on PA. It is expected that the binding of the alternative moiety to this site would make the site unavailable for the other moiety (192). To address a potential issue of steric constraints, we exposed neutrophils for two hours to increasing concentrations of ET and LT (50-500 ng/ml) of a 2:1:1 weight ratio of PA, EF and LF. The cAMP response

again remained at a low level (data not shown). Next we exposed neutrophils and HeLa cells to a 5:1:1 weight ratio of PA, EF and LF, which leaves PA molecules free and assures that any effects seen were not the consequence of LF competing with EF for PA binding sites. Again, cAMP levels remained low in neutrophils (Fig. 4-14B) and HeLa cells treated with ET+LT (data not shown). Increasing concentrations of ET and LT did not increase cAMP in a dose dependent manner as observed with ET alone nor did we find the >50-fold increase seen with ET treatment. Increasing the ratio of moieties to overcome any steric constraints did not improve the four-fold increase in cAMP levels noted with dual toxin treatment. These findings indicate the low levels of cAMP associated with dual toxin treatment are not the consequence of competitive inhibition of EF by LF for their binding partner PA.

We sought to determine if the concentration of the individual toxins played a role in cAMP inhibition. Neutrophils (Fig. 4-14D) and HeLa cells (Fig. 4-14E) were treated with 100 ng/ml of LT in addition to increasing concentrations of ET (5:1:1 weight ratio used for PA, EF and LF). A 100 ng/ml concentration of LT was able to impair the ability of ET to increase cAMP levels in both neutrophils and HeLa cells.

Signaling Pathway Utilized by LT to Decrease ET cAMP Production

We next sought to examine if LT cleavage and inactivation of the MEK pathway played a role in decreased cAMP response. We treated neutrophils (Fig. 4-15A) and HeLa cells (Fig. 4-15B) with 500 ng/ml of ET (5:1 weight ratio) for one hour followed by the addition of MEK inhibitors for the second hour. MEK inhibitors were: SB203580 (inhibits the p38 pathway), SP600125 (inhibits the JNK pathway) and PD98059 (inhibits the ERK pathway). All three inhibitors significantly impaired the ability of ET to increase intracellular cAMP levels ($p<0.001$).

cAMP levels are down-regulated by phosphodiesterases. To rule out LT as a potential phosphodiesterase, neutrophils (Fig. 4-16A) and HeLa cells (Fig. 4-16B) were again exposed to 500 ng/ml of ET and 100 ng/ml of LT (5:1:1 weight ratio of PA, EF and LF) for one hour followed by an additional hour of treatment with 50 mM of theophylline. Theophylline is an inhibitor of phosphodiesterase enzymes and would be expected to allow for increased cAMP levels after LT exposure if LT had phosphodiesterase characteristics. The addition of theophylline still led to a dramatic decrease in intracellular cAMP levels with dual toxin treatment ($p<0.001$). These results (Fig. 4-16) led us to conclude that LT does not activate phosphodiesterases and appears to impair increased cAMP levels by inhibiting one or more of the MEK pathways. We also confirmed that the chemical inhibitors did not react with the assay itself (data not shown).

Effects of ET+LT Exposure to cAMP Downstream Target PKA

Previous work from our lab (106) has shown that ET-induced rise in cAMP is accompanied by the phosphorylation of PKA and downstream phosphorylation of VASP at S157 (in press). After ET+LT treatment, is ET still able to activate its downstream signaling pathway? Untreated neutrophils were compared to neutrophils treated for two hours with 6-db-cAMP (positive control), 100 ng/ml of LT, 500 ng/ml of ET and increasing concentrations of ET with 100 ng/ml of LT (5:1:1 weight ratio) ($p<0.001$) (Fig. 4-16A). LT does not appear to inhibit the ability of ET to phosphorylate PKA as a two-fold increase in P-PKA was detected.

Neutrophils were next treated with a 100 ng/ml of LT and 500 ng/ml of ET (5:1:1 weight ratio) in a time-dependent manner to determine if the 2-fold increase in PKA was still able to phosphorylate VASP at S157. VASP phosphorylation at S157A is noted one

hour after dual toxin treatment (Fig. 4-16B). The two-fold increase in PKA noted after ET+LT treatment is sufficient to activate its downstream effector molecule VASP.

Timing of Toxin Entry

Even though LT impairs increases in cAMP levels at two hours post exposure, PKA phosphorylation is still occurring. This led us to speculate that what we were seeing was related to the timing of toxin activity. It is highly likely that both EF and LF enter at the same time; however LF takes time to cleve the MEKs. Neutrophils were exposed to buffer only, 500 ng/ml of ET or 500 ng/ml of ET and 100 ng/ml of LT (5:1:1 weight ratio) over a time course ranging from 30 minutes to two hours (Fig. 4-17A). ET begins increasing intracellular cAMP levels at 30 minutes post-exposure and steadily increases cAMP levels up to the two-hour time point. The addition of 100 ng/ml of LT caused cAMP levels to increase up to the one and a half hour time point, and at two hours LT impaired the increase in cAMP, bringing the levels back to physiologically normal levels. We are able to conclude that ET is able to significantly affect intracellular cAMP levels by 30 minutes.

Previous work from our lab found that experiments conducted on neutrophils exposed to LT needed a minimum two-hour incubation period before impairing neutrophil actin-based motility (39). To assess LT activity we exposed neutrophils to 100 ng/ml of LT over a two-hour time course (Fig. 4-17B). Neutrophil lysates were subjected to western blot analysis using an antibody against the amino-terminus of MEK. MEK cleavage begins at one hour but does not reach its maximal cleavage until two hours post-exposure. During, et al. (39) showed that neutrophils treated with 50 ng/ml of LT at one hour had no effect on polarity or chemotaxis; however, two hours post-exposure caused a 50% reduction in the ability of neutrophils not only to polarize

but also to chemotax, which corresponds to the two hours necessary for complete MEK cleavage. We conclude that ET acts quickly within 30 minutes to increase cAMP and phosphorylate PKA, and then its activity is shut off by LT's at 1.5 to 2 hours after toxin exposure. Sequential toxin effects serves to limit the duration of cAMP.

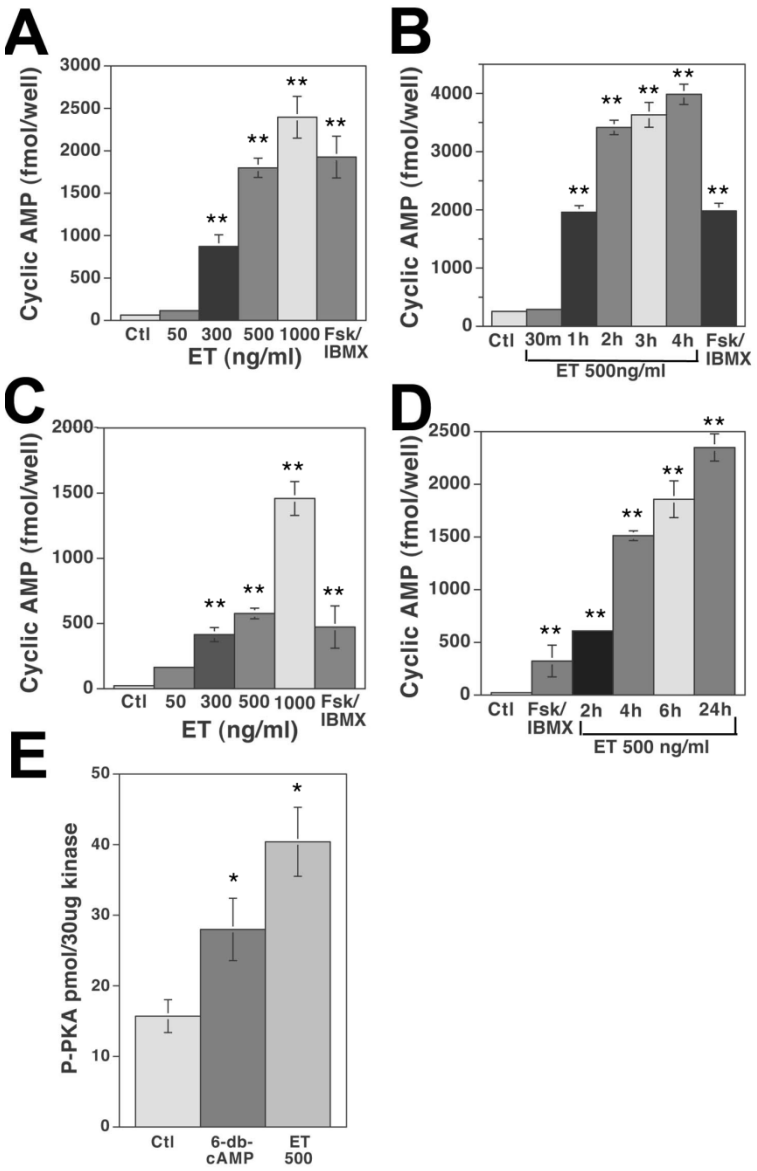

Figure 4-1. Effects of ET on Intracellular cAMP levels and PKA phosphorylation. A) Concentration dependent increase in intracellular cAMP levels in human neutrophils treated with ET. The far right bar shows neutrophils treated with the cAMP agonists Fsk (10 mM) and IBMX (100 mM) for 15 min at 37°C. B) Effects of incubation time on ET induced rise in intracellular cAMP levels. Neutrophils were treated with 500 ng/ml of ET. C) Concentration dependence of ET induced intracellular cAMP levels in HeLa cells. Experimental conditions are identical to A. D) Effects of incubation time on ET induced rise in intracellular cAMP levels in HeLa cells. Conditions are identical to B. E) Phosphorylation of PKA was determined using 25 μg of radiolabeled protein lysate and measuring the transfer of radioactive phosphate from ATP into Kemptide. A > 4-fold increase in phosphorylated PKA was observed after ET treatment. Standard errors indicate the SEM of 3 experiments. * = $p<0.001$ and ** = $p<0.0001$ compared to Ctl treated cells.

Table 4-1. Effects of ET on cell necrosis and apoptosis

Neutrophils	% Viable Cells	% Necrosis	% Apoptosis
Control	96.7	3.3	0
50ng/ml ET	89.9	10.1	<1
300ng/ml ET	95.8	4.2	0
500ng/ml ET	92.0	8.0	<1
HeLa Cells			
Control	93.9	6.1	<1
50ng/ml ET	98.5	1.5	<1
300ng/ml ET	96.3	3.7	<1
500ng/ml ET	96.0	4.0	<1

†Cells were treated with ET for 2h and stained with annexin V and propidium iodide, followed by FACS analysis (see Materials and Methods). HeLa cells were scraped from tissue culture dishes, explaining the relatively high percentage of necrosis in control HeLa cells (p=1.0, Fisher's exact test).

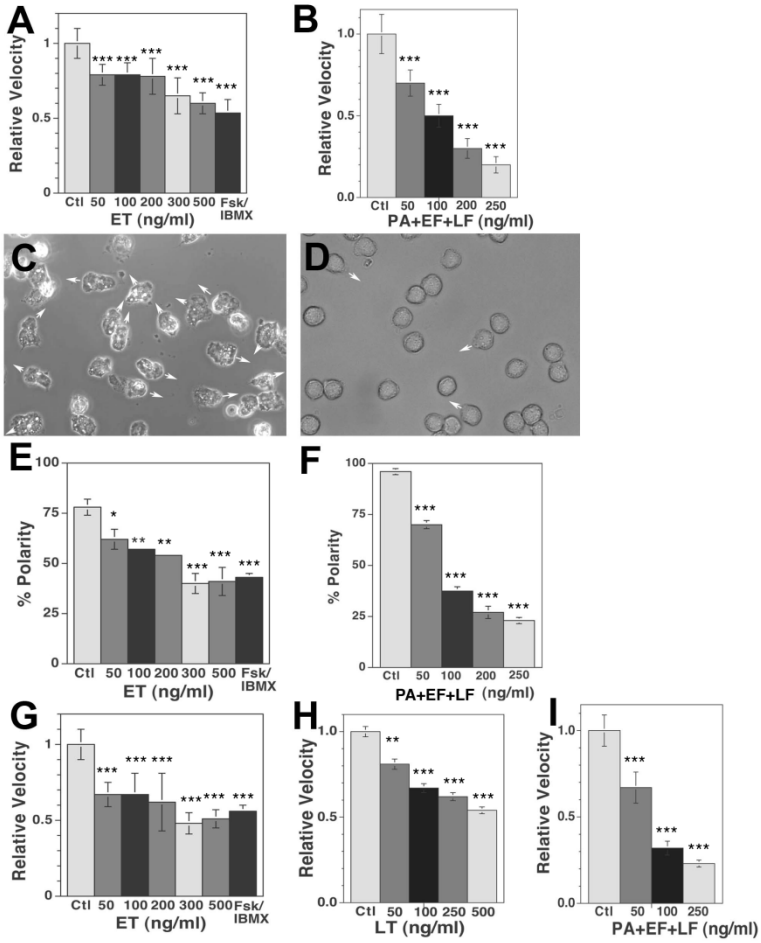

Figure 4-2. Effects of anthrax toxins on neutrophil chemokinesis, polarity, and chemotaxis. A) Mean relative velocity of human neutrophil chemokinesis after treatment with buffer (Ctl), increasing concentrations of ET or Fsk/IBMX (10 nM/100 nM). Error bars indicate the SEM of 7 experiments. B) Effects of PA, EF, and LF on neutrophil chemokinesis. Standard errors indicate the SEM of 3 experiments. C) Phase contrast micrograph of control PMNs 5 min after the addition of 1 µM FMLP. The arrows point to the direction of polarity and movement of each cell. D) Phase contrast micrograph of PA + EF +LF - treated (PMN 5 min after the addition of 1 µM FMLP. E) Percentage of polarized PMNs after FMLP exposure. Standard errors = SEM of 7 experiments. For each condition, 130 cells were analyzed per experiment. F) Effects of PA, EF, and LF on neutrophil polarity. Error bars indicate the SEM of 3 experiments. G) Relative velocity of human neutrophil chemotaxis after treatment with buffer (Ctl), increasing concentrations of ET or Fsk/IBMX (10 nM/100 nM). Error bars indicate the SEM of 3 experiments. H) Relative velocity of human neutrophil chemotaxis after treatment with buffer (Ctl) or increasing concentration of I) Effects of PA, EF, and LF on neutrophil chemotaxis. Error bars indicate the SEM of 3 experiments. Note the additive inhibition of chemotaxis as compared to ET and LT alone (G and H). * = $p>0.05$, ** = $p<0.001$ and *** = $p<0.0001$.

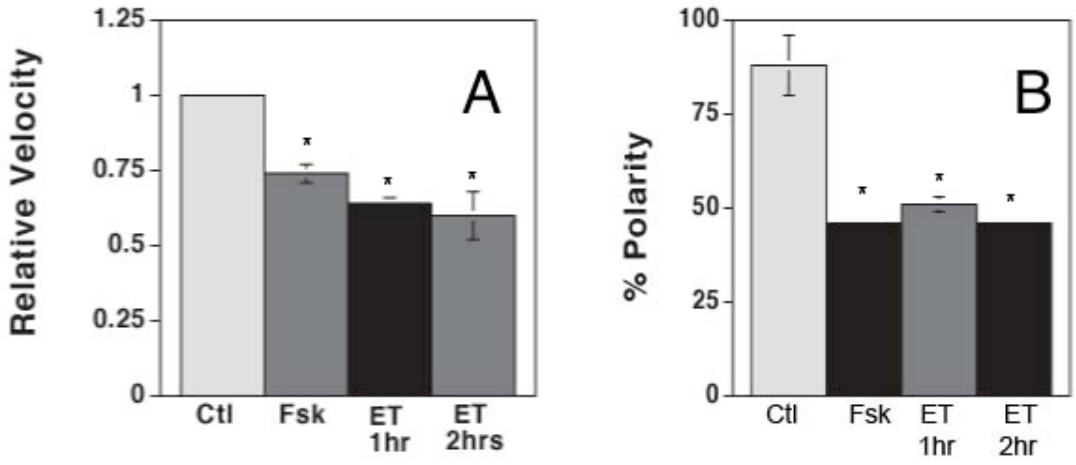

Figure 4-3. Time course of ET on neutrophil chemokinesis and polarity. A) Mean relative velocity of human neutrophils after treatment with buffer only (Ctl), 500 ng/ml of ET (weight ratio of 5:1) for 1 to 2 h and 10 nM of Fsk for 20 min. The differences in relative velocity of ET at 1 and 2 h are not statistically different ($p>0.05$). Error bars are indicative of SEMs of 2 experiments ($n=210$). ET significantly impairs the velocity of neutrophils 1 h post exposure. B) Percentage of polarized neutrophils 5 min after the addition of 1 mmol/L of FMLP. Error bars indicate the SEMs of 2 separate experiments ($n=100$). * = $p<0.001$.

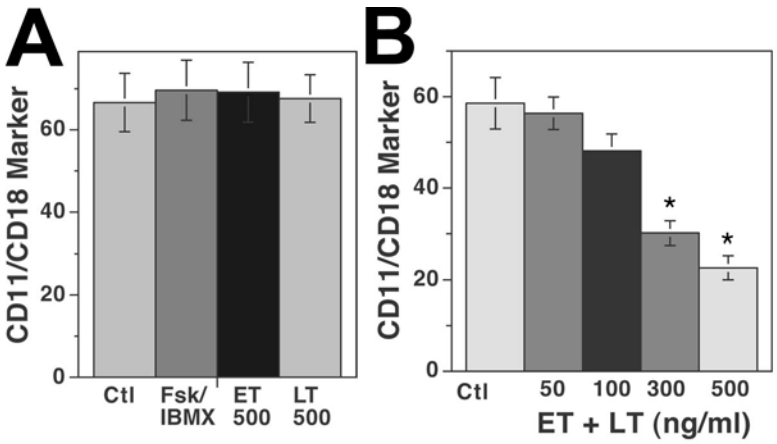

Figure 4-4. Effects of anthrax toxins on CD11/CD18 surface expression by neutrophils. A) Neutrophils were treated with buffer, 500ng/ml ET or LT (500 ng/ml PA + 500 ng/ml of EF or LF) for 2 h, or with Fsk/IBMX (10 mM/100 mM) for 15 min followed by surface staining and FACS analysis of 10,000 cells. As compared to buffer alone, no significant differences in receptor expression were observed in toxin or Fsk/IBMX-treated cells. B) Neutrophils were treated with 1 µg/ml of PA plus increasing concentrations of a 1:1 weight ration of EF and LF (identical to conditions in Fig 2 F) for 2 h, followed by staining and sorting as described above. A 50% reduction in the CD11/CD18 surface receptor expression was observed with 300 ng/ml (1 µg/ml PA + 300 ng/ml EF + 300 ng/ml LF). Error bars indicate the SEM of 3 experiments. *= $p<0.001$ compared with Ctl.

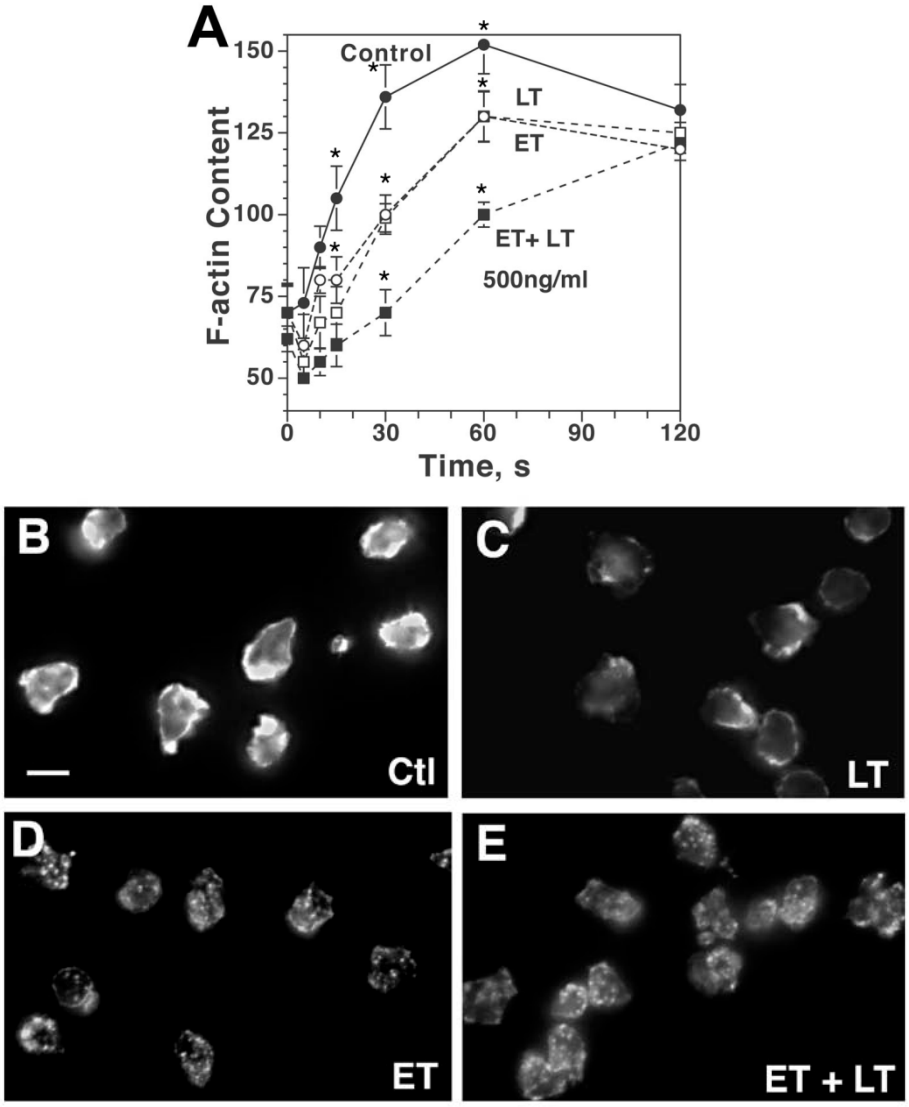

Figure 4-5. Effects of anthrax toxins on FMLP-induced neutrophil actin assembly. A) Effects of ET (open circles), LT (open squares) as well as the combination of ET and LT (closed squares) on actin filament content of neutrophils as compared to cells incubated in buffer (Control, closed circles). The median fluorescence intensity was determined by FACS analysis of 10,000 cells for each time point. Both ET and LT alone and in combination slowed the onset of actin assembly and the combination resulted in an additive reduction in peak F-actin content, 34% as compared to ET (15% reduction) and LT (15% reduction) alone ($p<0.001$). Error bars = SEM of 3 experiments. B) Fluorescence micrograph of human neutrophils incubated with buffer for 2 h, allowed to attach to fibronectin coated glass slides. Bar = 10 µm. C) Fluorescence micrograph of human neutrophils incubated with 500 ng/ml LT D) Fluorescence micrograph of human neutrophils incubated with 500 ng/ml ET E) Fluorescence micrograph of human neutrophils incubated with ET +. * = $p<0.001$ compared to control.

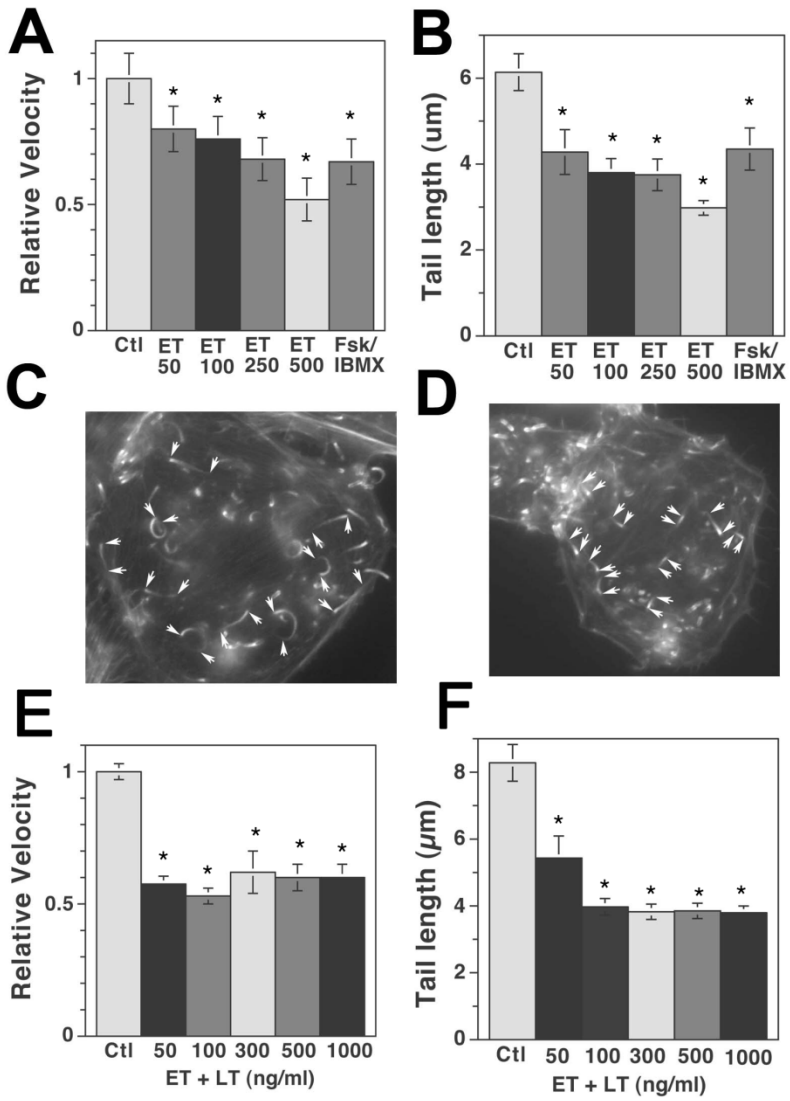

Figure 4-6. Effects of anthrax toxins on *Listeria* actin-based motility. A) Relative mean velocities of intracellular *Listeria* in HeLa cells after treatment for 2 h with buffer (Ctl), and increasing concentrations of ET or 15 min with Fsk/IBMX. Error bars indicate the SEM, n=730. Measurements were made 5-6 hours after initial *Listeria* infection. B) Comparing mean lengths of *Listeria*-induced actin filament tails. Error bars indicates the SEM, n=100. C) Fluorescent micrographs of buffer-treated HeLa cells infected with *Listeria* for 6 h fixed and stained with Alexa-488 phalloidin. Note the long *Listeria* actin rocket tails (arrows: point to the beginning and end of selected tails). Bar = 10 µm. D) Fluorescent micrograph of ET-treated HeLa cells infected with *Listeria*. Cells were fixed and stained as described in C. Note the shorter *Listeria* actin tails. E) Effects of increasing concentrations of LF, EF, and PA in combination on the velocity of *Listeria*. Error bars indicate the SEM, n=50. F) Mean *Listeria* tail lengths under the same conditions as E. Error bars indicate the SEM, n=50. * = $p<0.001$ compared to control (Ctl).

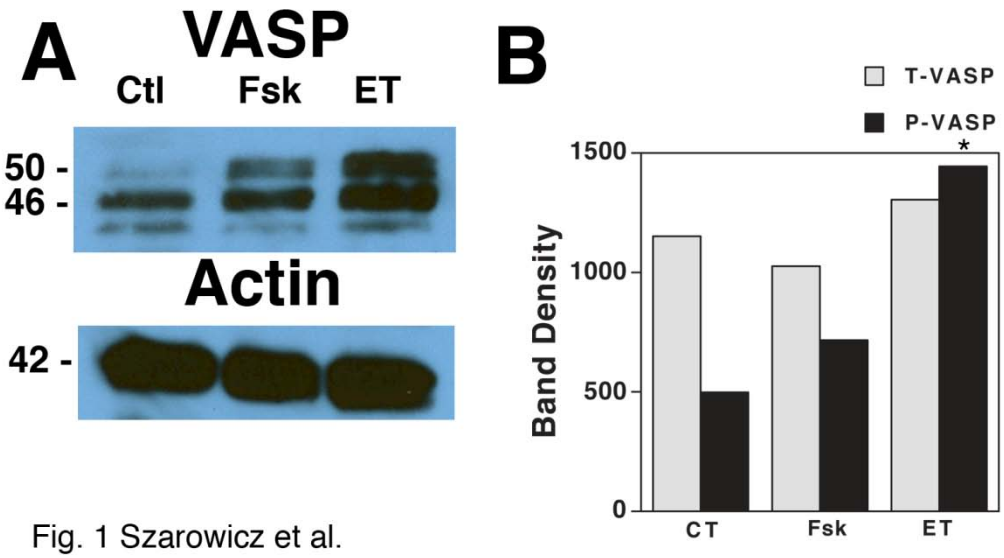

Fig. 1 Szarowicz et al.

Figure 4-7. Effects of ET on P S157 VASP. A) Purified neutrophils were treated from left to right with buffer only, Fsk (10 mM) or 500 ng/ml of ET for 2 h at 37°C. Equal protein amounts of each treatment were analyzed for P S157 by western blot analysis. A >5-fold increase in P S157 was observed after ET treatment, $p<0.001$. Blots are representative of 2 separate experiments. The lower blot is beta-actin for load control. Numbers on the right side represents molecular weight markers in kilodaltons. Ctl=control (buffer only); Fsk=forskolin. B) Densitometry was performed, and the densities of the lower 46-kDa and upper 50-kDa bands were measured. * = $p<0.001$.

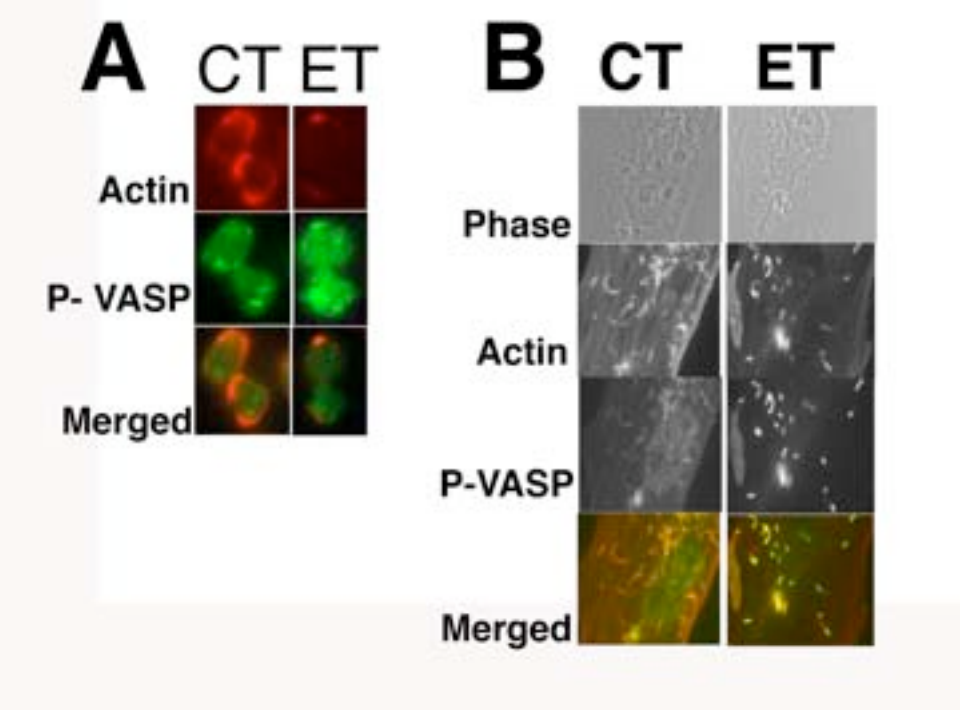

Figure 4-8. The effects of ET on P S157 VASP localization on neutrophils and *Listeria* infected HeLa cells. A) Fluorescent micrograph of human neutrophils incubated with buffer for 2 h, allowed to adhere to fibronectin coated glass slides, and then exposed to 1 µM FMLP for 10 min, followed by formalin fixation, permeabilization, and staining with Alexa-Rhodamine (red) and P S157 VASP antibody (green). Note the high concentration of filamentous actin at the leading edge with small amount of P S157 VASP staining towards the rear of the neutrophil. Fluorescent micrograph of human neutrophils incubated with 500 ng/ml of ET for 2 h have a reduction in fluorescence intensity, indicative of reduced filamentous actin with increased amounts of P S157 VASP staining at the plasma membrane. B) Fluorescent micrograph of buffer treated HeLa cells infected with *Listeria* for 6 h and treated as described in panel A. Note not only the long *Listeria* actin rocket tails but also the P S157 staining around the back portion of the bacteria. Fluorescent micrograph of ET treated HeLa cells infected with *Listeria* for 6 h. Cells were fixed and stained as described in panel A. Note the shorter *Listeria* actin rocket tails and the increased staining intensity of P S157 around the back portion of the bacteria. Ctl=control (buffer treated); Fsk=forskolin.

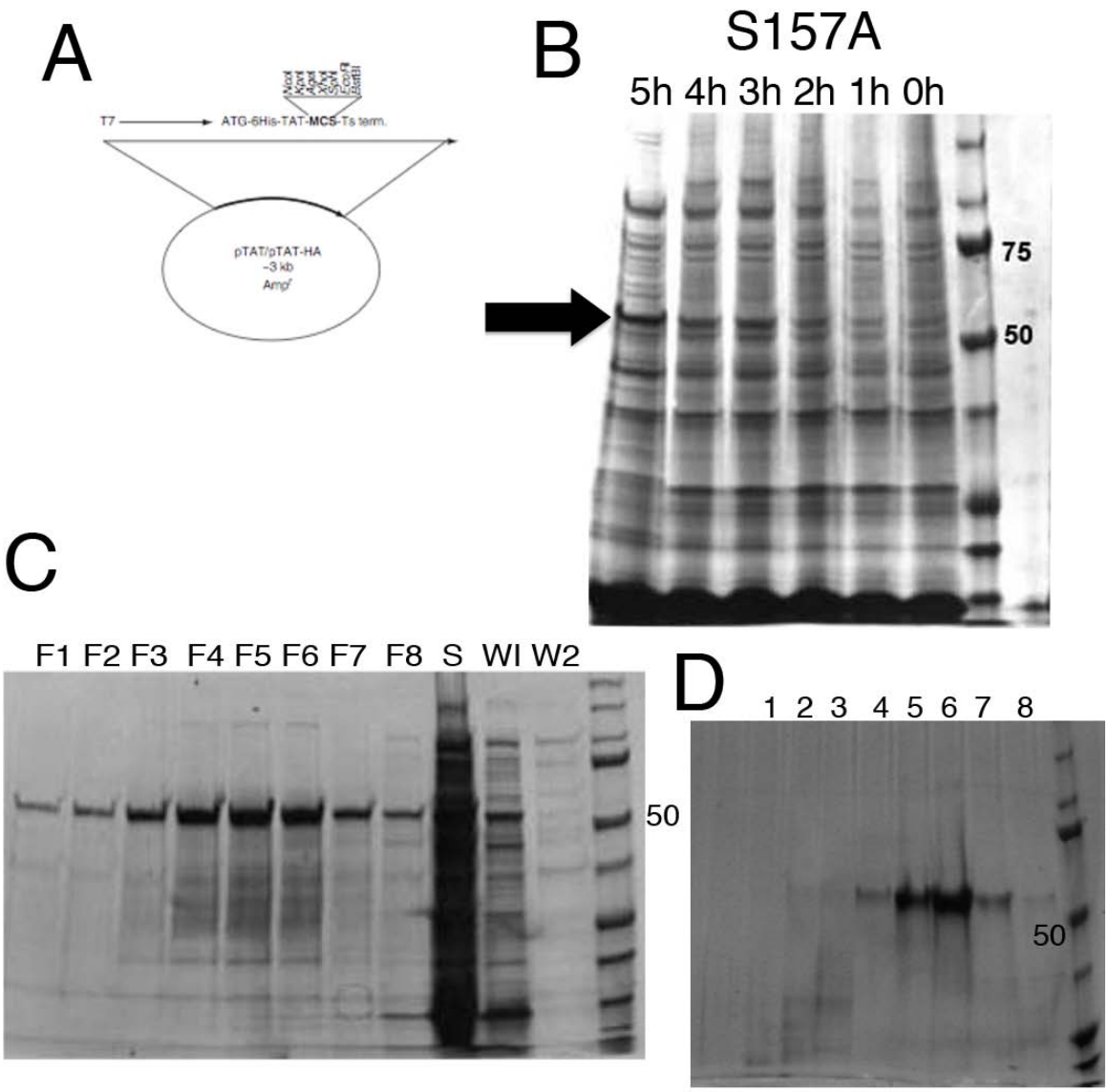

Figure 4-9. Characterization of pTAT vector and the steps involved in protein synthesis. A) pTAT expression vector. B) Induction of pTAT-VASP S157A expression. pTAT-VASP S157A was induced with 500 mM IPTG. Black arrow points to the induction of the pTAT-VASP protein of interest. C) Purification of pTAT-VASP S157A fusion protein over a cobalt resin (Frac, fractions 1-8; S, sample prior to purification; W, washes) were resolved by SDS-Page and stained with Coomassie blue. D) Purification of pTAT-VASP S157A fusion protein over an S200 size exchange column (Fraction 1-8).

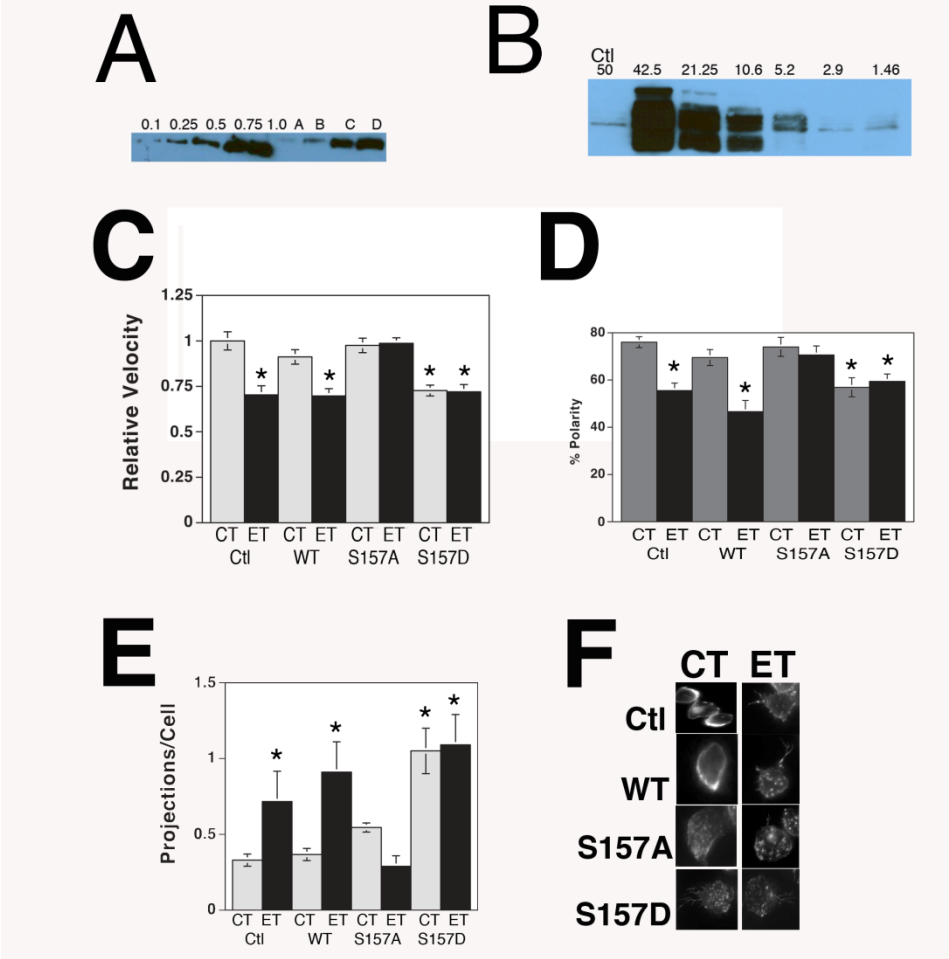

Figure 4-10. Effects of P S157 VASP on regulating actin assembly in human neutrophils. A) Concentration curve of VASP present in human neutrophils. A defined amount of native VASP (0.1 ng, 0.25 ng, 0.5 ng, 0.75 ng and 1 ng) was resolved by SDS-Page and probed with anti-VASP antibody. Protein lysates from human neutrophils at various concentrations were also resolved to determine the concentration of VASP in human neutrophils (A=$2.5X10^3$, B=$2.5X10^4$, C=$2.5X10^5$ and D=$2.5X10^6$ cells/mL). B) Concentration curve of pTAT-VASP wild-type fusion protein. C) Relative velocity of neutrophils transduced with buffer only, pTAT-VASP wild-type (VASP), pTAT-VASP S157A (S157A) and pTAT-VASP S15D (S157D) followed by treatment for 2 h with buffer only (Ctl), Fsk (10 mM) or 500 ng/ml of ET. Error bars indicate the SEMs of the results of 4 experiments. D) Percentage of polarized neutrophils. Error bars show SEMs of 2 experiments. For each condition, 50 cells per experiment were analyzed. E) Number of filopodia per cell formed in neutrophils. Error bars indicate the SEMs 2 experiments, n=50. F) Fluorescent micrograph of human neutrophils transduced with buffer only, pTAT-VASP wild-type, pTAT-VASP S157A or pTAT-VASP S157D for 30 min then treated with buffer only (Ctl) or 500ng/ml of ET. These images are representative of neutrophils observed during polarity analysis. * = $p<0.001$.

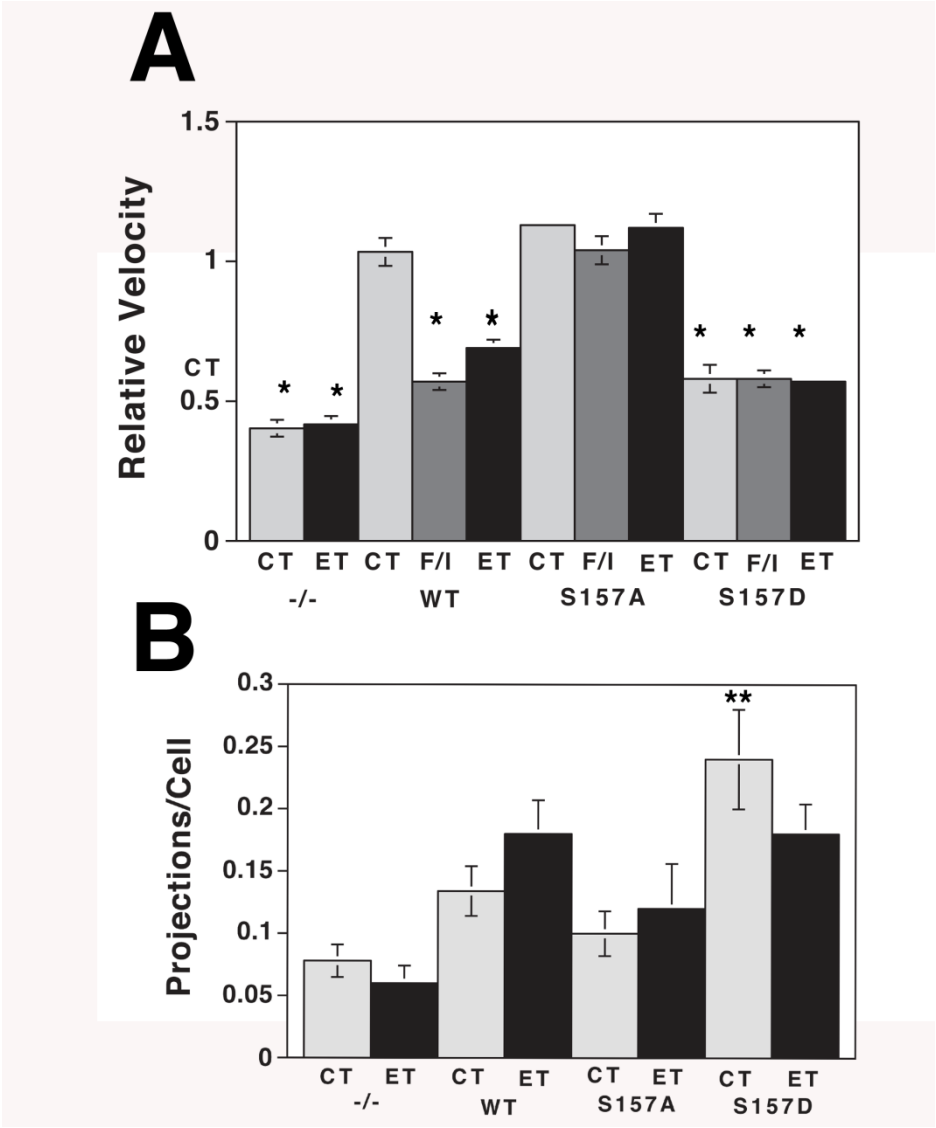

Figure 4-11. Pseudophosphorylated VASP mimics the effects of ET on *Listeria* motility. A) The relative velocity of intracellular *Listeria* in MVd7 cells expressing no Ena/Mena/VASP (-/-), wild-type VASP (VASP), VASP S157A (S157A) or VASP S157D (S157D) after treatment for 2 h with buffer only, Fsk/IBMX (10 mM/100 mM) or 500 ng/ml of ET. Phosphorylation of VASP at S157 decreases *Listeria* motility. Error bars indicate the SEMs n=115. B) Number of filopodia per cell formed by intracellular infection of *Listeria* in MVd7 cells expressing -/-, WT VASP, S157A or S157D VASP after treatment for 2 h with buffer or 500 ng/ml of ET. Phosphorylation of VASP at S157 increases *Listeria* induced filopodia formation. Error bars indicate the SEMs n=50. * = $p<0.001$ and ** = $p<0.046$.

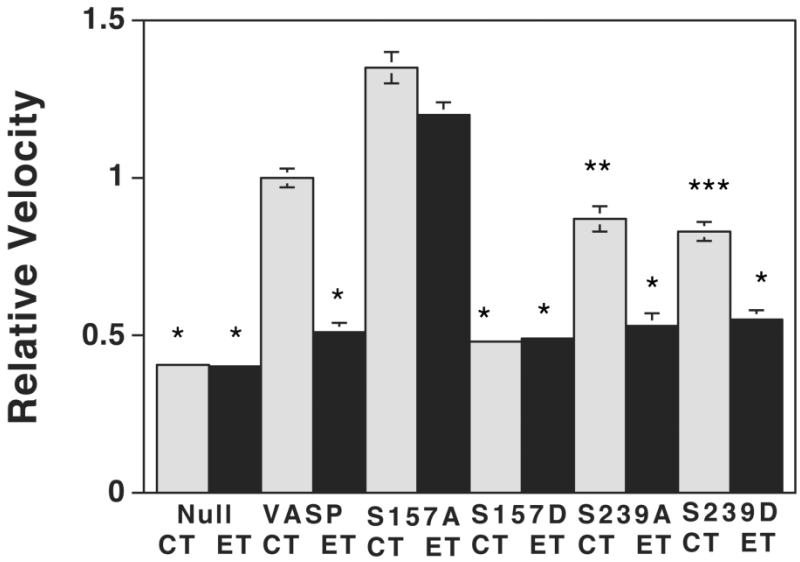

Figure 4-12. Effects of P S239 VASP on regulating actin assembly in human neutrophils. Relative velocity of intracellular *Listeria* in MVd7 cells expressing no Ena/Mena/VASP (-/- null), wild-type VASP (VASP), S157A, S157D, S239A and S239D after treatment for 2 h with buffer only (CT) or 500 ng/ml of ET. Phosphorylation of VASP at S157 significantly decreased *Listeria* motility while ET appeared to only have a slight effect on *Listeria* motility. Error bars indicate the SEMs (n=73). * = $p<0.0001$, ** = $p<0.0091$ and *** = $p<0.0011$.

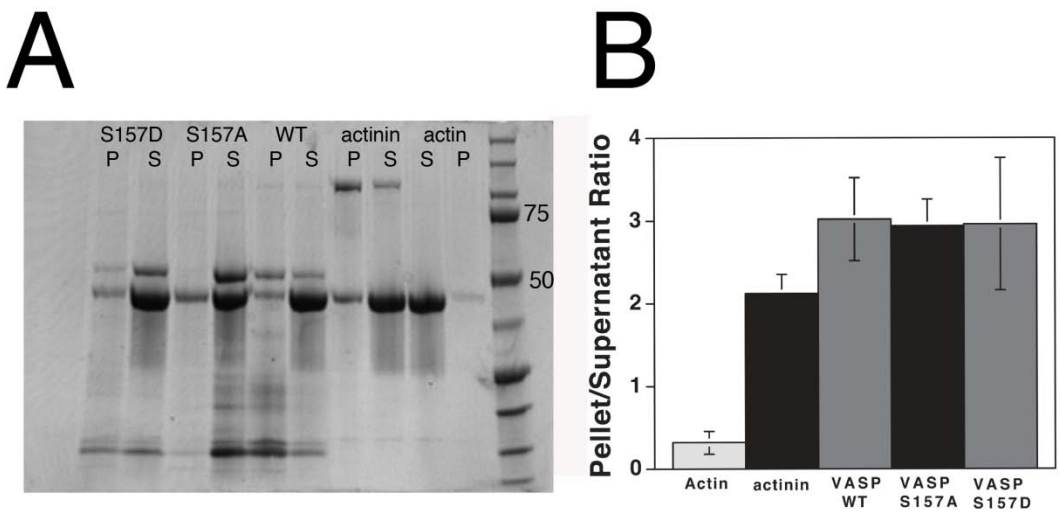

Figure 4-13. Actin Bundling Assay. A) Bundled F-actin was pelleted by 10,000 X g centrifugation, and pellets (P) and supernatants (S) were run on an SDS-PAGE gel. Only in the presence of the F-actin bundling protein alpha-actinin and all three isoforms of VASP (wild-type (WT), S157A and S157D) was actin pelleted at this centrifugation speed. B) Pellet to supernantant ratios were determined. All three VASP isoforms bundle the same pellet/supernatant ratios. $P<0.001$ for actinin and all VASP isoforms compared to actin alone. *, $p<0.001$.

Table 4-2. VASP S157D Interacts with CKAP4

Protein	Wild-type	S157A	S157D
VASP	√	√	√
EIF5A	√	√	√
SFPQ	√	√	√
CKAP4	√	√	√
Similar to non-POU domain	√	√	√

EIF5A: eukaryotic initiation translocation factor 5A; SFPQ: isoform long of splicing factor, proline-glutamine rich; CKAP4: isoform of cytoskeleton associated protein 4; similar to non-POU: octomer binding isoform 1.

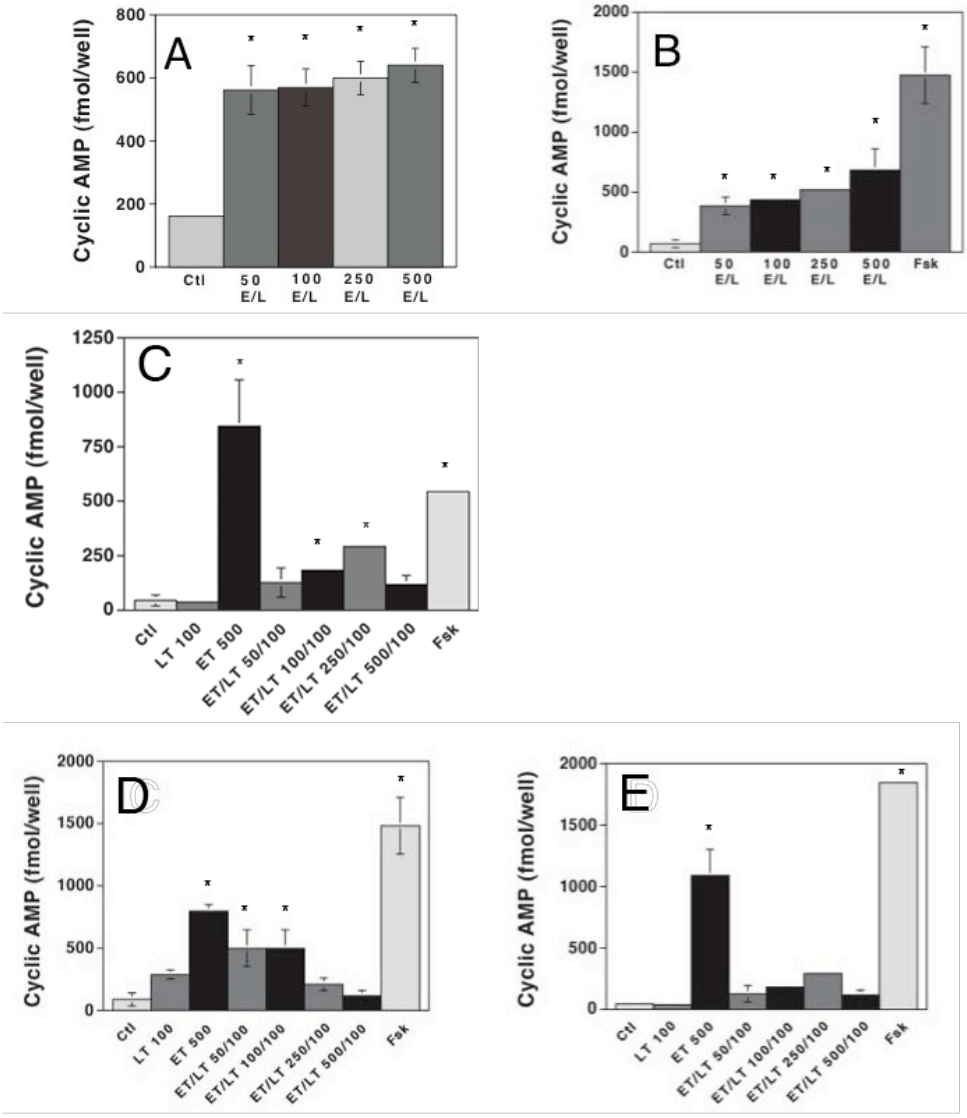

Figure 4-14. Effects of ET+LT on intracellular cAMP levels. A) Decreased ability of ET to increase cAMP levels while in the presence of LT. Neutrophils were treated with increasing amounts of ET and LT (1:1:1 of PA, EF and LF). Error bars indicate the SEM results of 3 separate experiments run in duplicate. B) Decreased ability of ET to increase cAMP levels while in the presence of LT. Neutrophils were treated with increasing amounts of ET and LT (5:1:1 of PA, EF and LF). Error bars indicate the SEM results of 2 separate experiments run in duplicate. C) Decreased ability of ET to increase cAMP levels while in the presence of LT. HeLa cells were treated with increasing amounts of ET and LT (5:1:1 of PA, EF and LF). Error bars indicate the SEM results of 2 separate experiments run in duplicate. D) Complete inhibition of ET to increase cAMP levels in the presence of 100 ng/ml of LT. Error bars indicate the SEM results of 2 experiments run in duplicate. E) Complete inhibition of ET to increase cAMP levels in the presence of 100 ng/ml of LT. Error bars indicate the SEM results of 2 experiments run in duplicate. * = $p<0.001$.

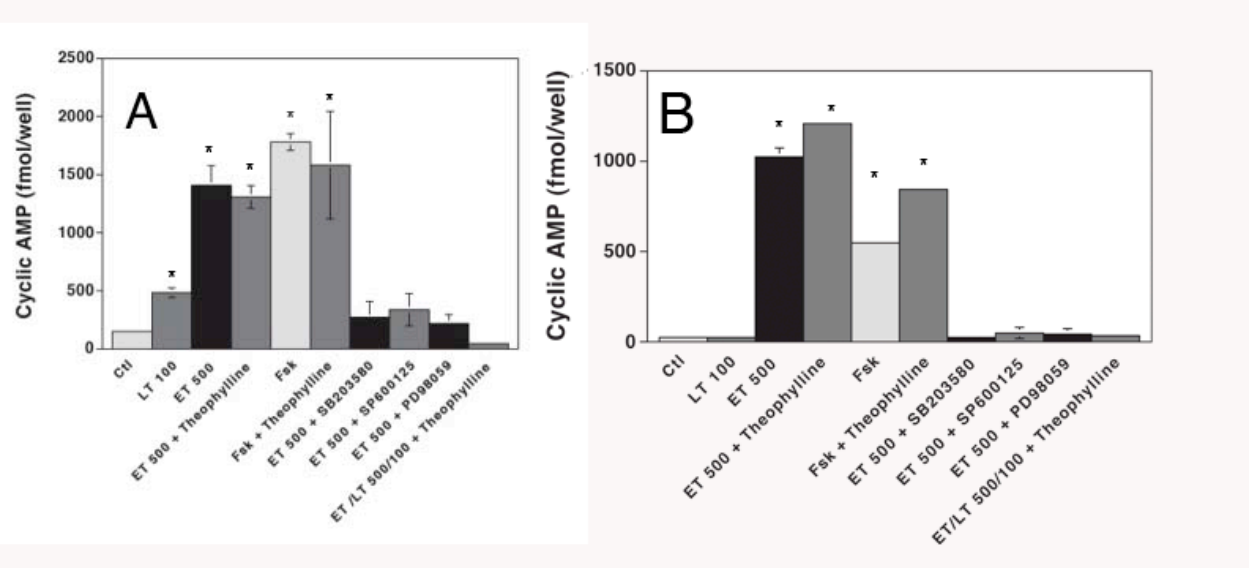

Figure 4-15. How LT inhibits intracellular cAMP levels induced by ET. A) Complete inhibition of cAMP levels in neutrophils after ET and LT treatment, which appears to be due to LT inhibiting one or more MEK pathways. Neutrophils were treated with: buffer only (Ctl), 500 ng/ml of ET (weight ratio 5:1), 100 ng/ml of LT (weight ratio of 5:1), cAMP agonist Fsk at 10 mM, theophylline (50 mM) with 500 ng/ml of ET and then with 500 ng/ml of ET and 100 ng/ml of LT (weight ratio of 5:1:1). Neutrophils were also treated with 500 ng/ml of ET (weight ratio of 5:1) and an individual MAPK inhibitor: SB203880 (100 mM), SP600125 (10 mM) and PD98059 (10 mM). Neutrophils were treated with toxins for 2 h at 37°C. 1 h into the toxin exposure inhibitors were added. Error bars indicate the SEMs results of 2 experiments run in duplicate. All three MEK inhibitors were able to decrease cAMP levels to physiological normal levels while theophylline had no effect on the effects of LT on cAMP. B) Complete inhibition of cAMP levels in HeLa cells after ET and LT treatment. HeLa cells were treated as described in panel A above. Error bars indicate the SEM results of 2 experiments run in duplicate. * = $p<0.0001$ compared to control treated cells.

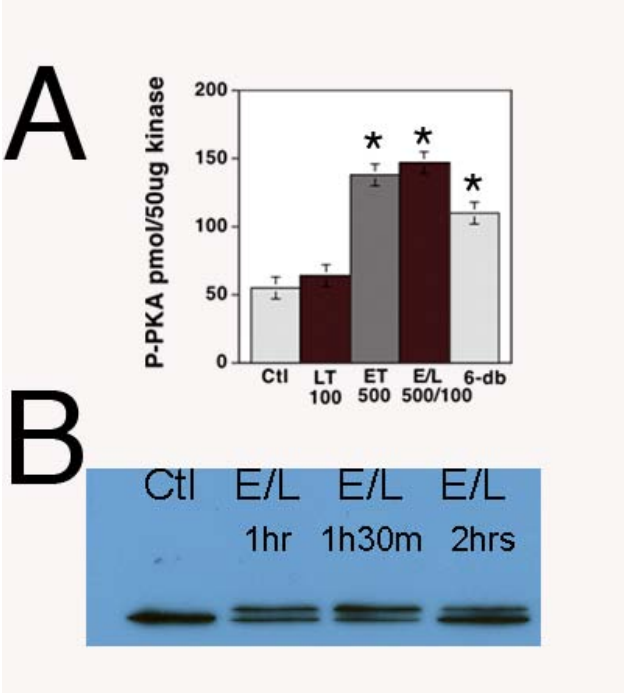

Figure 4-16. Effects of ET+LT on PKA phosphorylation. Bar graph showing the effects of ET+LT on Protein Kinase A (PKA) phosphorylation. Neutrophils were exposed to buffer only (Ctl), treated with 6-db-cAMP (100 mM) for 1 h, and treated with 100 ng/ml LT (weight ratio of 5:1), 500 ng/ml of ET (weight ratio of 5:1) and 100 ng/ml of LT with 500 ng/ml of ET (weight ratio of 5:1:1 of PA, EF and LF) for 2 h at 37°C. A >2-fold increase in phosphorylated PKA was observed not only with ET treatment but also with ET+LT treatment. Control versus 100 ng/ml of LT was not statistically significant ($p>0.05$) nor was 500 ng/ml of ET versus the ET+LT dose response ($p>0.05$). There was no statistical difference between ET and the various concentrations of ET+LT on PKA phosphorylation independent of LT concentrations. Error bars indicate the SEM results of 3 separate experiments. B) Western Blot depicting a time course of VASP phosphorylation at S157 in HeLa cells after ET+LT treatment at 500 ng/ml of each toxin. As with PKA phosphorylation, VASP phosphorylation has been initiated prior to LT entry into the HeLa cell. * = $p<0.001$ compared to control treated cells.

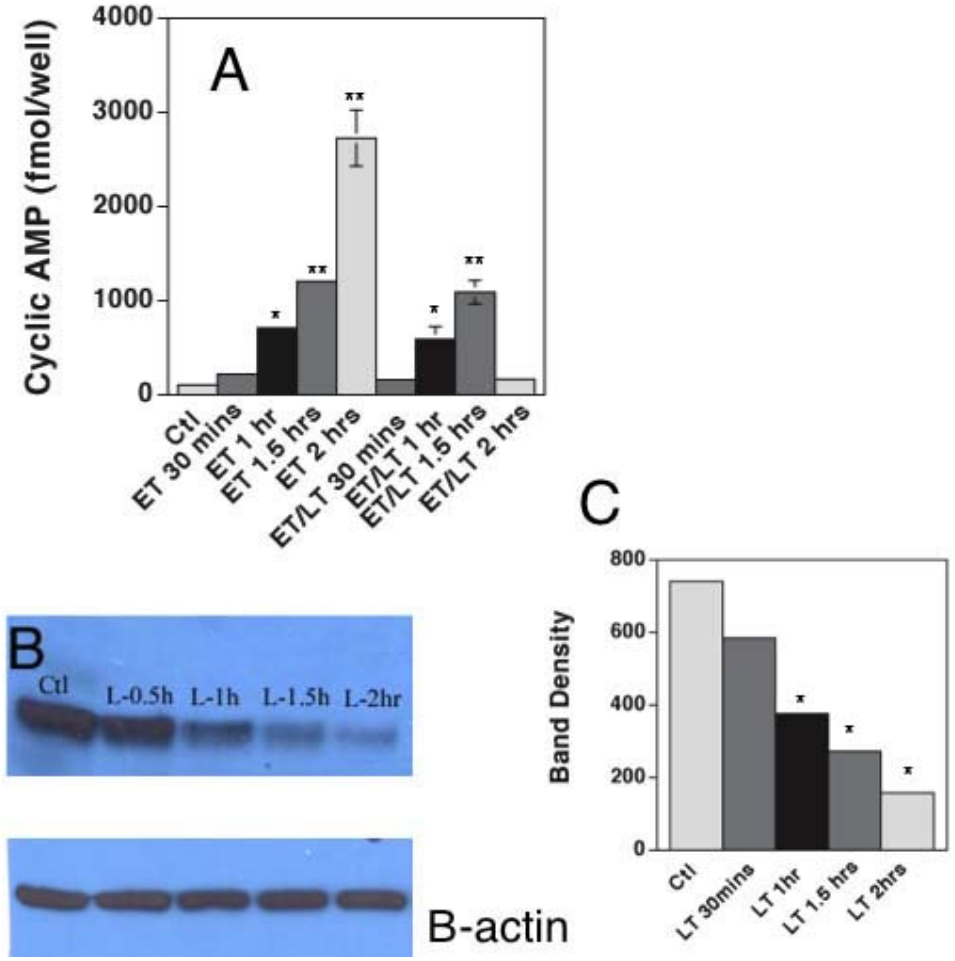

Figure 4-17. Effects of ET+LT on intracellular cAMP levels over time. A) Time dependent response of ET and ET+LT induced intracellular cAMP levels in human neutrophils. Neutrophils were treated with 500 ng/ml of ET (weight ratio of 5:1) or 500 ng/ml of ET and 100 ng/ml of LT (weight ratio of 5:1:1) and incubated at 37°C. Error bars indicate the SEMs of the results of 2 separate experiments run in duplicate. B) Western blot analysis of extracts from buffer only treated (Ctl) and 100 ng/ml LT treated HeLa cells over a 2 h time course using an anti-amino terminal MEK antibody. Under the conditions of our experiment MEK was almost fully cleaved by LT at the 2 h time point. Western blot image is representative of 2 separate experiments. D) Densitometry readings of band intensity from MEK cleavage following LT exposure. * = $p<0.001$ and ** = $p<0.0001$.

CHAPTER 5
DISCUSSION

ET and ET+LT Inhibit Neutrophil Actin-Based Assembly and Impair *Listeria monocytogenes* Intracellular Motility

Neutrophils are a primary component of the innate immune response and are the earliest responders to invasion by bacterial pathogens (213). Recently, we investigated the effects of lethal toxin (LT) on neutrophil motile function and discovered that relatively low concentrations of lethal toxin (50-100 ng/ml) impair neutrophil chemotaxis and chemoattractant-induced actin assembly (39). Both LT and ET have been shown to markedly impair activation of neutrophil NADPH oxidase activity; thus, disarming the powerful superoxide bactericidal system (49).

Less is known about the effects of edema toxin on cell motility. Over two decades have passed since the effects of ET on human neutrophil chemotaxis were last examined (214). Recently investigators have been able to express edema toxin in *E. coli* and have shown that this purified recombinant protein has comparable binding affinity and biological activity to toxin purified from *B. anthracis (192, 193)*. This advance has allowed us to reexamine the biological effects of this calcium-sensitive calmodulin-dependent adenylate cyclase on neutrophil motility. Unlike the original study that noted a doubling of directed neutrophil migration in response to ET, as well as to the combination of PA + EF + LF (191), we find that ET treatment resulted in a concentration dependent reduction in neutrophil chemotaxis (Fig. 4-2G). We utilized a different assay for chemotaxis, video microscopy of neutrophils adherent to a fibronectin-coated surface, rather than migration through agarose, and our utilization of this assay may account for our contradictory findings. As further support for ET-mediated impairment of chemotaxis, we find that ET-treatment also reduces

chemokinesis (Fig. 4-2A) and the ability of neutrophils to polarize in response to the chemoattractant FMLP (Fig. 4-2E). These findings suggested that ET may globally impair neutrophil actin assembly, and our assessment of filament assembly kinetics using Alexa-phalloidin staining revealed that ET slows both the onset and extent of chemoattractant-stimulated neutrophil actin assembly (Fig. 4-5A). The ET-mediated reduction in actin filament content is accompanied by distinct changes in the actin filament localization. Rather than homogeneously concentrating at the leading edge in lamellipodia, as observed in untreated neutrophils exposed to FMLP, actin filaments in ET-treated neutrophils concentrate in discrete small foci dispersed throughout the cell near the adherent membrane surface. This staining pattern is reminiscent of actin filament clusters associated with focal contacts in neutrophils adhered to uncoated plastic surfaces, a condition shown to stimulate actin assembly in the absence of FMLP (154, 187), and suggests that ET may act through similar signal transduction pathways.

Because systemic anthrax infection would be expected to expose neutrophils to the combination of lethal factor, edema factor, and protective antigen, we also examined the effects of this combination. We found that inhibition of chemotaxis, chemokinesis, polarization, as well as FMLP-induced actin assembly are additive. These findings suggest that LF and EF act by different pathways to impair actin-based motility. In addition, the combination of both toxins can reduce the surface expression of the adherence receptor CD11/CD18 (Fig. 4-4), and this effect may contribute to the poor delivery of neutrophils to the sites of infection. It has previously been reported that cAMP elevating agents lead to decreased respiratory burst of neutrophils due to decreased CD18 and impaired actin filament assembly (215). Given the close

association between the cytoskeleton and integrins, it is likely that the marked reduction in actin filament assembly induced by dual toxin treatment may contribute the reduction in CD11/CD18 surface expression. ET-mediated activation of PKA would be expected to phosphorylate and inactivate the actin regulatory protein VASP, as well as activate the G-proteins CDC42 and Rac (216), while LT would be expected to block the activation of ERK, a necessary step in early focal contact formation (217). Future experiments will focus on assessing the contributions of these pathways to adherence and actin assembly. It is of interest that in HeLa cells this same combination does not result in an additive reduction in *Listeria* actin-based motility, each individual toxin, as well as the combination resulting in similar inhibition (Fig. 4-6). However, *Listeria* bypasses many of the signal transduction pathways required for FMLP-induced actin assembly, and therefore, the pathways by which these two toxins inhibit *Listeria* may differ from receptor-induced actin assembly. The shape changes associated with chemotaxis, cell spreading, and phagocytosis are complex and make analysis of rates and directionality of actin assembly difficult. Furthermore, these events involve several steps of receptor-mediated signal transduction. *Listeria* intracellular infection and movement are a particularly useful model for examining the parameters of *in vivo* actin assembly, allowing discrete temporal and spatial resolution of actin filament formation (218).

We have recently discovered that one of the primary downstream targets for LT is the actin monomer sequestering protein heat-shock protein 27 (198). The inability of LT-treated cells to phosphorylate Hsp27 prevents the shuttling of actin monomers to the leading edge of motile cells (198). We are presently beginning to explore the pathway,

or pathways, by which ET interferes with actin assembly. As previously reported (49, 191), we find that ET induces a rise in cAMP levels, and under the conditions of our experiments we observe a >50 fold rise of cAMP in neutrophils. Our findings are consistent with previous observations in neutrophils and T lymphocytes showing that agents inducing a rise in cAMP impair actin assembly and chemotaxis (67, 189, 214, 219-221). However, a simple quantitative relationship between cAMP levels and alterations in chemotaxis has not been observed, suggesting that additional signal transduction pathways can modify the effects of cAMP (67, 214, 219).

For the first time, we document that the ET-induced rise in cAMP is accompanied by the phosphorylation of PKA in human neutrophils. Our findings are consistent with previous observations that ET treatment increases cAMP levels and activates PKA in many other cell types (196, 222-224). Our experiments utilizing the intracellular bacteria *Listeria* help to narrow the potential downstream targets for ET and activated PKA. *Listeria* requires the bacterial surface protein ActA, and this protein directly activates the host cell Arp2/3 complex (225). ActA also attracts the actin-regulatory protein VASP (139). On the other hand, *Shigella* requires the bacterial surface protein IcsA (226). IcsA directly attracts and activates the host cell protein N-WASP, and this protein in-turn activates Arp2/3 complex (227). Also *Shigella*, unlike *Listeria,* does not require VASP for intracellular actin-based motility (208). Finally, *Listeria* requires PI3 kinase activity, while Shigella does not (218). Thus the ability of ET to impair *Listeria*, but not *Shigella* actin-based motility, points to three potential mechanisms of ET action: 1. impairment of ActA-induced activation of the Arp2/3 complex, 2. inhibition of VASP binding or activation by ActA, or 3. inhibition of PI3 kinase activity. It is also possible that an

additional previously unappreciated difference in the pathways by which *Listeria* and *Shigella* direct the actin-regulatory protein pathways of the host cell, accounts for our observations.

VASP Phosphorylation Impairs Neutrophil and *Listeria* Actin-Based Motility

Inhalation anthrax is a rapidly progressive disease that is associated with high levels of mortality with death occurring shortly after the onset of symptoms (228). Genomic analysis has revealed that, as compared with its close phylogenetic neighbor *Bacillus cereus, B. anthracis* is unique in possessing edema and lethal toxin (229). These toxins primarily enhance anthrax virulence by paralyzing the host's innate immune response. Neutrophils are a primary component of the innate immune response and are considered the first responders during infection. Recently, we showed that ET impairs neutrophil chemotaxis and chemoattractant induced actin assembly (106).

Previous work from our lab and others (106, 222-224, 230) has shown that ET-induces a marked rise in cAMP and this rise is accompanied by the phosphorylation of PKA, a condition that would be expected to activate this kinase. In addition to reducing actin filament assembly and chemotaxis in human neutrophils, ET slows *Listeria monocytogenes* actin-based intracellular motility in HeLa cells, but has no effect on another actin-mediated process, intracellular motility of *Shigella flexerni* (1). *Listeria* is known to require VASP for efficient intracellular motility, while *Shigella* does not (231). Furthermore, VASP S157 is known to be a substrate for PKA phosphorylation (63, 111, 144, 145, 148, 160, 184, 232). These observations point to VASP as a potential downstream target for ET-mediated neutrophil paralysis.

Ena/VASP was originally discovered in platelets as a substrate for PKA and PKG (233). VASP localizes to sites of dynamic actin remodeling, such as filopodia, lamellipodia and focal adhesions (147, 159). VASP has several effects on actin including enhancing actin assembly (164, 234), and bundling of actin filaments (153, 164, 179, 234-236). Phosphorylation of VASP at S157 (VASP P157) has been shown to lower the affinity of VASP for actin filaments (163, 237), as well as the SH3 domains of Abl (63), Src and αII-spectrin (237). However, the *in vivo* contribution of VASP phosphorylation to the regulation of actin filament assembly and architecture remains unclear. Chemoattractant stimulation of human neutrophils induces a rapid and transient PKA-dependent phosphorylation of VASP Ser 157, the percentage of total VASP phosphorylated at S157 increasing from 40 to 60% within 30 s of exposure to FMLP, and returning to baseline within 20 minutes. In ET-treated PMN, VASP phosphorylation persists for greater than 2 h preventing the cycling of VASP between the phosphorylated and dephosphorylated forms (See Fig. 4-7). ET treatment also results in an increase VASP P157 content at the leading edge of neutrophils associated with impaired chemotaxis, chemokinesis and neutrophil polarity, suggesting that persistent VASP phosphorylation may impair neutrophil actin-based motility. In addition to neutrophils, accumulation of phosphorylated VASP S157 at sites of high actin dynamics has been observed in the cell periphery of forskolin-treated endothelial cells (165). ET treatment also results in an increase in VASP P157 content around intracellular *Listeria* (Fig. 4-8) and is associated with a decrease in *Listeria*-actin based motility (106).

The above findings suggest that persistent phosphorylation of VASP S157 impairs actin-based motility. To substantiate this possibility we utilized recombinant pseudophosphorylated and unphosphorylated VASP constructs and introduced them into neutrophils utilizing a TAT-chimera proteins and rescued ENA/VASP null MVd7 cells with VASP wild-type and mutant proteins. Consistent with ET treatment, introduction of pseudo-phosphorylated VASP (S157D) impaired neutrophil chemokinesis and polarity and slowed *Listeria* motility in MVd7 cells (Figs. 4-9, 4-11 and 4-12). While introduction of pseudo-unphosphorylated VASP (S157A) accelerated *Listeria* motility and rendered both MVd7 cells and neutrophils resistant to the inhibition of actin-based motility by ET. Using these same methods, we found that pseudo-phosphorylated and unphosphorylated VASP S239 had no effect on actin-based motility in our cells. We conclude that persistent VASP S157 phosphorylation is the primary mechanism by which anthrax edema toxin impairs actin-based motility.

An unexpected additional dividend of our investigations was the discovery of an association between VASP phosphorylation and filopodia formation. Filopodia have been implicated in a number of cellular processes including neuronal growth cone path finding, embryonic development, wound healing, and metastasis. Recent work in neuronal cells demonstrates the crucial role Ena/VASP proteins have in filopodia formation (211). Similarly, in *Dictyostelium*, genetic ablation of dVASP, the sole Ena/VASP member present in the organism, decreases filopodia formation and causes chemotactic defects (143). Hyperphosphorylation of VASP S157 in human platelets is associated with hyper-production of filopodia and increased platelet aggregation in response to collagen (166, 238). Much to our initial surprise, we discovered that ET

treatment of human neutrophils significantly increased the number of filopodia per cell. Similarly, introduction of pseudophophoshorlated VASP S157D increased while pseudo-unphosphorlated VASP S157A reduced filopodia number (Fig. 4-11). *Listeria* are also known to form membrane projections that mimic the actin architecture of filopodia (157) and we found that introduction of pseudophophorylated VASP significantly increased the number of membrane projections containing bacteria (Fig. 4-9). Such membrane projections push into adjacent cells and promote *Listeria* spread to adjacent cells while avoiding the extracellular environment. Thus VASP phosphorylation not only accounts for ET effects on actin-based motility, and is also likely to play an important role in *Listeria* cell-to-cell spread. It has been proposed that Ena/VASP protein promotes actin filament bundling, (179, 235, 239, 240) bringing filaments into closer proximity to allow fascin to strengthen filopodia bundles, and fascin as well as VASP are found in both filopodia and *Listeria* membrane projections (241-243). It is of interest that filopodia fail to form in *Dictyostelium* lacking VASP and are markedly reduced in neural cells lacking Ena/Mena/VASP (143, 244, 245). To test the possibility that VASP S157 phosphorylation enhances VASP actin filament bundling; we compared the bundling function of purified wild-type, pseudo-phosphorylated and pseudo-unphosphorylated VASP, but found no differences in their abilities to bundle purified actin filaments (Figure 6). We suspect that enhanced binding of phospho-VASP to Abl, α-spectrin (163, 237) may facilitate filopodia formation, and these possibilities warrant future investigation.

The profound effects of ET on VASP S157 phosphorylation, cell motility and filopodia formation emphasize the importance of cAMP/PKA pathway for actin-based

motility and filopodia formation. These findings not only help to explain how anthrax impairs the innate immune system, and *Listeria* spreads from cell-to-cell, but also may have relevance for neurite outgrowth, platelet shape change, wound healing, embryonic development and tumor metastasis.

Cell Entry and Manipulation of Host Signaling Pathways

The innate immune response is the first line of defense against invading pathogens, and it plays a central role in acute anthrax infection. *B. anthracis* triggers a strong inflammatory response by activating TLR4 on neutrophils and macrophages at the entry site into the host. LT and ET interfere with this process, as the MEK pathway cascade is essential for full induction of the oxidative burst and pro-inflammatory cytokine expression (246), for cell migration (32). The strong increase in cAMP induced by ET is a potent inhibitor of these processes (247). In general, bacterial toxins that increase cAMP levels mostly effect immune cells and dampen the immune system to facilitate the survival of bacteria, contributing to the establishment of infection (58).

Of the two toxins, LT has been more extensively investigated, with little attention has been paid to ET and ET+LT. During systemic anthrax infection, neutrophils are exposed to both LT and ET. Therefore, we examined the effects of ET+LT on human neutrophils. It was of great interest to find that exposure of neutrophils to ET+LT inhibits the rise in intracellular cAMP levels (Fig. 4-14).

cAMP levels are down-regulated by phosphodiesterases (63). Human neutrophils were treated with ET and LT in concert with theophylline, a known phosphodiestease inhibitor, to determine if LT had phosphodiesterase like characteristics (Fig. 4-15). These results led us to conclude that LT does not act by activating phosphodiesterases and appears to inhibit the increased cAMP levels by

impairing one or more MEK pathways. Even though LT impaired the intracellular increase in cAMP levels, there was still sufficient time for ET to enter the cell and cause its effects because there was no effect on PKA phosphorylation between ET and ET+LT and these effects were independent of the concentration of LT (Fig. 4-17). ET is still able to cause a two-fold increase in PKA phosphorylation after LT treatment.

Timing of toxin affects came to the forefront as an important factor. A time course of ET infection showed that cAMP levels began to increase at 30 minutes post-exposure and continued to increase throughout the two-hour time-course (Fig. 4-18). Neutrophils were subjected to the same time-course but were exposed to ET and LT. Neutrophils exposed to both toxins were able to increase intracellular cAMP levels until 1.5 hours post-exposure when the levels began to decrease, and by two hours were at physiologically normal levels. This led us to speculate that ET may only require an hour to affect cell physiology, increase intracellular cAMP levels and activate downstream effector molecules. Previous work done by our lab (39) has shown that LT requires a minimum of two hours for near complete cleavage of MEKs (Fig. 4-18), and this MEK cleavage at two hours correlates with maximal inhibition of neutrophil chemotaxis after LT treatment. A similar time course of chemokinesis and polarity was done with neutrophils exposed to ET (Fig. 4-3). We found that the mechanism of LT action takes longer due to the proteolytic cleavage of the MEKs, while once ET is in the cell I can immediately serve as an adenylate cyclase.

There must be a biological basis for the difference in the way ET and LT are processed. ET and LT are unique toxins in that they both share the common receptors of TEM8 and CMG2 for binding moieties and subsequent entry into the cell (31, 32). An

increase in surface expression of receptors has consequences for both toxins. It has recently been shown by Maldonado-Arocho, et al. (51) that ET is able to increase the mRNA levels of both receptors in murine macrophages. Due to the early entry of ET, we speculate this allows ET to increase receptors during the first 20-60 minutes allowing increased entry of LT. Perhaps the concentration requirements of LT to effectively cleave all the MEKs are higher, necessitating ET to aid in increased LT entry. This would be of technical benefit for allowing more complete paralysis of the innate immune function allowing anthrax to readily survive in the host.

ET is a key component utilized by *B. anthracis* to thwart the host immune defenses and potentially helps to establish a successful infection. Having continuously high levels of cAMP may be deleterious to the bacteria itself. With *Bordetella pertussis,* an adenylate cyclase producing bacteria generates high levels of cAMP for a short period of time and then down-regulates cAMP for the duration of infection (249). LT appears to decrease ET's increase in intracellular cAMP similar to what *B. pertussis* does once it has established an infection within the host. Similar to *B. pertussis*, ET is important in establishment of infection but prolonged exposure to supraphysiological levels of cAMP could hamper the bacteria in the long run. It appears that allowing LT to enter the cell later gives ET time to establish its downstream mechanism of action. The exact mechanism of action is the bases of future research in our lab.

CHAPTER 6
FUTURE WORK

Vascular Sepsis Caused During Inhalation Anthrax

Hemorrhage and pleural effusion are prominent pathological features of systemic anthrax infection. There is growing evidence for LT having a direct effect on endothelial cell function during infection ultimately leading to septic shock. Primary human endothelial cells exposed to LT have previously shown that the loss of MEK function inhibits the ability of p38 phosphorylation and its subsequent downstream effects on phosphorylating the actin monomer binding protein Hsp27 (198). Blockage of hsp27 phosphorylation by LT prevents hsp27 from releasing sequestered actin monomers for new actin filament assembly (198). LT induces a time and concentration dependent decrease in transendothelial electrical resistance (impedance) and an increase in permeability of fluorescently labeled albumin (unpublished work) (250). These changes in permeability following LT treatment are accompanied by altered distribution of actin fibers and the adherence junctional protein VE-cadherin, which are both necessary for barrier function (250). These findings support a role for LT induced barrier dysfunction in the vascular permeability changes associated with systemic anthrax infection.

To date, the effects of ET on vascular endothelial cell junctions have not been studied. Previous research (220) has shown that cAMP inducing agents like Fsk inhibit F-actin assembly in stimulated T cells via the direct activation of the cAMP-PKA pathway. We have shown that ET, LT and ET+LT at low concentrations impair neutrophil chemotaxis and chemotactic movement, which is associated with the ability of neutrophils to undergo actin assembly (251). ET affects actin assembly by increasing cAMP, which activates PKA causing the phosphorylation of VASP at S157 to

impair F-actin polymerization (in press). Our prior research suggests that in addition to VASP phosphorylation and inhibition of Hsp27 phosphorylation, ET and LT are likely to alter the functions of one or more additional actin regulatory proteins.

The vascular system is integrated with endothelial cells that serve as a barrier and join junctions together to retain fluid and red blood cells within the intravascular space. Breakdown of cell-cell junctions can lead to extravasations of intravascular fluid resulting in shock. One mechanism by which pathogens can weaken the endothelial cell-cell junctions is by altering the underlying actin cytoskeleton. There are two types of junctions, adherens junctions and a more exclusive barrier called the tight junction (Figure 6-1). VE-cadherin is the outermost protein that serves to glue the vascular cells together in the adherens junctions. The intracellular portion of VE-cadherin binds to β-catenin, α-catenin, α-actinin and vinculin. α-catenin, actinin and vinculin can all bind to actin filaments and serve to attract large bundles of filamentous actin to this region to help stabilize the cell junction (252). However, the mechanisms underlying actin filament assembly and disassembly in the region of cell-cell junctions are poorly understood. We do know that disassembly of actin filaments impairs cell junctions indicating that actin filaments are vital for the integrity of the cell junctions.

Once adherens junctions have formed, tight junctions can be created. Tight junctions prevent small molecules from leaking through the vascular endothelial junctions. Two transmembrane proteins, occludin and claudin, are the primary components (253). Phosphorylation of occludin is required for proper membrane localization. Claudin-5 possesses a binding sequence for ZO-1 (254), which associates

with the cytoskeletal protein α-spectrin. α-spectrin in turn binds VASP (237), which provides a link between tight junctions to the underlying actin cytoskeleton.

The ultimate consequence of inhalation anthrax is septic shock, which is 80-100% lethal even with proper treatment. To date, the only treatment for sepsis is supportive care because we do not understand the underlying physiological condition to provide better care. One of the major components responsible for maintaining the integrity of vascular junctions is filamentous actin. The signal transduction mechanisms that regulate actin found at cell junctions are poorly understood. Future work will analyze septic shock and promises to lead to new therapeutic approaches for all forms of septic shock associated with vascular leakage. A better understanding of biochemical pathways regulating vascular cell junctions could also provide new therapies to alter the permeability of the blood-brain barrier and allow for more efficient delivery of chemotherapeutic agents to the cerebral cortex.

The Role of VASP in Filopodia Formation

The actin cytoskeleton plays a central role in cell-cell junctions. Over time the actin cytoskeleton is able to remodel itself along with remodeling the cell-cell junctional proteins (255). The exact mechanism underlying this rearrangement has yet to be fully elucidated. Several reports suggest that small GTPases of the Rho family may be involved (256). Recent work on adherence junctions has found that when primary cells are stimulated, they form intercellular junctions by an active process driven by actin polymerization. The process requires the production of filopodia, which penetrate neighboring cells. The physical force exerted by the filopodia draws the opposing cells together to form adherence junctions. Vasioukhin, et al. (168) were able to show that

production of filopodia with adherence proteins at the tip yielded adherence junction, whose stabilization depended on α-catenin, VASP, and actin polymerization and reorganization. To date, limited research on epithelial cells and the formation of adherence junctions has been performed, and virtually no studies have examined the formation of both adherence and tight junctions in endothelial cells. In our work with neutrophils and MVd7 cells, we found that VASP isoform S157D increased filopodia formation (Fig. 4-14 and Fig. 4-16). This is in direct correlation with what was recently reported in macrophages. Kim, et al. (224) found that the filopodia increased in quantity after ET treatment in macrophages, but they also found an increase in chemokinesis whereas we have found a decrease in neutrophil chemokinesis. We attribute the difference in chemotaxis to the different nature of cell motility in neutrophils and macrophages. The forward movement of the macrophage requires the extension of the filopodia and lamellipodia. In neutrophils, filopodia formation is not common and the neutrophil relies on the extension of the lamellipodia for forward movement (257).

It has been shown that when primary endothelial cells are stimulated, they form intercellular junctions by an active and dynamic process of filopodial formation, which penetrates and embeds into neighboring cells. The physical force of drawing two opposing membranes together is maximized at the tips of the filopodia, by clusters of adherence junctional proteins, VASP, vinculin and zyxin. The stabilization of the junctions depends on VASP and actin polymerization and reorganization (168). We hypothesize that ET's enhanced filopodia formation will serve to at least partly reverse LT's effects on vascular tight junctions.

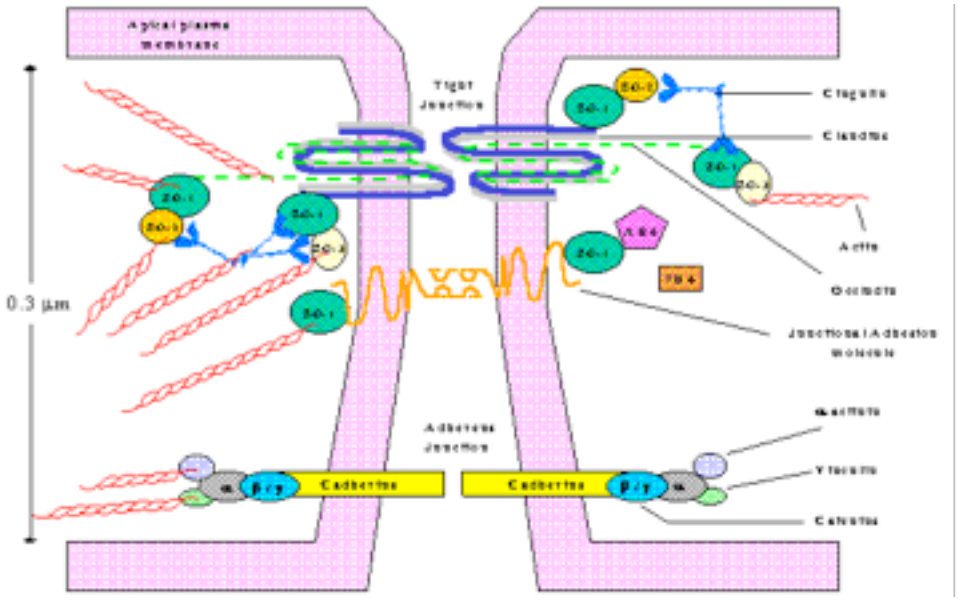

Figure 6-1. Schematic Diagram of Vascular Endothelial Junctions. There are two types of junctions: 1) Adherens junctions (lower junction) made up of VE-cadherin, the catenins, alpha-actinin, and vinculin. 2) Tight Junctions (upper junction) made up of occluding and claudins, ZO-1, spectrin and VASP (black). Both junctions link to the actin cytoskeleton (red helical structures).

LIST OF REFERENCES

1. Jernigan JA*, et al.* (2001) Bioterrorism-related inhalational anthrax: the first 10 cases reported in the United States. *Emerg Infect Dis* 7(6):933-944.

2. Guarner J*, et al.* (2003) Pathology and pathogenesis of bioterrorism-related inhalational anthrax. *Am J Pathol* 163(2):701-709.

3. Tournier J-N, Ulrich RG, Quesnel-Hellmann A, Mohamadzadeh M, & Stiles BG (2009) Anthrax, toxins and vaccines: a 125-year journey targeting *Bacillus anthracis*. *Expert Review of Anti-infective Therapy* 7(2):219-236.

4. Keim P & Smith KL (2002) *Bacillus anthracis* evolution and epidemiology. *Curr Top Microbiol Immunol* 271:21-32.

5. Koch R (1843-1910) Historical views and diseases and epidemics. in *Harvard University Library Open Collections Program*.

6. Schwartz M (2009) Dr. Jekyll and Mr. Hyde: a short history of anthrax. *Mol Aspects Med* 30(6):347-355.

7. Spencer RC (2003) *Bacillus anthracis*. *J Clin Pathol* 56(3):182-187.

8. Hawley RJ & Eitzen EM, Jr. (2001) Biological weapons--a primer for microbiologists. *Annu Rev Microbiol* 55:235-253.

9. Abramova AA & Grinberg LM (1993) Pathology of anthrax sepsis according to materials of the infectious outbreak in 1979 in Sverdlovsk (microscopic changes. *Arkh Patol* 55(1):18-23.

10. Inglesby TV*, et al.* (2002) Anthrax as a biological weapon, 2002: updated recommendations for management. *JAMA* 287(17):2236-2252.

11. Peters CJ & Hartley DM (2002) Anthrax inhalation and lethal human infection. *Lancet* 359(9307):710-711.

12. Ruthel G, Ribot WJ, Bavari S, & Hoover TA (2004) Time-lapse confocal imaging of development of *Bacillus anthracis* in macrophages. *J Infect Dis* 189(7):1313-1316.

13. Dixon AE*, et al.* (1999) Alloreactive Th1 cells localize in lung and induce acute lung injury. *Chest* 116(1 Suppl):36S-37S.

14. Brittingham KC*, et al.* (2005) Dendritic cells endocytose *Bacillus anthracis* spores: Implications for anthrax pathogenesis. *J Immunol* 174(9):5545-5552.

15. Bozue JA*, et al.* (2005) Construction of a rhamnose mutation in *Bacillus anthracis* affects adherence to macrophages but not virulence in guinea pigs. *Microbial Pathogenesis* 38(1):1-12.

16. Henderson DW, Peacock S, & Belton FC (1956) Observations on the prophylaxis of experimental pulmonary anthrax in the monkey. *J Hyg (Lond)* 54(1):28-36.

17. Dai Z, Sirard JC, Mock M, & Koehler TM (1995) The atxA gene product activates transcription of the anthrax toxin genes and is essential for virulence. *Mol Microbiol* 16(6):1171-1181.

18. Guidi-Rontani C*, et al.* (1999) Identification and characterization of a germination operon on the virulence plasmid pXO1 of *Bacillus anthracis*. *Mol Microbiol* 33(2):407-414.

19. Mignot T, Mock M, & Fouet A (2003) A plasmid-encoded regulator couples the synthesis of toxins and surface structures in *Bacillus anthracis. Mol Microbiol* 47(4):917-927.

20. Schneerson R*, et al.* (2003) Poly(gamma-D-glutamic acid) protein conjugates induce IgG antibodies in mice to the capsule of *Bacillus anthracis*: a potential addition to the anthrax vaccine. *Proc Natl Acad Sci U S A* 100(15):8945-8950.

21. Makino Y, Negoro S, Urabe I, & Okada H (1989) Stability-increasing mutants of glucose dehydrogenase from *Bacillus megaterium* IWG3. *J Biol Chem* 264(11):6381-6385.

22. Shannon JG, Ross CL, Koehler TM, & Rest RF (2003) Characterization of anthrolysin O, the *Bacillus anthracis* cholesterol-dependent cytolysin. *Infect. Immun.* 71(6):3183-3189.

23. Alouf JE (2001) Pore-forming bacterial protein toxins: an overview. *Curr Top Microbiol Immunol* 257:1-14.

24. Kayal S & Charbit A (2006) Listeriolysin O: a key protein of *Listeria monocytogenes* with multiple functions. *FEMS Microbiol Rev* 30(4):514-529.

25. Mosser EM & Rest RF (2006) The *Bacillus anthracis* cholesterol-dependent cytolysin, Anthrolysin O, kills human neutrophils, monocytes and macrophages. *BMC Microbiol* 6:56.

26. Park JM, Ng VH, Maeda S, Rest RF, & Karin M (2004) Anthrolysin O and other gram-positive cytolysins are toll-like receptor 4 agonists. *J Exp Med* 200(12):1647-1655.

27. Jernigan DB*, et al.* (2002) Investigation of bioterrorism-related anthrax, United States, 2001: epidemiologic findings. *Emerg Infect Dis* 8(10):1019-1028.

28. Bravata DM*, et al.* (2006) Reducing mortality from anthrax bioterrorism: strategies for stockpiling and dispensing medical and pharmaceutical supplies. *Biosecur Bioterror* 4(3):244-262.

29. Friedlander AM (1986) Macrophages are sensitive to anthrax lethal toxin through an acid-dependent process. *J. Biol. Chem.* 261(16):7123-7126.

30. Gordon VM, Leppla SH, & Hewlett EL (1988) Inhibitors of receptor-mediated endocytosis block the entry of *Bacillus anthracis* adenylate cyclase toxin but not that of *Bordetella pertussis* adenylate cyclase toxin. *Infect. Immun.* 56(5):1066-1069.

31. Bradley KA, Mogridge J, Mourez M, Collier RJ, & Young JA (2001) Identification of the cellular receptor for anthrax toxin. *Nature* 414(6860):225-229.

32. Scobie HM, Rainey GJ, Bradley KA, & Young JA (2003) Human capillary morphogenesis protein 2 functions as an anthrax toxin receptor. *Proc Natl Acad Sci U S A* 100(9):5170-5174.

33. Gordon VM, Klimpel KR, Arora N, Henderson MA, & Leppla SH (1995) Proteolytic activation of bacterial toxins by eukaryotic cells is performed by furin and by additional cellular proteases. *Infect Immun* 63(1):82-87.

34. Milne JC, Furlong D, Hanna PC, Wall JS, & Collier RJ (1994) Anthrax protective antigen forms oligomers during intoxication of mammalian cells. *J Biol Chem* 269(32):20607-20612.

35. Mogridge J, Cunningham K, Lacy DB, Mourez M, & Collier RJ (2002) The lethal and edema factors of anthrax toxin bind only to oligomeric forms of the protective antigen. *Proc Natl Acad Sci U S A* 99(10):7045-7048.

36. Wesche J, Elliott JL, Falnes PO, Olsnes S, & Collier RJ (1998) Characterization of membrane translocation by anthrax protective antigen. *Biochemistry* 37(45):15737-15746.

37. Duesbery NS*, et al.* (1998) Proteolytic inactivation of MAP-Kinase-Kinase by anthrax lethal factor. *Science* 280(5364):734-737.

38. Pellizzari R, Guidi-Rontani C, Vitale G, Mock M, & Montecucco C (2000) Lethal factor of *Bacillus anthracis* cleaves the N-terminus of MAPKKs: analysis of the intracellular consequences in macrophages. *Int J Med Microbiol* 290(4-5):421-427.

39. During RL*, et al.* (2005) Anthrax lethal toxin paralyzes neutrophil actin-based motility. *The Journal of Infectious Diseases* 192(5):837-845.

40. Kassam A, Der SD, & Mogridge J (2005) Differentiation of human monocytic cell lines confers susceptibility to *Bacillus anthracis* lethal toxin. *Cell Microbiol* 7(2):281-292.

41. Wu AG*, et al.* (2003) Anthrax toxin induces hemolysis: an indirect effect through polymorphonuclear cells. *J Infect Dis* 188(8):1138-1141.

42. Alileche A, Serfass ER, Muehlbauer SM, Porcelli SA, & Brojatsch J (2005) Anthrax lethal toxin-mediated killing of human and murine dendritic cells impairs the adaptive immune response. *PLoS Pathog* 1(2):e19-29.

43. Ribot WJ*, et al.* (2006) Anthrax lethal toxin impairs innate immune functions of alveolar macrophages and facilitates *Bacillus anthracis* survival. *Infect Immun* 74(9):5029-5034.

44. Webster JI*, et al.* (2003) Anthrax lethal factor represses glucocorticoid and progesterone receptor activity. *Proc Natl Acad Sci U S A* 100(10):5706-5711.

45. Kumar P, Ahuja N, & Bhatnagar R (2002) Anthrax edema toxin requires influx of calcium for inducing cyclic AMP toxicity in target cells. *Infect. Immun.* 70(9):4997-5007.

46. Kumar B*, et al.* (2002) Mevastatin induces degeneration and decreases viability of cAMP-induced differentiated neuroblastoma cells in culture by inhibiting proteasome activity, and mevalonic acid lactone prevents these effects. *J Neurosci Res* 68(5):627-635.

47. Welkos S, Little S, Friedlander A, Fritz D, & Fellows P (2001) The role of antibodies to *Bacillus anthracis* and anthrax toxin components in inhibiting the early stages of infection by anthrax spores. *Microbiology* 147(Pt 6):1677-1685.

48. Kent EG (1989) The Albert Lasker Medical Awards. Role of the cyclic AMP-dependent protein kinase in signal transduction. *JAMA* 262(13):1815-1818.

49. Crawford MA, Aylott CV, Bourdeau RW, & Bokoch GM (2006) *Bacillus anthracis* toxins inhibit human neutrophil NADPH oxidase activity. *J Immunol* 176(12):7557-7565.

50. O'Brien J, Friedlander A, Dreier T, Ezzell J, & Leppla S (1985) Effects of anthrax toxin components on human neutrophils. *Infect. Immun.* 47(1):306-310.

51. Maldonado-Arocho FJ, Fulcher JA, Lee B, & Bradley KA (2006) Anthrax edema toxin induces anthrax toxin receptor expression in monocyte-derived cells. *Mol Microbiol* 61(2):324-337.

52. Moss J*, et al.* (1984) NIH conference. Cyclic nucleotides: mediators of bacterial toxin action in disease. *Ann Intern Med* 101(5):653-666.

53. Jalink K & Moolenaar WH (2010) G protein-coupled receptors: the inside story. *Bioessays* 32(1):13-16.

54. Sutherland EW & Rall TW (1958) Fractionation and characterization of a cyclic adenine ribonucleotide formed by tissue particles. *J Biol Chem* 232(2):1077-1091.

55. Baillie GS (2009) Compartmentalized signalling: spatial regulation of cAMP by the action of compartmentalized phosphodiesterases. *FEBS J* 276(7):1790-1799.

56. Hong J*, et al.* (2005) Anthrax edema factor potency depends on mode of cell entry. *Biochem Biophys Res Commun* 335(3):850-857.

57. Kamenetsky M*, et al.* (2006) Molecular details of cAMP generation in mammalian cells: a tale of two systems. *J Mol Biol* 362(4):623-639.

58. Ahuja N, Kumar P, & Bhatnagar R (2004) The adenylate cyclase toxins. *Crit Rev Microbiol* 30(3):187-196.

59. Soderling SH & Beavo JA (2000) Regulation of cAMP and cGMP signaling: new phosphodiesterases and new functions. *Current Opinion in Cell Biology* 12(2):174-179.

60. Conti M*, et al.* (2003) Cyclic AMP-specific PDE4 phosphodiesterases as critical components of cyclic AMP signaling. *J Biol Chem* 278(8):5493-5496.

61. Brunton LL HJ, and Mayer SE (1981) Functional compartmentation of cyclic AMP and protein kinase in heart. *Adv Cyclic Nucleotide Res* (14):391-397.

62. Carr DW*, et al.* (1991) Interaction of the regulatory subunit (RII) of cAMP-dependent protein kinase with RII-anchoring proteins occurs through an amphipathic helix binding motif. *J Biol Chem* 266(22):14188-14192.

63. Howe AK, Baldor LC, & Hogan BP (2005) Spatial regulation of the cAMP-dependent protein kinase during chemotactic cell migration. *Proc Natl Acad Sci U S A* 102(40):14320-14325.

64. Fimia GM & Sassone-Corsi P (2001) Cyclic AMP signalling. *J Cell Sci* 114(11):1971-1972.

65. Iwasaki T, Chen JD, Kim JP, Wynn KC, & Woodley DT (1994) Dibutyryl cyclic AMP modulates keratinocyte migration without alteration of integrin expression. *J Invest Dermatol* 102(6):891-897.

66. Edin ML, Howe AK, & Juliano RL (2001) Inhibition of PKA blocks fibroblast migration in response to growth factors. *Exp Cell Res* 270(2):214-222.

67. Ydrenius L, Molony L, Ng-Sikorski J, & Andersson T (1997) Dual action of cAMP-dependent protein kinase on granulocyte movement. *Biochem Biophys Res Commun* 235(3):445-450.

68. Taylor SS*, et al.* (2005) Dynamics of signaling by PKA. *Biochimica et Biophysica Acta (BBA) - Proteins & Proteomics* 1754(1-2):25-37.

69. Moore MJ, Kanter JR, Jones KC, & Taylor SS (2002) Phosphorylation of the catalytic subunit of protein kinase A. Autophosphorylation versus phosphorylation by phosphoinositide-dependent kinase-1. *J Biol Chem* 277(49):47878-47884.

70. Diviani D, Soderling J, & Scott JD (2001) AKAP-Lbc anchors protein kinase A and nucleates Galpha 12-selective Rho-mediated stress fiber formation. *J Biol Chem* 276(47):44247-44257.

71. Klussmann E & Rosenthal W (2001) Role and identification of protein kinase A anchoring proteins in vasopressin-mediated aquaporin-2 translocation. *Kidney Int* 60(2):446-449.

72. Nauert JB, Klauck TM, Langeberg LK, & Scott JD (1997) Gravin, an autoantigen recognized by serum from myasthenia gravis patients, is a kinase scaffold protein. *Curr Biol* 7(1):52-62.

73. Dransfield DT*, et al.* (1997) Ezrin is a cyclic AMP-dependent protein kinase anchoring protein. *EMBO J* 16(1):35-43.

74. Westphal RS, Soderling SH, Alto NM, Langeberg LK, & Scott JD (2000) Scar/WAVE-1, a Wiskott-Aldrich syndrome protein, assembles an actin-associated multi-kinase scaffold. *EMBO J* 19(17):4589-4600.

75. Michel JJ & Scott JD (2002) AKAP mediated signal transduction. *Annu Rev Pharmacol Toxicol* 42:235-257.

76. Wegner A & Isenberg G (1983) 12-fold difference between the critical monomer concentrations of the two ends of actin filaments in physiological salt conditions. *Proc Natl Acad Sci U S A* 80(16):4922-4925.

77. Higgs H (2001) *Molecular Interactions of Actin: Actin Structure and Actin-Binding Proteins* (La Jolla).

78. Pantaloni D, Le Clainche C, & Carlier MF (2001) Mechanism of actin-based motility. *Science* 292(5521):1502-1506.

79. Kang F, Purich DL, & Southwick FS (1999) Profilin promotes barbed-end actin filament assembly without lowering the critical concentration. *J Biol Chem* 274(52):36963-36972.

80. Carlier MF PD (1994) Actin assembly in response to extracellular signals: role of capping proteins, thymosin beta4 and profilin. *Semin Cell Biol* 5(3):183-191.

81. Mishra VS, Henske EP, Kwiatkowski DJ, & Southwick FS (1994) The human actin-regulatory protein cap G: gene structure and chromosome location. *Genomics* 23(3):560-565.

82. Yin HL (1987) Gelsolin: calcium- and polyphosphoinositide-regulated actin-modulating protein. *Bioessays* 7(4):176-179.

83. McGough A (2001) The ADF/cofilin family: accelerators of actin reorganization. *Results and problems in cell differentiation* 32:135-137.

84. Lin KM, Mejillano M, & Yin HL (2000) Ca2+ regulation of gelsolin by its C-terminal tail. *J Biol Chem* 275(36):27746-27752.

85. Mullins RD, Heuser JA, & Pollard TD (1998) The interaction of Arp2/3 complex with actin: nucleation, high affinity pointed end capping, and formation of branching networks of filaments. *Proc Natl Acad Sci U S A* 95(11):6181-6186.

86. Mullins RD & Pollard TD (1999) Rho-family GTPases require the Arp2/3 complex to stimulate actin polymerization in *Acanthamoeba* extracts. *Curr Biol* 9(8):405-415.

87. Machesky LM*, et al.* (1999) Scar, a WASp-related protein, activates nucleation of actin filaments by the Arp2/3 complex. *Proc Natl Acad Sci U S A* 96(7):3739-3744.

88. Dabiri GA, Sanger JM, Portnoy DA, & Southwick FS (1990) *Listeria monocytogenes* moves rapidly through the host-cell cytoplasm by inducing directional actin assembly. *Proc Natl Acad Sci U S A* 87(16):6068-6072.

89. Witko-Sarsat V, Rieu P, Descamps-Latscha B, Lesavre P, & Halbwachs-Mecarelli L (2000) Neutrophils: molecules, functions and pathophysiological aspects. *Lab Invest* 80(5):617-653.

90. Furze RC & Rankin SM (2008) Neutrophil mobilization and clearance in the bone marrow. *Immunology* 125(3):281-288.

91. Gabrilovich DI (2005) *The Neutrophils: New Outlook for Old Cells* (Imperial College Press, Danvers) p 355-365.

92. Dale DC, Ward SB, Kimball HR, & Wolff SM (1972) Studies of neutrophil production and turnover in grey collie dogs with cyclic neutropenia. *J Clin Invest* 51(8):2190-2196.

93. Pliyev BK (2008) Chemotactically active proteins of neutrophils. *Biochemistry (Mosc)* 73(9):970-984.

94. Siddiqui RA, Akard LP, Garcia JG, Cui Y, & English D (1999) Chemotactic migration triggers IL-8 generation in neutrophilic leukocytes. *J Immunol* 162(2):1077-1083.

95. English D*, et al.* (1999) Induction of endothelial cell chemotaxis by sphingosine 1-phosphate and stabilization of endothelial monolayer barrier function by lysophosphatidic acid, potential mediators of hematopoietic angiogenesis. *J Hematother Stem Cell Res* 8(6):627-634.

96. Mock Ml & Fouet As (2001) Anthrax. *Annual Review of Microbiology* 55(1):647-671.

97. Creagh EM & O'Neill LAJ (2006) TLRs, NLRs and RLRs: a trinity of pathogen sensors that co-operate in innate immunity. *Trends in Immunology* 27(8):352-357.

98. Topham MK, Carveth HJ, McIntyre TM, Prescott SM, & Zimmerman GA (1998) Human endothelial cells regulate polymorphonuclear leukocyte degranulation. *FASEB J* 12(9):733-746.

99. Vulcano M, Alves Rosa MF, Minnucci FS, Chernavsky AC, & Isturiz MA (1998) N-formyl-methionyl-leucyl-phenylalanine (fMLP) inhibits tumour necrosis factor-alpha (TNF-alpha) production on lipopolysaccharide (LPS)-stimulated human neutrophils. *Clin Exp Immunol* 113(1):39-47.

100. Xing L & Remick DG (2003) Relative cytokine and cytokine inhibitor production by mononuclear cells and neutrophils. *Shock* 20(1):10-16.

101. Bainton DF (1973) Sequential degranulation of the two types of polymorphonuclear leukocyte granules during phagocytosis of microorganisms. *J Cell Biol* 58(2):249-264.

102. Howard TH & Watts RG (1994) Actin polymerization and leukocyte function. *Curr Opin Hematol* 1(1):61-68.

103. Delves PJ & Roitt IM (2000) The immune system. First of two parts. *N Engl J Med* 343(1):37-49.

104. Delves PJ & Roitt IM (2000) The immune system. Second of two parts. *N Engl J Med* 343(2):108-117.

105. Abbassi O, Kishimoto TK, McIntire LV, & Smith CW (1993) Neutrophil adhesion to endothelial cells. *Blood Cells* 19(2):245-259; discussion 259-260.

106. Szarowicz SE*, et al.* (2009) *Bacillus anthracis* edema toxin impairs neutrophil actin-based motility. *Infect. Immun.* 77(6):2455-2464.

107. Southwick FS, Dabiri GA, & Stossel TP (1988) Neutrophil actin dysfunction is a genetic disorder associated with partial impairment of neutrophil actin assembly in three family members. *J Clin Invest* 82(5):1525-1531.

108. Alves-Filho JC, Benjamim C, Tavares-Murta BM, & Cunha FQ (2005) Failure of neutrophil migration toward infectious focus in severe sepsis: a critical event for the outcome of this syndrome. *Mem Inst Oswaldo Cruz* 100 Suppl 1:223-226.

109. Alves-Filho JC*, et al.* (2006) Neutrophil function in severe sepsis. *Endocr Metab Immune Disord Drug Targets* 6(2):151-158.

110. Ridley AJ*, et al.* (2003) Cell migration: integrating signals from front to back. *Science* 302(5651):1704-1709.

111. Eckert RE & Jones SL (2007) Regulation of VASP serine 157 phosphorylation in human neutrophils after stimulation by a chemoattractant. *J Leukoc Biol* 82(5):1311-1321.

112. Jones SL (2002) Protein kinase A regulates beta2 integrin avidity in neutrophils. *J Leukoc Biol* 71(6):1042-1048.

113. Jones SL & Sharief Y (2005) Asymmetrical protein kinase A activity establishes neutrophil cytoskeletal polarity and enables chemotaxis. *J Leukoc Biol* 78(1):248-258.

114. Ananthakrishnan R & Ehrlicher A (2007) The forces behind cell movement. *Int J Biol Sci* 3(5):303-317.

115. Wu D (2005) Signaling mechanisms for regulation of chemotaxis. *Cell Res* 15(1):52-56.

116. Sasaki T*, et al.* (2000) Function of PI3Kgamma in thymocyte development, T cell activation, and neutrophil migration. *Science* 287(5455):1040-1046.

117. Zhelev DV & Alteraifi A (2002) Signaling in the motility responses of the human neutrophil. *Ann Biomed Eng* 30(3):356-370.

118. Pollard TD, Blanchoin L, & Mullins RD (2000) Molecular mechanisms controlling actin filament dynamics in nonmuscle cells. *Annu Rev Biophys Biomol Struct* 29:545-576.

119. Chang PS, Axelrod D, Omann GM, & Linderman JJ (2005) G protein threshold behavior in the human neutrophil oxidant response: measurement of G proteins available for signaling in responding and nonresponding subpopulations. *Cell Signal* 17(5):605-614.

120. Alteraifi AM & Zhelev DV (1997) Transient increase of free cytosolic calcium during neutrophil motility responses. *J Cell Sci* 110 (Pt 16):1967-1977.

121. Haribabu B*, et al.* (1999) Chemoattractant receptors activate distinct pathways for chemotaxis and secretion. Role of G-protein usage. *J Biol Chem* 274(52):37087-37092.

122. Higgs HN & Pollard TD (2000) Activation by Cdc42 and PIP(2) of Wiskott-Aldrich syndrome protein (WASp) stimulates actin nucleation by Arp2/3 complex. *J Cell Biol* 150(6):1311-1320.

123. Zigmond SH*, et al.* (1998) Mechanism of Cdc42-induced actin polymerization in neutrophil extracts. *J Cell Biol* 142(4):1001-1012.

124. Schlech WF, 3rd (1997) *Listeria* gastroenteritis--old syndrome, new pathogen. *N Engl J Med* 336(2):130-132.

125. Gouin E, Welch MD, & Cossart P (2005) Actin-based motility of intracellular pathogens. *Curr Opin Microbiol* 8(1):35-45.

126. Kocks C*, et al.* (1992) *L. monocytogenes*-induced actin assembly requires the actA gene product, a surface protein. *Cell* 68(3):521-531.

127. Dold FG, Sanger JM, & Sanger JW (1994) Intact alpha-actinin molecules are needed for both the assembly of actin into the tails and the locomotion of *Listeria monocytogenes* inside infected cells. *Cell Motil Cytoskeleton* 28(2):97-107.

128. Tilney LG & Portnoy DA (1989) Actin filaments and the growth, movement, and spread of the intracellular bacterial parasite, *Listeria monocytogenes*. *J Cell Biol* 109(4 Pt 1):1597-1608.

129. Chong R*, et al.* (2009) Regulatory mimicry in *Listeria monocytogenes* actin-based motility. *Cell Host Microbe* 6(3):268-278.

130. Welch MD, Iwamatsu A, & Mitchison TJ (1997) Actin polymerization is induced by Arp2/3 protein complex at the surface of *Listeria monocytogenes*. *Nature* 385(6613):265-269.

131. Bierne H*, et al.* (2005) WASP-related proteins, Abi1 and Ena/VASP are required for *Listeria* invasion induced by the Met receptor. *J Cell Sci* 118(Pt 7):1537-1547.

132. Mengaud J, Ohayon H, Gounon P, Mege RM, & Cossart P (1996) E-cadherin is the receptor for internalin, a surface protein required for entry of *L. monocytogenes* into epithelial cells. *Cell* 84(6):923-932.

133. Shen Y, Naujokas M, Park M, & Ireton K (2000) InIB-dependent internalization of *Listeria* is mediated by the Met receptor tyrosine kinase. *Cell* 103(3):501-510.

134. Imamura Y, Itoh M, Maeno Y, Tsukita S, & Nagafuchi A (1999) Functional domains of alpha-catenin required for the strong state of cadherin-based cell adhesion. *J Cell Biol* 144(6):1311-1322.

135. Glomski IJ, Decatur AL, & Portnoy DA (2003) *Listeria monocytogenes* mutants that fail to compartmentalize listerolysin O activity are cytotoxic, avirulent, and unable to evade host extracellular defenses. *Infect Immun* 71(12):6754-6765.

136. Tilney LG & Tilney MS (1993) The wily ways of a parasite: induction of actin assembly by *Listeria*. *Trends Microbiol* 1(1):25-31.

137. Theriot JA, Mitchison TJ, Tilney LG, & Portnoy DA (1992) The rate of actin-based motility of intracellular *Listeria monocytogenes* equals the rate of actin polymerization. *Nature* 357(6375):257-260.

138. Chakraborty T*, et al.* (1995) A focal adhesion factor directly linking intracellularly motile *Listeria monocytogenes* and *Listeria* ivanovii to the actin-based cytoskeleton of mammalian cells. *EMBO J* 14(7):1314-1321.

139. Niebuhr K*, et al.* (1997) A novel proline-rich motif present in ActA of *Listeria monocytogenes* and cytoskeletal proteins is the ligand for the EVH1 domain, a protein module present in the Ena/VASP family. *EMBO J* 16(17):5433-5444.

140. Bear JE*, et al.* (2002) Antagonism between Ena/VASP proteins and actin filament capping regulates fibroblast motility. *Cell* 109(4):509-521.

141. Loisel TP, Boujemaa R, Pantaloni D, & Carlier MF (1999) Reconstitution of actin-based motility of *Listeria* and Shigella using pure proteins. *Nature* 401(6753):613-616.

142. Auerbuch V, Loureiro JJ, Gertler FB, Theriot JA, & Portnoy DA (2003) Ena/VASP proteins contribute to *Listeria monocytogenes* pathogenesis by controlling temporal and spatial persistence of bacterial actin-based motility. *Mol Microbiol* 49(5):1361-1375.

143. Han YH*, et al.* (2002) Requirement of a vasodilator-stimulated phosphoprotein family member for cell adhesion, the formation of filopodia, and chemotaxis in dictyostelium. *J Biol Chem* 277(51):49877-49887.

144. Halbrugge M & Walter U (1989) Purification of a vasodilator-regulated phosphoprotein from human platelets. *Eur J Biochem* 185(1):41-50.

145. Butt E*, et al.* (1994) cAMP- and cGMP-dependent protein kinase phosphorylation sites of the focal adhesion vasodilator-stimulated phosphoprotein (VASP) in vitro and in intact human platelets. *J Biol Chem* 269(20):14509-14517.

146. Waldmann R, Nieberding M, & Walter U (1987) Vasodilator-stimulated protein phosphorylation in platelets is mediated by cAMP- and cGMP-dependent protein kinases. *Eur J Biochem* 167(3):441-448.

147. Holt MR, Critchley DR, & Brindle NP (1998) The focal adhesion phosphoprotein, VASP. *Int J Biochem Cell Biol* 30(3):307-311.

148. Smolenski A*, et al.* (1998) Analysis and regulation of vasodilator-stimulated phosphoprotein serine 239 phosphorylation in vitro and in intact cells using a phosphospecific monoclonal antibody. *J Biol Chem* 273(32):20029-20035.

149. Draijer R*, et al.* (1995) Expression of cGMP-dependent protein kinase I and phosphorylation of its substrate, vasodilator-stimulated phosphoprotein, in human endothelial cells of different origin. *Circ Res* 77(5):897-905.

150. Rottner K, Behrendt B, Small JV, & Wehland J (1999) VASP dynamics during lamellipodia protrusion. *Nat Cell Biol* 1(5):321-322.

151. Smith GA, Theriot JA, & Portnoy DA (1996) The tandem repeat domain in the *Listeria monocytogenes* ActA protein controls the rate of actin-based motility, the percentage of moving bacteria, and the localization of vasodilator-stimulated phosphoprotein and profilin. *J Cell Biol* 135(3):647-660.

152. Laurent V*, et al.* (1999) Role of proteins of the Ena/VASP family in actin-based motility of *Listeria monocytogenes. J Cell Biol* 144(6):1245-1258.

153. Skoble J, Auerbuch V, Goley ED, Welch MD, & Portnoy DA (2001) Pivotal role of VASP in Arp2/3 complex-mediated actin nucleation, actin branch-formation, and *Listeria monocytogenes* motility. *J Cell Biol* 155(1):89-100.

154. Lawrence DW & Pryzwansky KB (2001) The vasodilator-stimulated phosphoprotein is regulated by cyclic GMP-dependent protein kinase during neutrophil spreading. *J Immunol* 166(9):5550-5556.

155. Gertler FB, Niebuhr K, Reinhard M, Wehland J, & Soriano P (1996) Mena, a relative of VASP and Drosophila Enabled, is implicated in the control of microfilament dynamics. *Cell* 87(2):227-239.

156. Kwiatkowski AV, Gertler FB, & Loureiro JJ (2003) Function and regulation of Ena/VASP proteins. *Trends Cell Biol* 13(7):386-392.

157. Sechi AS & Wehland J (2004) ENA/VASP proteins: multifunctional regulators of actin cytoskeleton dynamics. *Front Biosci* 9:1294-1310.

158. Ball LJ*, et al.* (2000) Dual epitope recognition by the VASP EVH1 domain modulates polyproline ligand specificity and binding affinity. *EMBO J* 19(18):4903-4914.

159. Reinhard M, Jouvenal K, Tripier D, & Walter U (1995) Identification, purification, and characterization of a zyxin-related protein that binds the focal adhesion and microfilament protein VASP (vasodilator-stimulated phosphoprotein). *Proc Natl Acad Sci U S A* 92(17):7956-7960.

160. Krause M, Dent EW, Bear JE, Loureiro JJ, & Gertler FB (2003) Ena/VASP proteins: regulators of the actin cytoskeleton and cell migration. *Annu Rev Cell Dev Biol* 19:541-564.

161. Krause M, Bear JE, Loureiro JJ, & Gertler FB (2002) The Ena/VASP enigma. *J Cell Sci* 115(Pt 24):4721-4726.

162. Blume C*, et al.* (2007) AMP-activated protein kinase impairs endothelial actin cytoskeleton assembly by phosphorylating vasodilator-stimulated phosphoprotein. *J Biol Chem* 282(7):4601-4612.

163. Lambrechts A*, et al.* (2000) cAMP-dependent protein kinase phosphorylation of EVL, a Mena/VASP relative, regulates its interaction with actin and SH3 domains. *J Biol Chem* 275(46):36143-36151.

164. Barzik M*, et al.* (2005) Ena/VASP proteins enhance actin polymerization in the presence of barbed end capping proteins. *J Biol Chem* 280(31):28653-28662.

165. Benz PM*, et al.* (2009) Differential VASP phosphorylation controls remodeling of the actin cytoskeleton. *J Cell Sci* 122(Pt 21):3954-3965.

166. Reinhard M*, et al.* (1992) The 46/50 kDa phosphoprotein VASP purified from human platelets is a novel protein associated with actin filaments and focal contacts. *EMBO J* 11(6):2063-2070.

167. Scott JA*, et al.* (2006) Ena/VASP proteins can regulate distinct modes of actin organization at cadherin-adhesive contacts. *Mol Biol Cell* 17(3):1085-1095.

168. Vasioukhin V, Bauer C, Yin M, & Fuchs E (2000) Directed actin polymerization is the driving force for epithelial cell-cell adhesion. *Cell* 100(2):209-219.

169. Mejillano MR*, et al.* (2004) Lamellipodial versus filopodial mode of the actin nanomachinery: pivotal role of the filament barbed end. *Cell* 118(3):363-373.

170. Rorth P (2003) Communication by touch: role of cellular extensions in complex animals. *Cell* 112(5):595-598.

171. Porter KR & Yegian D (1945) Some artifacts encountered in stained Preparations of tubercle bacilli: II. Much granules and beads. *J Bacteriol* 50(5):563-575.

172. Small JV (1988) The actin cytoskeleton. *Electron Microsc Rev* 1(1):155-174.

173. Jacinto A*, et al.* (2000) Dynamic actin-based epithelial adhesion and cell matching during Drosophila dorsal closure. *Curr Biol* 10(22):1420-1426.

174. Jacinto A & Wolpert L (2001) Filopodia. *Curr Biol* 11(16):R634-637.

175. Dent EW & Gertler FB (2003) Cytoskeletal dynamics and transport in growth cone motility and axon guidance. *Neuron* 40(2):209-227.

176. Vasioukhin V & Fuchs E (2001) Actin dynamics and cell-cell adhesion in epithelia. *Curr Opin Cell Biol* 13(1):76-84.

177. Nobes CD & Hall A (1995) Rho, rac, and cdc42 GTPases regulate the assembly of multimolecular focal complexes associated with actin stress fibers, lamellipodia, and filopodia. *Cell* 81(1):53-62.

178. Faix J, Breitsprecher D, Stradal TE, & Rottner K (2009) Filopodia: Complex models for simple rods. *Int J Biochem Cell Biol* 41(8-9):1656-1664.

179. Applewhite DA*, et al.* (2007) Ena/VASP proteins have an anti-capping independent function in filopodia formation. *Mol Biol Cell* 18(7):2579-2591.

180. Kerber ML*, et al.* (2009) A novel form of motility in filopodia revealed by imaging myosin-X at the single-molecule level. *Curr Biol* 19(11):967-973.

181. Lim KB*, et al.* (2008) The Cdc42 effector IRSp53 generates filopodia by coupling membrane protrusion with actin dynamics. *J Biol Chem* 283(29):20454-20472.

182. Faix J & Rottner K (2006) The making of filopodia. *Curr Opin Cell Biol* 18(1):18-25.

183. Yeager LA, Chopra AK, & Peterson JW (2009) *Bacillus anthracis* edema toxin suppresses human macrophage phagocytosis and cytoskeletal remodeling via the protein kinase A and exchange protein activated by cyclic AMP pathways. *Infect Immun* 77(6):2530-2543.

184. Bear JE*, et al.* (2000) Negative regulation of fibroblast motility by Ena/VASP proteins. *Cell* 101(7):717-728.

185. Harbeck B, Huttelmaier S, Schluter K, Jockusch BM, & Illenberger S (2000) Phosphorylation of the vasodilator-stimulated phosphoprotein regulates its interaction with actin. *J Biol Chem* 275(40):30817-30825.

186. Ascenzi P*, et al.* (2002) Anthrax toxin: a tripartite lethal combination. *FEBS Lett* 531(3):384-388.

187. Southwick FS, Dabiri GA, Paschetto M, & Zigmond SH (1989) Polymorphonuclear leukocyte adherence induces actin polymerization by a transduction pathway which differs from that used by chemoattractants. *J Cell Biol* 109(4 Pt 1):1561-1569.

188. Twenhafel NA, Leffel E, & Pitt ML (2007) Pathology of inhalational anthrax infection in the african green monkey. *Vet Pathol* 44(5):716-721.

189. Downey GP*, et al.* (1991) Biophysical properties and microfilament assembly in neutrophils: modulation by cyclic AMP. *J Cell Biol* 114(6):1179-1190.

190. Affolter M & Weijer CJ (2005) Signaling to cytoskeletal dynamics during chemotaxis. 9(1):19-34.

191. Wade BH, Wright GG, Hewlett EL, Leppla SH, & Mandell GL (1985) Anthrax toxin components stimulate chemotaxis of human polymorphonuclear neutrophils. *Proc Soc Exp Biol Med* 179(2):159-162.

192. Kumar P, Ahuja N, & Bhatnagar R (2001) Purification of anthrax edema factor from *Escherichia coli* and identification of residues required for binding to anthrax protective antigen. *Infect Immun* 69(10):6532-6536.

193. Soelaiman S*, et al.* (2003) Structure-based inhibitor discovery against adenylyl cyclase toxins from pathogenic bacteria that cause anthrax and whooping cough. *J Biol Chem* 278(28):25990-25997.

194. Leppla SH (1982) Anthrax toxin edema factor: a bacterial adenylate cyclase that increases cyclic AMP concentrations of eukaryotic cells. *Proc Natl Acad Sci U S A* 79(10):3162-3166.

195. van Sorge NM*, et al.* (2008) Anthrax toxins inhibit neutrophil signaling pathways in brain endothelium and contribute to the pathogenesis of meningitis. *PLoS One* 3(8):e2964.

196. Quinn CP, Shone CC, Turnbull PC, & Melling J (1988) Purification of anthrax-toxin components by high-performance anion-exchange, gel-filtration and hydrophobic-interaction chromatography. *Biochem J* 252(3):753-758.

197. Cartier C*, et al.* (2003) Active cAMP-dependent protein kinase incorporated within highly purified HIV-1 particles is required for viral infectivity and interacts with viral capsid protein. *J Biol Chem* 278(37):35211-35219.

198. During RL*, et al.* (2007) Anthrax lethal toxin paralyzes actin-based motility by blocking Hsp27 phosphorylation. *EMBO J* 26(9):2240-2250.

199. Zeile WL, Purich DL, & Southwick FS (1996) Recognition of two classes of oligoproline sequences in profilin-mediated acceleration of actin-based Shigella motility. *J Cell Biol* 133(1):49-59.

200. Schafer D & Baenkler HW (2005) Functional eicosanoid test and typing (FET) of peripheral blood cells in eicosanoids related diseases. *J Physiol Pharmacol* 56 Suppl 5:103-118.

201. Schevchenko VA*, et al.* (1996) Human cytogenetic consequences of the Chernobyl accident. *Mutat Res* 361(1):29-34.

202. Walsh DA, Perkins JP, & Krebs EG (1968) An adenosine 3',5'-monophosphate-dependant protein kinase from rabbit skeletal muscle. *J Biol Chem* 243(13):3763-3765.

203. Razin VF (1978) Characteristics of the manifestation of acute peritonitis in persons with developmental anomalies of the inguinal canal. (*Klin Khir* (4):59-60.

204. Takei K, Tokuyama K, Kato M, & Morikawa A (1998) Role of cyclic adenosine monophosphate in reducing superoxide anion generation in guinea pig alveolar macrophages. *Pharmacology* 57(1):1-7.

205. Ar'Rajab A*, et al.* (1996) The role of neutrophils in peritoneal adhesion formation. *J Surg Res* 61(1):143-146.

206. Bernardini ML, Mounier J, d'Hauteville H, Coquis-Rondon M, & Sansonetti PJ (1989) Identification of icsA, a plasmid locus of *Shigella flexneri* that governs bacterial intra- and intercellular spread through interaction with F-actin. *Proc Natl Acad Sci U S A* 86(10):3867-3871.

207. Sanger JM, Sanger JW, & Southwick FS (1992) Host cell actin assembly is necessary and likely to provide the propulsive force for intracellular movement of *Listeria monocytogenes*. *Infect Immun* 60(9):3609-3619.

208. Cossart P & Sansonetti PJ (2004) Bacterial invasion: the paradigms of enteroinvasive pathogens. *Science* 304(5668):242-248.

209. Zhao T*, et al.* (2007) Silencing the PTEN gene is protective against neuronal death induced by human immunodeficiency virus type 1 Tat. *J Neurovirol* 13(2):97-106.

210. Svitkina TM*, et al.* (2003) Mechanism of filopodia initiation by reorganization of a dendritic network. *J Cell Biol* 160(3):409-421.

211. Lebrand C*, et al.* (2004) Critical role of Ena/VASP proteins for filopodia formation in neurons and in function downstream of netrin-1. *Neuron* 42(1):37-49.

212. Geese M*, et al.* (2002) Contribution of Ena/VASP proteins to intracellular motility of *Listeria* requires phosphorylation and proline-rich core but not F-actin binding or multimerization. *Mol Biol Cell* 13(7):2383-2396.

213. Fialkow L, Wang Y, & Downey GP (2007) Reactive oxygen and nitrogen species as signaling molecules regulating neutrophil function. *Free Radic Biol Med* 42(2):153-164.

214. Harvath L, Robbins JD, Russell AA, & Seamon KB (1991) cAMP and human neutrophil chemotaxis. Elevation of cAMP differentially affects chemotactic responsiveness. *J Immunol* 146(1):224-232.

215. Nathan C & Sanchez E (1990) Tumor necrosis factor and CD11/CD18 (beta 2) integrins act synergistically to lower cAMP in human neutrophils. *J Cell Biol* 111(5 Pt 1):2171-2181.

216. DeMali KA, Wennerberg K, & Burridge K (2003) Integrin signaling to the actin cytoskeleton. *Curr Opin Cell Biol* 15(5):572-582.

217. Fincham VJ, James M, Frame MC, & Winder SJ (2000) Active ERK/MAP kinase is targeted to newly forming cell-matrix adhesions by integrin engagement and v-Src. *EMBO J* 19(12):2911-2923.

218. Sidhu G*, et al.* (2005) Phosphoinositide 3-kinase is required for intracellular *Listeria monocytogenes* actin-based motility and filopod formation. *J Biol Chem* 280(12):11379-11386.

219. Rivkin I, Rosenblatt J, & Becker EL (1975) The role of cyclic AMP in the chemotactic responsiveness and spontaneous motility of rabbit peritoneal neutrophils. The inhibition of neutrophil movement and the elevation of cyclic AMP levels by catecholamines, prostaglandins, theophylline and cholera toxin. *J Immunol* 115(4):1126-1134.

220. Selliah N, Bartik MM, Carlson SL, Brooks WH, & Roszman TL (1995) cAMP accumulation in T-cells inhibits anti-CD3 monoclonal antibody-induced actin polymerization. *J Neuroimmunol* 56(1):107-112.

221. Ydrenius L, Majeed M, Rasmusson BJ, Stendahl O, & Sarndahl E (2000) Activation of cAMP-dependent protein kinase is necessary for actin rearrangements in human neutrophils during phagocytosis. *J Leukoc Biol* 67(4):520-528.

222. Dal Molin F*, et al.* (2008) cAMP imaging of cells treated with pertussis toxin, cholera toxin, and anthrax edema toxin. *Biochem Biophys Res Commun* 376(2):429-433.

223. Dal Molin F*, et al.* (2006) Cell entry and cAMP imaging of anthrax edema toxin. *EMBO J* 25(22):5405-5413.

224. Kim C*, et al.* (2008) Antiinflammatory cAMP signaling and cell migration genes co-opted by the anthrax bacillus. *Proc Natl Acad Sci U S A* 105(16):6150-6155.

225. Welch MD, Rosenblatt J, Skoble J, Portnoy DA, & Mitchison TJ (1998) Interaction of human Arp2/3 complex and the *Listeria monocytogenes* ActA protein in actin filament nucleation. *Science* 281(5373):105-108.

226. Goldberg MB, Theriot JA, & Sansonetti PJ (1994) Regulation of surface presentation of IcsA, a Shigella protein essential to intracellular movement and spread, is growth phase dependent. *Infect Immun* 62(12):5664-5668.

227. Egile C*, et al.* (1999) Activation of the CDC42 effector N-WASP by the S*higella flexneri* IcsA protein promotes actin nucleation by Arp2/3 complex and bacterial actin-based motility. *J Cell Biol* 146(6):1319-1332.

228. Holty JE*, et al.* (2006) Systematic review: a century of inhalational anthrax cases from 1900 to 2005. *Ann Intern Med* 144(4):270-280.

229. Read TD*, et al.* (2003) The genome sequence of *Bacillus anthracis* Ames and comparison to closely related bacteria. *Nature* 423(6935):81-86.

230. Puhar A, Dal Molin F, Horvath S, Ladants D, & Montecucco C (2008) Anthrax edema toxin modulates PKA- and CREB-dependent signaling in two phases. *PLoS One* 3(10):e3564.

231. Southwick FS & Purich DL (1998) *Listeria* and Shigella actin-based motility in host cells. *Trans Am Clin Climatol Assoc* 109:160-172; discussion 172-163.

232. Li Z, Ajdic J, Eigenthaler M, & Du X (2003) A predominant role for cAMP-dependent protein kinase in the cGMP-induced phosphorylation of vasodilator-stimulated phosphoprotein and platelet inhibition in humans. *Blood* 101(11):4423-4429.

233. Halbrugge M, Friedrich C, Eigenthaler M, Schanzenbacher P, & Walter U (1990) Stoichiometric and reversible phosphorylation of a 46-kDa protein in human platelets in response to cGMP- and cAMP-elevating vasodilators. *J Biol Chem* 265(6):3088-3093.

234. Pasic L, Kotova T, & Schafer DA (2008) Ena/VASP proteins capture actin filament barbed ends. *J Biol Chem* 283(15):9814-9819.

235. Bachmann C, Fischer L, Walter U, & Reinhard M (1999) The EVH2 domain of the vasodilator-stimulated phosphoprotein mediates tetramerization, F-actin binding, and actin bundle formation. *J Biol Chem* 274(33):23549-23557.

236. Bear JE, Krause M, & Gertler FB (2001) Regulating cellular actin assembly. *Current Opinion in Cell Biology* 13(2):158-166.

237. Benz PM*, et al.* (2008) Cytoskeleton assembly at endothelial cell-cell contacts is regulated by alphaII-spectrin-VASP complexes. *J Cell Biol* 180(1):205-219.

238. Pula G*, et al.* (2006) PKCdelta regulates collagen-induced platelet aggregation through inhibition of VASP-mediated filopodia formation. *Blood* 108(13):4035-4044.

239. Schirenbeck A, Arasada R, Bretschneider T, Schleicher M, & Faix J (2005) Formins and VASPs may co-operate in the formation of filopodia. *Biochem Soc Trans* 33(Pt 6):1256-1259.

240. Kuhnel K*, et al.* (2004) The VASP tetramerization domain is a right-handed coiled coil based on a 15-residue repeat. *Proc Natl Acad Sci U S A* 101(49):17027-17032.

241. Block J*, et al.* (2008) Filopodia formation induced by active mDia2/Drf3. *J Microsc* 231(3):506-517.

242. Vignjevic D*, et al.* (2006) Role of fascin in filopodial protrusion. *J Cell Biol* 174(6):863-875.

243. Vignjevic D, Peloquin J, & Borisy GG (2006) *In vitro* assembly of filopodia-like bundles. *Methods Enzymol* 406:727-739.

244. Dent EW*, et al.* (2007) Filopodia are required for cortical neurite initiation. *Nat Cell Biol* 9(12):1347-1359.

245. Kwiatkowski AV*, et al.* (2007) Ena/VASP is required for neuritogenesis in the developing cortex. *Neuron* 56(3):441-455.

246. Abramova AA & Grinberg LM (1993) Pathology of anthrax sepsis according to materials of the infectious outbreak in 1979 in Sverdlovsk (macroscopic changes). *Arkh Patol* 55(1):12-17.

247. Moayeri M, Haines D, Young HA, & Leppla SH (2003) *Bacillus anthracis* lethal toxin induces TNF-α independent hypoxia-mediated toxicity in mice. *The Journal of Clinical Investigation* 112(5):670-682.

248. Abrami L, Lindsay M, Parton RG, Leppla SH, & van der Goot FG (2004) Membrane insertion of anthrax protective antigen and cytoplasmic delivery of lethal factor occur at different stages of the endocytic pathway. *J Cell Biol* 166(5):645-651.

249. Gordon VM*, et al.* (1989) Adenylate cyclase toxins from *Bacillus anthracis* and *Bordetella pertussis.* Different processes for interaction with and entry into target cells. *J Biol Chem* 264(25):14792-14796.

250. Warfel JM, Steele AD, & D'Agnillo F (2005) Anthrax lethal toxin induces endothelial barrier dysfunction. *Am J Pathol* 166(6):1871-1881.

251. Condeelis J (1993) Life at the leading edge: The formation of cell protrusions. *Annual Review of Cell Biology* 9(1):411-444.

252. Dejana E, Corada M, & Lampugnani MG (1995) Endothelial cell-to-cell junctions. *FASEB J* 9(10):910-918.

253. Bazzoni G (2006) Endothelial tight junctions: permeable barriers of the vessel wall. *Thromb Haemost* 95(1):36-42.

254. Fanning AS & Anderson JM (2009) Zonula occludens-1 and -2 are cytosolic scaffolds that regulate the assembly of cellular junctions. *Ann N Y Acad Sci* 1165:113-120.

255. Adams CL & Nelson WJ (1998) Cytomechanics of cadherin-mediated cell-cell adhesion. *Curr Opin Cell Biol* 10(5):572-577.

256. Kodama A, Takaishi K, Nakano K, Nishioka H, & Takai Y (1999) Involvement of Cdc42 small G protein in cell-cell adhesion, migration and morphology of MDCK cells. *Oncogene* 18(27):3996-4006.

257. Jones GE, Ridley AJ, & Zicha D (2000) Rho GTPases and cell migration: measurement of macrophage chemotaxis. *Methods Enzymol* 325:449-462.

BIOGRAPHICAL SKETCH

Sarah Elizabeth Szarowicz was born Sarah Elizabeth Guilmain of Massachusetts. Sarah grew up the only daughter and middle child of two hard working middle class parents. Sarah began her higher educational career by attending Becker College in Leicester, MA where in May of 2000 she received her AS in Veterinary Technology. Her desire and passion for education sent her that fall to the University of Maine to attain her BS in May 2002 in animal and veterinary science. Sarah then decided to try her hand at research and was accepted into the University of Maine's master's program in animal science.

During her master's program, Sarah had the great fortune of working with a group of passionate professors who gave her the drive to ask questions and further sparked her interest in research. After completing her master's on a project of hypothyroidism on hyt/hyt mice Sarah received a job working at the National Institutes of Health (NIH) working with Dr. Jim Pickel in the mental health mouse transgenic core facility. Here, Dr. Pickel pushed Sarah to learn to work independently on various research projects she could call her own and he encouraged her to continue her education. Also, while working at NIH Sarah met her husband Mark Szarowicz.

Sarah was accepted in the summer of 2006 to the Inter-Disciplinary Program at the University of Florida. It was here that she found her mentor Dr. Frederick Southwick and worked to obtain her PhD in immunology and microbiology. Sarah has taken advantage of several opportunities to teach not only undergraduate students but also high school students in infectious diseases and the great opportunities that working in a lab on research can provide for undergraduate students. While attaining her PhD, Sarah

married her husband on October 04, 2009 in an intimate wedding held at the Bauman Center located on the campus of the University of Florida overlooking Lake Alice.

Sarah obtained a post-doctoral position at the United States Army Medical Research Institute of Infectious Disease (USAMRIID) where she will continue striving for excellence in infectious disease research.